GEOLOGICA ULTRAIECTINA

Mededelingen van de
Faculteit Geowetenschappen
Universiteit Utrecht

No. 252

The control of climate and base-level change on the stratigraphic architecture of fluvio-deltaic systems

investigated by quantitative analogue modelling

Aart-Peter van den Berg van Saparoea

This research was carried out at the Sedimentology Group,
Faculty of Geosciences, Utrecht University.

Address:
Budapestlaan 4
PO Box 80021
3508 TA Utrecht
The Netherlands

Internet site: www.geo.uu.nl
(research, research groups, sedimentology)

ISBN: 90-5744-114-4

The control of climate and base-level change on the stratigraphic architecture of fluvio-deltaic systems

investigated by quantitative analogue modelling

De invloed van klimaats- en base level veranderingen op de stratigrafische architectuur van fluvio-deltaische systemen

onderzocht door kwantitatief analoog modelleren

(met een samenvatting in het Nederlands)

Proefschrift

ter verkrijging van de graad van doctor
aan de Universiteit Utrecht
op gezag van de Rector Magnificus, Prof.dr. W. H. Gispen,
ingevolge het besluit van het College voor Promoties
in het openbaar te verdedigen
op maandag 17 oktober 2005 des namiddags te 12.45 uur

door

Aart Petrus Henricus van den Berg van Saparoea

geboren op 29 augustus 1974 te Wageningen

Promotor: Prof. dr. P.L. de Boer
Faculty of Geosciences
Utrecht University

Co-promotor: Dr. G. Postma
Faculty of Geosciences
Utrecht University

Aan mijn ouders

Members of the dissertation committee:

Prof. dr. E.A. Koster
Faculty of Geosciences, Utrecht University
Utrecht, The Netherlands

Prof. dr. S.B. Kroonenberg
Faculty of Civil Engineering and Geosciences, Delft University of Technology
Delft, The Netherlands

Dr. T. E. Törnqvist
Department of Earth and Environmental Sciences, University of Illinois
Chicago, United States of America

Prof. dr. J.F. Vandenberghe
Faculty of Earth and Life Sciences, Free University
Amsterdam, The Netherlands

Prof. dr. ir. A. Veldkamp
Department of Environmental Sciences, Wageningen University
Wageningen, The Netherlands

Contents

Chapter 1 **9**
Introduction

Chapter 2 **13**
Impact of discharge, sediment flux and sea-level change on the stratigraphic architecture of river-delta-shelf systems
(Submitted for publication in IAS Special Publication 'Analogue and Numerical Forward Modelling of Sedimentary Systems; from Understanding to Prediction', Editors: P.L. de Boer, G. Postma et al.)

Chapter 3 **29**
Control of climate change on the yield of river systems
(Submitted for publication in SEPM Special Publication 'Recent advances in shoreline-shelf stratigraphy', Editors: G.J. Hampson et al.)

Chapter 4 **61**
Intersecting river terraces as the result of complex response to simple climate forcing

Chapter 5 **73**
Matlab tool for constructing synthetic stratigraphy from sequential DEMs

Chapter 6 **85**
Epilogue

References **87**

Samenvatting **93**
(Summary in Dutch)

Dankwoord **97**
(Acknowledgements)

Curriculum Vitae **99**

Chapter 1

Introduction

The fluvial system

River systems transport approximately 95% of the detrital sediment supplied to the ocean basins (Hay, 1998). Sediments are transferred from continental areas through deltas and continental shelves to the continental slope. Large quantities of sediment are stored on the continental shelf for long periods. Although the volume of strictly fluvial sediments is comparatively small, fluvial transfer systems play an important role in the filling of most sedimentary basins. The stratigraphy of river systems and their associated deposits record the history of the external forcing processes, the most important of which are climate, tectonics and sea-level change. Where e.g. lacustrine and cave deposits offer excellent records of terrestrial environmental change over relatively short periods, the fluvial stratigraphic record provides a more or less continuous, onshore archive of Quaternary climate change and provides a good stratigraphic framework for correlating detailed records to the global marine record (Bridgland, 2002; Bridgland et al., 2004).

In addition to the geological importance of river systems, fluvial deposits are of economic importance. Fluvial sediments serve as reservoirs for oil, gas and water, and host coal and placer mineral deposits. This makes understanding the generation of fluvial stratigraphy and the controls on sediment delivery to basins highly relevant in this context as well.

River systems can be divided into three basic parts: the catchment area where water and sediment are collected, the transfer valley through which the river transports the sediment, and the depositional basin where the sediment is ultimately deposited.

The transfer valley is not simply a conveyor belt that automatically transports all sediment it receives to the depositional basin. The longitudinal profile of a river system is controlled by water discharge and sediment flux. The gradient is proportional to the sediment flux and inversely proportional to the water discharge. In other words: a high sediment flux and/or a low discharge lead to a steep river valley gradient. Changes in the valley gradient go hand in hand with changes in the volume of sediment in the river valley. Thus river valleys act as a buffer: sediment is stored temporarily or released from temporary storage in response to changing water discharge and sediment supply.

Thus, climate exerts control on the production and release of sediment in the catchment area, on the transport of sediment through the fluvial system, and consequently on the amount of sediment delivered to the depositional basin. Two other major external forcing processes are tectonics and sea-level fluctuations. Tectonics control the generation of sediments in the catchment area and the amount of accommodation space in the transfer valley and in the depositional basin. Sea-level fluctuations control the accommodation space on the continental shelves, and the base level to which rivers are graded if given enough time.

The interplay between these three external forcing processes results in very complex behaviour of the river system. Neither their individual impact on the system, nor their relative importance or the results of their interaction are clearly understood. These processes occur on time scales of thousands to millions of years, and thus river-delta architecture can only be

studied on the basis of the final product, the stratigraphy. That makes a correct interpretation and understanding of its genesis very difficult. Additionally, Quaternary climate conditions, in which the most recent and best preserved river systems formed, are not representative of the past. For example, Quaternary sea-level fluctuations have been of a greater magnitude and frequency than sea-level fluctuations in ice-age-free periods. Finally, equifinality (Schumm, 1998), the notion that (combinations of) different processes can produce a similar result, introduces further uncertainty in the interpretation of stratigraphy.

Current conceptual models explain the development of sedimentary systems on the basis of a limited number of forcing processes that exert simple control on the system. A well known and successful example is the sequence-stratigraphy concept (Vail et al., 1977), which regards (the rate of) eustatic sea-level change as the main control on the stratigraphic architecture of river-shelf-basin systems along passive margins. The elegance of the concept is, no doubt, its simplicity. In some systems it certainly offers a plausible explanation for the generation of the observed stratigraphic architecture. However, the strong focus on sea-level change probably is an oversimplification, and the lack of a successful extension into the continental domain is a major limitation of the concept. The broader concept of genetic stratigraphy, proposed by Galloway (1989), aims to divide stratigraphy into a systematic framework of sequences created in depositional episodes and bounded by hiatuses, independent of the processes responsible for the generation of these sequences. Therefore it can be applied to any sedimentary system, which makes this approach very useful. The concept focuses on the description of stratigraphic successions and not on explanations of the creation of the sequences, however. Additional concepts for the impact of individual forcing processes as well as their relative importance and interaction are required for these explanations. Before such concepts can be developed, more insight into the impact of the different external forcing processes - sea-level change, climate change, and tectonics – must be gained.

The aim of the analogue-modelling study presented in this thesis is to assess the impact of climate (i.e., discharge and sediment flux) on the development of the stratigraphic architecture of a river system in a passive margin setting, both in isolation and combined with sea-level fluctuations. More specifically, to:

- evaluate the relative importance of the impact of climate and sea-level change on the development of the stratigraphic architecture of river systems and their associated deposits on the continental shelf in a passive margin setting,
- to determine the impact of changes in discharge and of changes in sediment flux on the fluvial system and on the sediment yield at the mouth of the river system,
- to find a way to reconstruct, or at least to constrain, the development of a fluvial system by the analysis of its stratigraphic architecture, and
- to demonstrate the applicability of the results to natural systems.

Approach

We have chosen for an analogue modelling approach. The complexity of the fluvial system does not allow easy reconstruction or quantification of the processes controlling the generation of stratigraphy through the examination of real-world examples. Numerical and physical experiments offer a way to resolve some of this complexity. Analogue, i.e., physical, models can best be considered as models of miniature landscapes that provide important clues to

parameter sensitivity, which cannot be obtained from a numerical model. Analogue models do not model the actual processes in a river system, but they reproduce the long-term average effects and products of these processes. This top-down approach, in which the first-order behaviour of the system is studied, greatly reduces the complexity of the results. It provides a first-order framework, within which more detailed answers can be sought. Studies by Wood et al. (1993), Koss et al. (1994), Heller et al. (2001) and Van Heijst et al. (2001) are examples of successful application of the analogue modelling approach.

Summary

In **chapter 2** the interaction and relative impact of sea-level fluctuations and different discharge and sediment flux scenarios is investigated. Results obtained by Van Heijst and Postma (2001) on the impact of sea-level fluctuations are compared with results of experiments with constant discharge and sediment flux combined with a single sea-level change scenario. The results indicate that sea-level fluctuations are the dominant control on the large-scale stratigraphic architecture of the system, i.e., on the location of the depocentre and the timing of erosion episodes. The discharge and sediment flux in the river system, which are controlled by climate and tectonics (in the case of sediment flux) in the catchment area, have a secondary effect. They do not greatly influence the large-scale stratigraphic architecture of the system, but they do significantly affect the smaller scale stratigraphic architecture: they can cause a decrease or increase of the rate and extent of erosion, and they affect the relative size of systems tracts.

Chapter 3 discusses the impact of pulses in discharge and sediment flux on the yield of the river system. The experiments described in this chapter reveal a fundamental difference between the fluvial response to changes in water discharge and changes in sediment flux. The response of the yield at the river mouth to changes in discharge is rapid and has a relatively high magnitude, while the response to changes in sediment flux is slower and weaker. This behaviour causes the river system to act as a buffer for rapid changes in sediment influx. The consequence of this buffering is that the small-scale stratigraphy at the river mouth is controlled mainly by changes in discharge, whereas the large-scale stratigraphy at the river mouth is controlled by changes in sediment flux (and sea-level fluctuations, if present). Thus, high-resolution stratigraphy tells much about changes in discharge, i.e., climate, and low-resolution stratigraphy tells much about long-term changes in sediment influx, i.e., tectonic activity. The mass accumulation history at the mouth of a river can be used, in combination with the large-scale stratigraphic architecture of the fluvial domain, to constrain paleo-discharge and paleo-sediment flux. The important point of chapter 3 is that it is crucial to distinguish between changes in discharge and changes in sediment flux in the context of climate change.

Chapter 4 describes the complex response of a (model) fluvial system to a rapid increase in discharge. This behaviour may explain the creation of a certain type of stratigraphic architecture, called terrace intersection, which closely resembles the stratigraphic architecture resulting from the experiment described in this chapter. An example of this type of architecture is found in the Rhine River. Explaining the origin of such stratigraphy in terms of sea-level and climate change is difficult. The behaviour of the experiment offers a realistic explanation of the architecture of the lower Rhine River: an increase in water discharge while the system is already in a state of disequilibrium can cause rapid, simultaneous upstream erosion and downstream deposition, thereby creating a stratigraphic pattern that closely resembles the

terrace intersection geometry along the Rhine River. The most important conclusion of this chapter is that even the simplest of changes in external forcing processes in a very simple system (our model) can produce a complex response. In this particular case an increase in discharge does not simply cause a decrease in the gradient of the river valley, as might be expected, it also creates the more complicated terrace intersection geometry.

In **chapter 5** a new way of processing and presenting the data obtained from our experiments is explained. The main type of data generated in our experiments consists of series of sequential digital elevation models (DEMs), i.e., sets of surface elevation data on a fixed rectangular grid. By subtracting subsequent DEMs, deposition and erosion patterns in the period between the acquisition of the two DEMs can be obtained. This is the way in which such data are usually used. A series of DEMs, however, is the equivalent of a series of isochronous surfaces, i.e., timelines in three dimensions. Thus, all necessary information is available to generate a synthetic three-dimensional stratigraphy through model time and to present this information as, for example, geological maps, geological sections and Wheeler diagrams. Chapter 5 describes the logic behind the software that was made to generate synthetic stratigraphy from our model results. The ability to make synthetic stratigraphy is a significant advance in the amount, quality and presentation of information obtained from our experiments.

Chapter 2

Impact of discharge, sediment flux and sea-level change on the stratigraphic architecture of river-delta-shelf systems

G. Postma and A.P.H. van den Berg van Saparoea

Abstract

Variation in sediment transport and temporary sediment storage at large spatial and temporal scales is governed by inherited relief and by the interaction between climate change (water discharge and sediment yield), eustatic sea-level change and tectonics. These processes influence the character of sedimentary successions, and are difficult to reconstruct from stratigraphy alone. Physical modelling can help by allowing observation and quantification of processes that generate model stratigraphy. Sediment transport in the model setup shows diffusive behaviour. Non-dimensionalizing the relevant physical parameters that underlie model stratigraphy allows a comparison with real-world examples. The effect of (changes in) the forcing parameters (discharge, sediment yield, sea-level change and consequent shoreline position) on a loose bed of sand in a set of experiments is measured by laser. The resulting high-resolution digital elevation maps are transformed into both geological maps, profiles and Wheeler diagrams that allow detailed reconstruction of sediment flux and routing, storage time, and headward erosion rates. All raw data are stored in the Pangaea database, and are publicly available. A synthesis of all experimental results obtained over the last ten years has resulted in a first-order prediction of sediment flux that is induced solely by sea-level change. The flux changes with relaxation time (response time) of the system, transport efficiency of the river system (in terms of slope gradient), and the amount that sea level drops below the shelf edge (change in slope gradient); all variables are dimensionless. The results are presented as templates covering systematic trends in the effects of the dimensionless parameters on stratigraphic architecture, which allow assessment of the impact of sea-level change on sediment flux relative to the other forcing parameters.

Introduction

Reconstructions of cause-and-effect relationships in basin fills are usually inferred on the basis of deductive reasoning, since there is no direct record of the basin-fill history. Interpretations are qualitative and speculate about the way in which tectonic, eustatic sea-level change and sediment supply mechanisms have influenced the development of accommodation space and sediment supply. This qualitative approach logically implies many uncertainties. The various combinations of variables that can produce sedimentary cycles prohibits detailed reconstructions of the precise forcing mechanisms. A large number of factors, many of which are linked, may contribute to the stratigraphic product, and likely more than anywhere else the notion 'equifinality' is applicable to stratigraphic successions. This has provoked modellers

to quantitatively investigate stratigraphic models by constraining input parameters as sea-level change, tectonics, discharge, sediment flux and grain size (cf. Burgess & Allen, 1996; Kooi & Beaumont, 1996; Burgess & Hovius, 1998, Meijer, 2002).

One important and, as yet, underutilised tool are physical experiments on a sedimentary-systems scale. The obvious advantage of a physical experiment on a systems scale is that one can observe from start to end how systems are built up, and how they evolve under various conditions of imposed allocyclic forcing (e.g. Wood et al. 1993; Koss et al. 1994; Milana, 1998; Paola, 2000; Van Heijst et al. 2001; Van Heijst & Postma, 2001). The disadvantage of physical models on a landscape scale is that there is no commonly accepted scaling strategy, so that the applicability of the results to real-world systems is at best by analogue (e.g. Peackall et al., 1996). Conventional Froude scaling fails for geological-scale sediment transport and alternatives have, not yet, been investigated to the full extent. Paola (2000) discussed this problem, and Van Heijst et al. (2001) proposed a scaling strategy based on the diffusive behaviour of long-term sediment transport (cf. Begin, 1988; Paola et al., 1992).

The first objective of this paper is to address the progress and the outstanding problems in scaling long-term, geological-scale sediment transport. The second objective is to synthesize available data produced over the last ten years by various Utrecht workers and to create a template for flux induced by sea-level change. Sea-level oscillations in the sequence-stratigraphy concept are seen by many as the important independent variable controlling the stratigraphic architecture of sedimentary systems. Changes in relative sea level have a direct effect on accommodation space in the coastal realm and control, together with sediment supply, the large-scale architecture of delta and shelf systems on various time scales (Curray, 1964; Posamentier & Vail, 1988; Von Wagoner et al. 1990). The third objective is to investigate the applicability of the experimental results to real-world systems. We do this using the well studied source-sink example of the Gulf of Mexico, the Colorado River shelf system in Texas.

Approach

Basin-fill architecture is controlled by the initial topography and by the ratio of the rate of sediment supply and the rate of change in accommodation space (e.g. Curray, 1964; Posamentier & Vail, 1988). Since the rate of sediment supply at any point is the sum of what is produced and what is cannibalized upstream, it is important to consider the behaviour of the entire source-to-sink system when studying causality in stratigraphy. This will reveal, for instance, the consequences of local and temporal storage of sediment in the river valley and on the shelf. We approached this by modelling an entire source-sink system. The drainage system was represented by a sediment feeder, a fluvial valley system or transfer zone, where sediment can be cannibalised and temporarily stored in a rectangular duct, and the basin by a table covered with sediment that can act as a sink for sediment (Fig. 2.1). The basic shape and facies belts of the river-delta-shelf system in the flume and its evolution are similar to that of many common real-world systems, where river gradient is steeper than the coastal plain and shelf gradient. In particular, it represents the well investigated Colorado River shelf system in Texas, which we used as prototype before (Van Heijst et al., 2001).

Preparations for each experiment included the levelling of the sand according to a fixed initial topography (cf. Van Heijst & Postma, 2001). Each experiment started at sea-level highstand with a 15 hour run to establish a dynamic equilibrium stream profile as the initial condition.

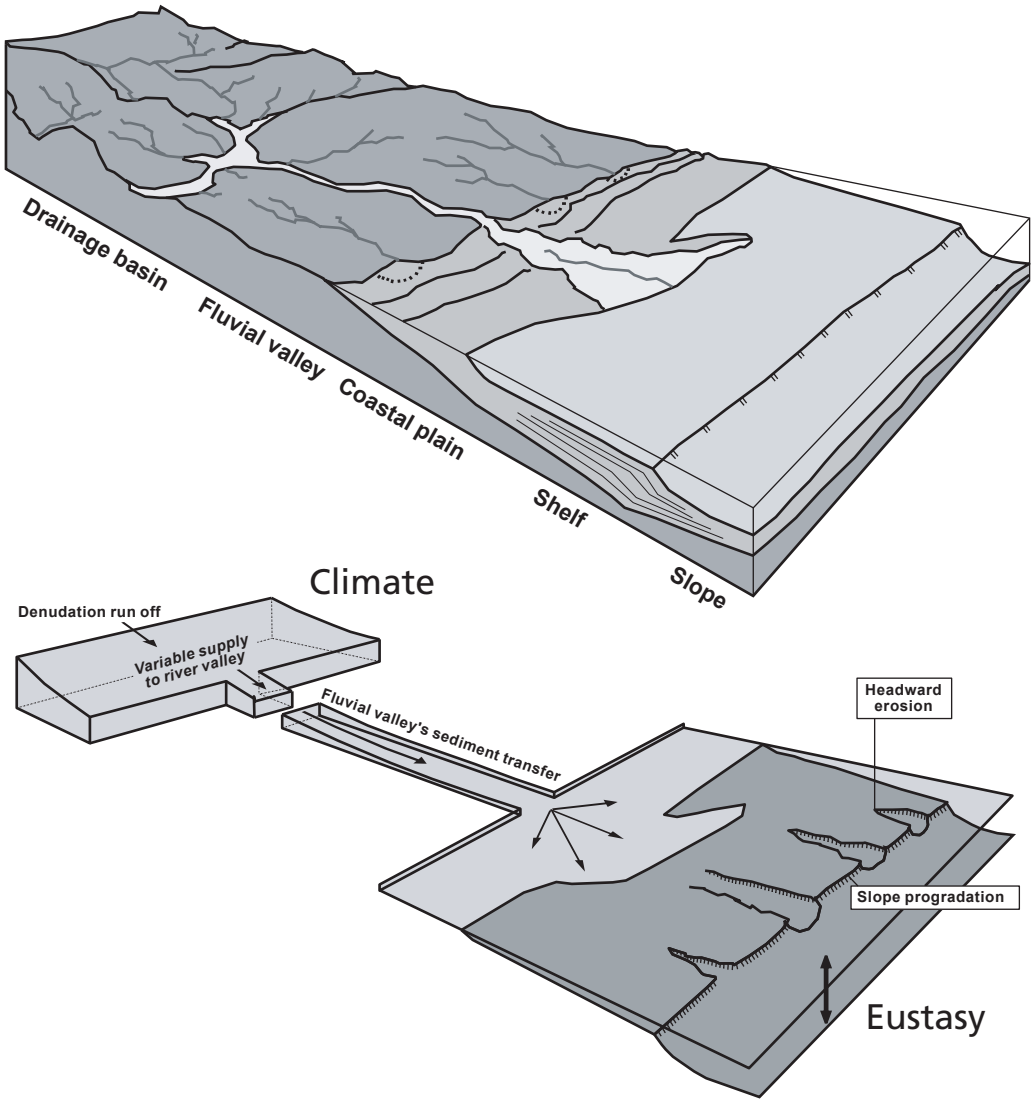

Figure 2.1 Real-world source – transfer – basin system simulated in our experiment. The dimensions of the setup are 3 m x 3.4 m x 1 m for the depositional basin and 4 m x 0.11 m x 0.5 m for the fluvial valley. A water tap with flow meter provides discharge, and a sediment feeder with adjustable conveyor-belt speed controls the sediment supply. Both are located at the upstream end of the fluvial valley and act as a surrogate for the drainage basin. The applied sediment is unimodal, medium, cohesionless quartz sand (D50 = 240 micron) that is supplied by the feeder and is also used as substrate. (Modified after Van Heijst et al., 2001.)

The sea-level change was imposed by adjustment of the level of overflow in the main tank at ten-minute intervals. Every hour, both discharge and sediment supply were checked, and the stream profile in the fluvial valley was measured by reading the rulers on the valleys' transparent wall. At five-hour intervals the topography in the main tank was measured using the automated bed profiler, for which the tank was drained slowly to avoid disturbance of the sediment. The topography was then measured by using a laser following a 2 cm x-y grid. The laser measurements had a vertical (z axis) precision of 300 microns and the background noise in the z direction was less than 1 mm.

A typical example of the evolution of a modelled system forced only by sea-level change is shown in Figure 2.2. During the early falling stage, the delta continued to aggrade. The shoreline prograded with the falling sea level. Local gradients and irregularities in the topography controlled the places where headward erosion induced by sea-level fall started incising the emerging shelf. The heads of the incisions (canyons) migrated upslope until one of them connected to the fluvial valley. The relative timing of connection of one of the shelf canyons with the fluvial valley has a strong bearing on the final volume of the slope fan and lowstand delta, because it determines the change from aggradation to degradation of the fluvial valley (Van Heijst & Postma, 2001). Overall, these experiments show that 1) the dynamic equilibrium gradient of the river profile, 2) the headward erosion rate (defining the amount of cannibalism) and 3) the relaxation time (the time that the system requires to restore equilibrium) all are important variables, which must be considered in a scaling strategy.

Scaling strategy

A critical question and point of ongoing research is the scaling of sediment transport over time scales of landscape evolution. How should we average catastrophic events of various intensities and frequencies combined with normal conditions? The most important point is that we do not attempt to accurately model sediment transport, but to model sediment preservation, the net result of sediment transport over geologically relevant time scales. Bed-load equations (e.g. Yalin, 1971) do not allow downscaling of spatial dimensions more than

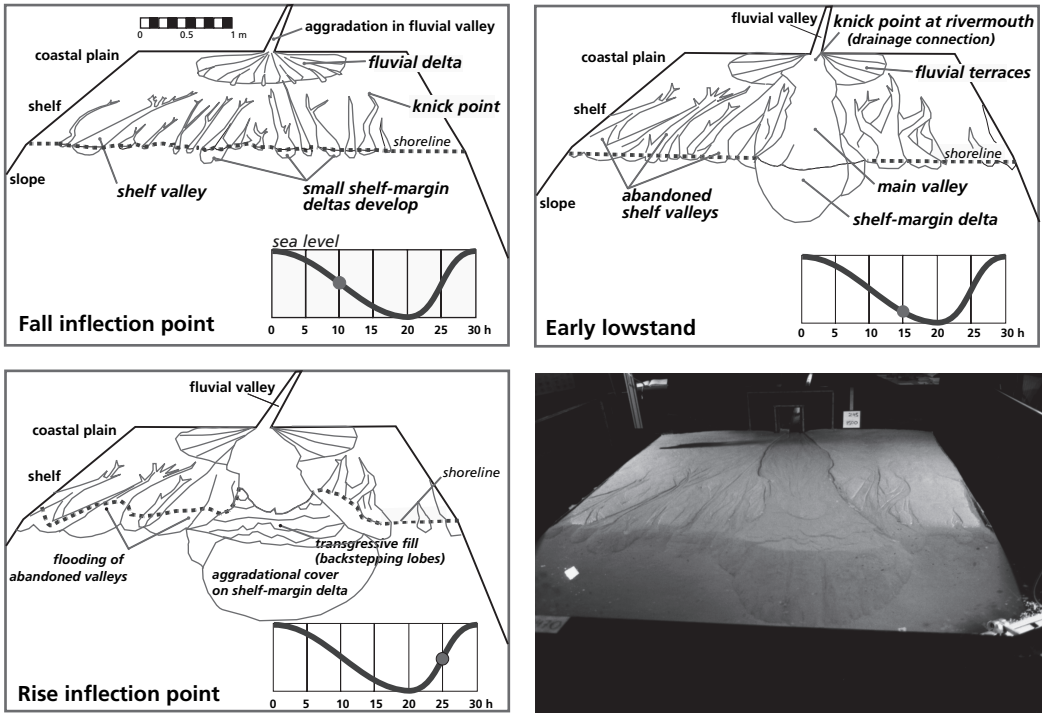

Figure 2.2 Photograph and drawings of experiment 240. The drawings show headward erosion of canyons that incise into the shelf. At about 13 hours, just after the fall inflection point, connection of the canyon with the fluvial valley occurred. At this point all the water and sediment discharge is funneled basinwards directly through the connected valley to the lowstand delta. Headward erosion now starts cannibalizing sediments in the fluvial feeder valley and the drainage basin increasing the yield at the valley outlet system (modified from Van Heijst & Postma, 2001).

1:50 (Peackall et al. 1996; Moreton et al., 2002), rendering the Froude scaling for downscaling entire systems impossible. This is why experiments on river-system scale are often referred to as analogues or analogue experiments. Hooke (1968) used analogue experiments to study evolving landscapes and referred to this scaling strategy as "similarity of process". By keeping the ratio between the size of the system and the time-averaged sediment transport rate in experiment and in real-world similar, spatial dimensions (volumes) can be scaled against time (Van Heijst et al. 2001):

$$Q_s = \frac{\Delta V_{(rw)}}{\Delta T_{(rw)}} = \frac{\Delta V_{(\exp)} \cdot \left(\lambda_x \cdot \lambda_y \cdot \lambda_z\right)}{\Delta T_{(\exp)} \cdot \left(\lambda_t\right)} \qquad \{L^3/T\} \qquad (1)$$

where Q_s is the time-averaged volumetric sediment transport rate (including normal and catastrophic events), ΔV is the displaced sediment volume and ΔT is the time period (normally of the order of 500-1000 years) over which the amount of displaced volume is determined. The scaling factors λ operate on the spatial dimensions (x-y-z) and time (t). In a perfect model, the up-scaled, time-averaged sediment flux observed in the experiment equals the value of the prototype.

Sediment-transport models for long time scales show diffusive behaviour (Begin, 1981, 1988; Andrews & Buckham, 1987; Paola et al., 1992; Kooi & Beaumont, 1996; Martin & Church, 1997; Paola, 2000). Begin et al. (1981) and Begin (1988) showed that channel degradation by base-level lowering closely follows the numerical solution of the simple diffusion equation

$$\frac{\partial <h>}{\partial t} = \frac{\partial}{\partial x} \cdot \left(k \cdot \frac{\partial <h>}{\partial x} \right) \qquad \{m/s\} \qquad (2)$$

where <h> is the average streambed height [m] with respect to origin, x is the horizontal position [m] with respect to origin, t is time [s] and k is the diffusivity constant for unit width [m^2/s]. The discharge variable appears in the diffusivity coefficient when the diffusion equation is derived from first principles (Paola et al., 1992):

$$k = \frac{-8Q \,.\, A\sqrt{c_f}}{C_o(s-1)} \qquad (3)$$

where Q is discharge per unit width [m^2/s], c_f is the drag coefficient (0.025), C_o is sediment concentration of the bed (0.67), and s is specific density, ρ_s/ρ_w (= 2.65). Changes in diffusivity depend on changes in discharge and riverbank erodability. A is a riverbank erodability constant with values of A = 1 for the meandering case and A = 0.15 - 0.4 for the braided case.

When the system is in equilibrium, the gradient of the equilibrium surface can be determined from

$$q = k \frac{\partial \langle <h> \rangle}{\partial x} \qquad (4)$$

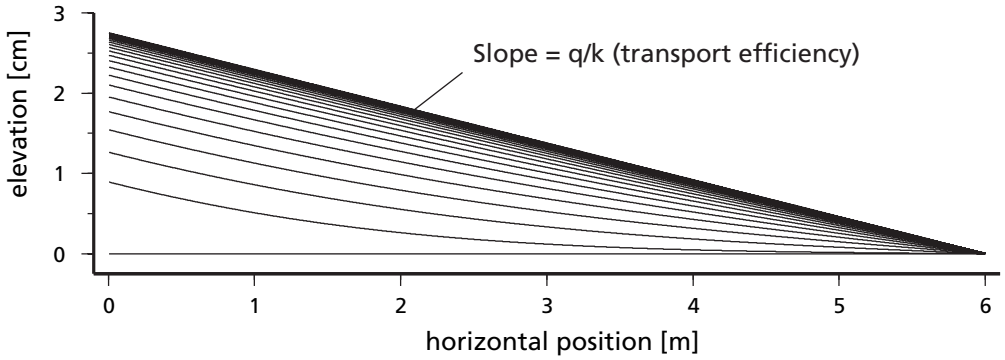

Figure 2.3 Numerical solution of the diffusion equation. The gradients in the solution are compared with sediment aggradation patterns (stratigraphy) in the experiment (cf. Begin, 1988, Paola et al., 1992). The equilibrium gradient is a consequence of transport efficiency, which is defined here as the ratio of sediment input (q) over diffusivity (k). The latter coefficient is directly related to discharge. (Modified from figure by Paul Meijer.)

where q is the sediment flux into the river system (sediment feed). The gradient of the fluvial valley river is dependent on the stream capacity and the available sediment load defined by the ratio q/k. Thus q/k denotes a dynamic equilibrium gradient, which is a measure for the transport efficiency of the system (Fig. 2.3). Very efficient systems have a low gradient and less efficient systems a higher gradient (see below).

The time and length scaling is obtained from non-dimensionless analysis of the diffusion equation as shown by Paola et al. (1992), who gave a first-order approximation of the relaxation time (T_{eq}) of the fluvial system by**:**

$$T_{eq} = \frac{L^2}{k} \qquad \{T\} \tag{5}$$

where L is the basin length. Basins with different length L and/or different values for *k* will have different relaxation times, and thus different response times to imposed changes.

Any allocyclic forcing mechanism can only be determined from the stratal record if its duration is longer than the systems relaxation time. In other words, if the system cannot return to its state of dynamic equilibrium before the next allocyclic change, the allocyclic signal is unlikely to be clearly recognisable is the stratal record. It is thus important to establish the frequency of change relative to the relaxation time of a system. Paola et al. (1992) and Heller & Paola (1992) proposed the dimensionless ratio T/T_{eq}. Van Heijst et al. (2001) referred to the ratio as the Basin Response factor (Br):

$$Br = \frac{T_{(rw)}}{T_{eq(rw)}} = \frac{T_{(\exp)}}{T_{eq(\exp)}} \qquad \{-\} \tag{6}$$

where T is the duration of one period of allocyclic change (e.g. duration of one sea-level cycle) and the response time of the sedimentary system in the real world (rw) and experiment (exp).

For the purpose of geological modelling of sedimentary systems it is important to be able to compare the vertical stacking of depositional environments in model and prototype. This is

done by considering the time-averaged sedimentation rate per unit area (R_s), which is obtained by dividing the time-averaged sediment deposition ($\Delta Q_s \geq 0$) by the depositional area (A):

$$R_s = \frac{\Delta Q_s}{A} \qquad \{L/T\} \qquad (7)$$

Applying the concept of Curray (1964), we use a Basin Fill factor (Bf), a non-dimensional parameter that describes the time-averaged sedimentation rate in relation to the rate of increase in accommodation space:

$$Bf = \frac{R_{s(rw)}}{R_{acc(rw)}} = \frac{R_{s(\exp)}}{R_{acc(\exp)}} \qquad \{-\} \qquad (8)$$

where R_{acc} accounts for the rate of change in accommodation space per unit area for both the fluvial and marine realm in real world (rw) and experiment (exp). Hence, the basin fill factor is a dimensionless parameter that describes progradation, aggradation and retrogradation of sedimentary systems. Note that R_s and R_{acc} should both be time-averaged over the same time span ΔT.

In studying evolutionary trends in sedimentary systems by experiment we thus focus on the volumetric changes per time slice, i.e., time-averaged sediment flux. The sand that we use is merely an isotropic medium, the mass of the grain influencing the value of the diffusivity coefficient k. It is important to realise that we only value the large-scale topographical features that are built over similar time scales as our time average sediment transport (eq. 1). Hence, we look at the scale of canyon and valley formation over time steps of ~6500 years, which are equivalent to the five hours between each two measurements, and not at the scale of individual channel incisions. Thus the scale of observation and measurement in the model is well tailored to the scale where allocyclic forcing mechanisms produce regional bounding (erosional) surfaces and depositional units (stratigraphy).

It must be noted, however, that in applying the above outlined non-dimensional scaling ratios to real world systems there remains much uncertainty in the calculated values, because data on rainfall, valley width and stratigraphy are too poorly known. This is shown below when dealing with the Colorado prototype as an example.

Results

A series of experiments has been conducted to study the behaviour of the system under different frequencies of sea-level change (Fig. 2.4), i.e., different basin-response factors, ranging from 1 to 4, and various transport efficiencies (q/k) (Fig. 2.5). Observations include time-lapse video recordings, photographs and laser scans taken at 5 hour intervals. The laser scans provided Digital Elevation Models (DEMs) of the surface of the model. From the series of DEMs, isopach maps, geological maps and geological profiles were composed to establish the architecture (style) of the deposits in the model (Fig. 2.5). All DEMs are stored in the publicly accessible Pangaea database (www.pangaea.de) in ASCII files containing x, y and z values. The x, y, z data are compatible with almost any relevant software package. We have used Golden Software Surfer for making topographical maps and calculating volumes in isopach maps, and have developed in-house software for generating the syntetic stratigraphy

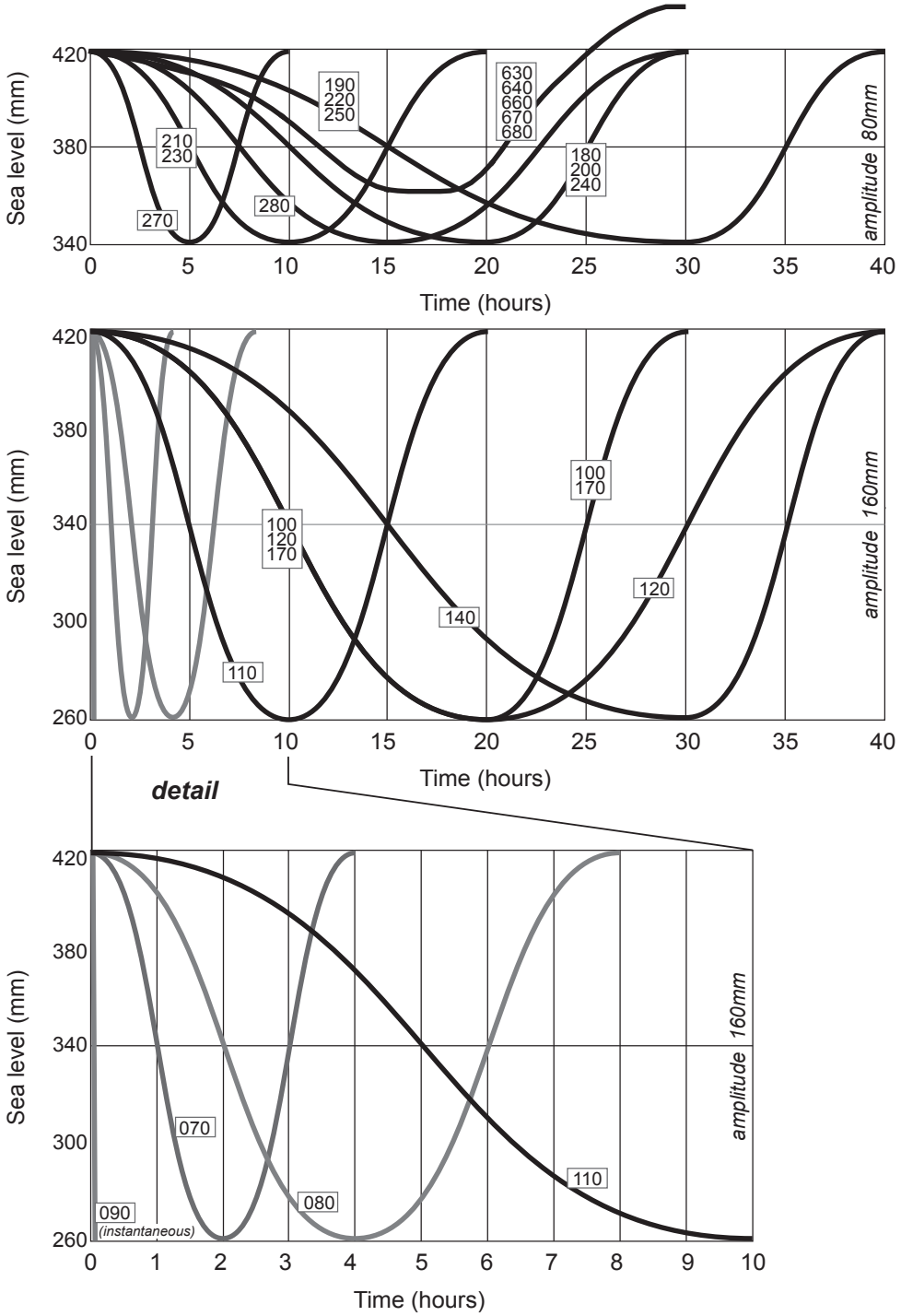

Figure 2.4 Sea-level curves used in the experiments plotted in the template in Figure 2.7. The labels represent experiment numbers.

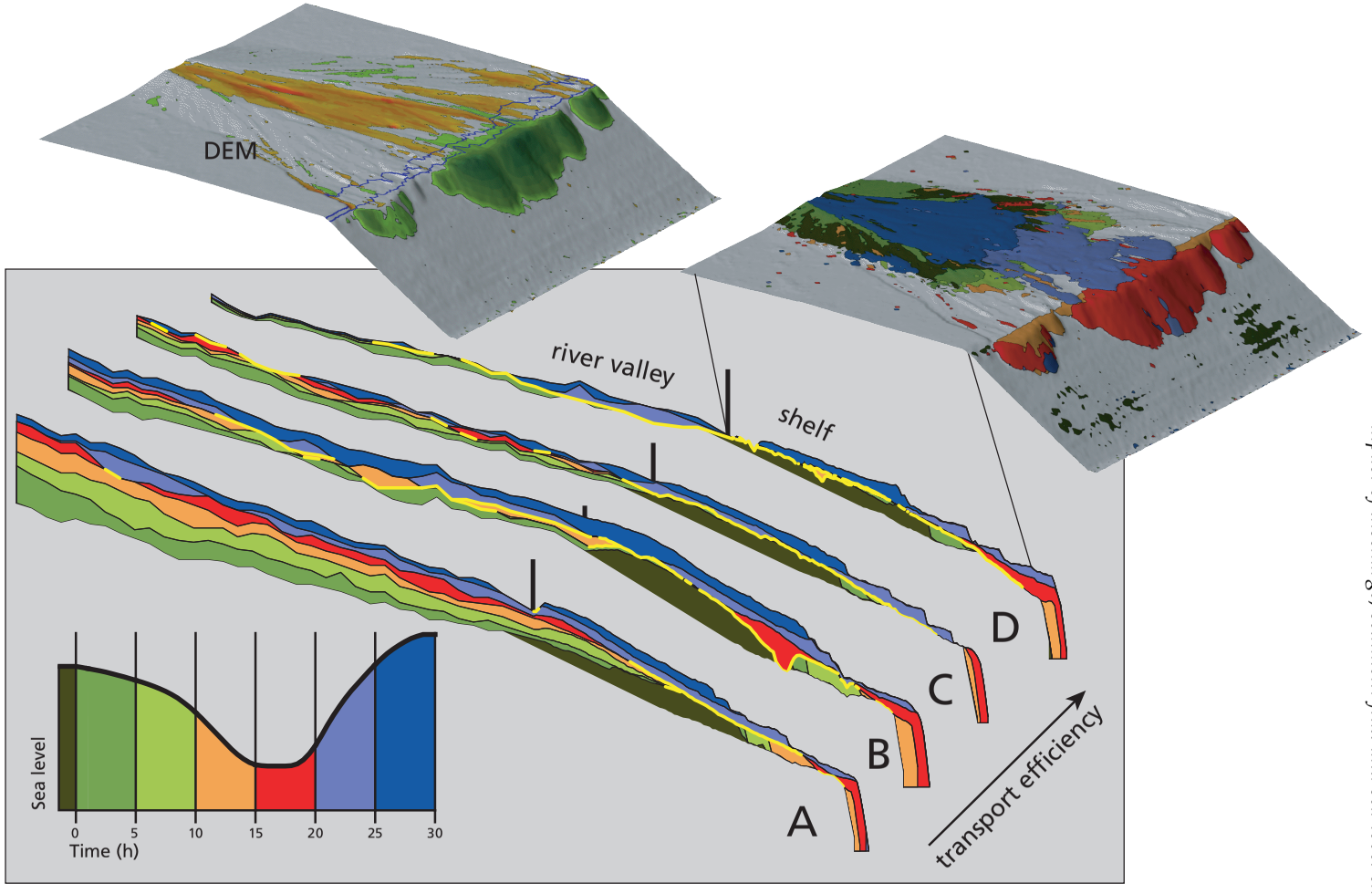

Figure 2.5 Longitudinal profiles of the stratigraphy of four experiments with different transport efficiencies. Other parameters were identical for each of these experiments. The sea-level curve given as inset in profile A was used. The colours of the stratigraphic units in the profiles correspond to the colours of the time slices indicated in the sea-level curve.

from the series of DEMs, which is the basis for the geological maps , geological profiles and Wheeler diagrams.

Examining systems behaviour for various discharges and sediment input, i.e., on transport efficiency q/k, we find a strong relationship between preserved stratigraphy in the fluvial and shelf realms and the transport efficiency. For instance, increasing values for q/k result in decreasing thicknesses (and preservation potential) of the highstand and falling stage systems tracts (Fig. 2.5). Converting the vertical sections to Wheeler diagrams (Fig. 2.6) reveals that the regional importance (length) of the sequence boundary clearly increases with transport efficiency. Furthermore, inefficient systems (high q/k ratio) are characterized by steep slopes, high preservation potential of all systems tracts in the river valley and poorly developed sequence boundaries developed only on the shelf, and we find the opposite for highly efficient systems.

Unfortunately, gradients in the experiments are different from those in the real world: to maintain bed load transport with the grain size and densities used in the experimental set up, steeper slopes are required. It is thus not possible to use q/k directly when comparing the experimental results with the real world. However, it can be used in a semi-quantitative way by referring to the preservation of deposits in the valley as shown by the profiles in Figure 2.5 and Wheeler diagrams in Figure 2.6. As a first approximation, we have distinguished four categories of transport efficiency in our template. Characteristic preservation patterns (architectural styles) are recognised, exemplified by the geological profiles (labelled A-D) in Figure 2.5. Type A is characteristic for high-supply systems, as for instance, is inferred for the Loranç del Munt fan-delta system (Steel et al. 2000). Type D is characteristic for a highly efficient system where the entire valley is flushed during lowstand. Type B and C take intermediate positions. Burgess and Allen (1996) come to very similar conclusions from a numerical modelling study. They found that increased gradients (comparable to our case A) in the fluvial domain go hand in hand with reduced vertical and lateral extent of erosion. The sequence boundary resulting from sea-level lowstand in these high-gradient systems is less extensive than in low-gradient systems under identical forcing parameters. It appears difficult to give real-world examples of each, since real-world data on valley systems have been insufficiently explored as yet.

Checking systems behaviour in response to sea-level change for various frequencies of sea-level fall using the data of Van Heijst & Postma 2001 (Fig. 2.4) and additional unpublished data for constant sediment supply, we find that the rate of cannibalization and the related sediment flux towards the shelf edge increases with increasing amplitude of sea-level change, i.e., the amount of sea-level fall below the shelf edge, and with the basin-response factor (Fig. 2.7). Also, with decreasing basin-response factor the connection of incised valleys with the river valley is delayed, resulting in a more diachronous sequence boundary and thicker transgressive systems tracts, which is also enhanced by the increasing amplitude (in particular increasing rate of fall) of sea-level change.

Figure 2.7 combines the results into a template for sediment flux induced by sea-level change for various scenarios of transport efficiency, frequency of sea-level change (i.e., basin response factor) and amplitude of sea-level change. The template indicates what systematic trends in yield relative to the sea-level curve (thus for systems tracts) can be expected in response to the external parameters investigated in this study: amplitude of sea-level change, transport efficiency and basin response factor (Fig. 2.7). Sediment fluxes are normalised to the sediment input from the catchment. Under equilibrium conditions,

Figure 2.6 Wheeler diagrams (deposition and erosion through time) for profiles A (low transport efficiency) and D (high transport efficiency). The solid lines indicate the final product at the end of an experiment (the equivalent of a Wheeler diagram for natural systems). Dashed lines indicate deposits that have been eroded. Sea-level oscillation is indicated on the left. In the low-efficiency system (A) deposition is continuous nearly everywhere. Erosion is limited to the shelf area and occurs only during sea-level fall. In the high-efficiency system (D) deposition is much more localized and intermittent. Most of the shelf and the whole river valley are subject to erosion, which starts immediately with sea-level fall and continues until late in the transgressive phase.

sediment influx from the catchment matches the yield of the river system, since its profile, and thus the volume of sediment in the river valley, does not change in equilibrium. Any deviation from a yield of 100% in Figure 2.7 is caused by changes in the external forcing parameters. In natural systems the sediment influx from the catchment must be estimated.

The Colorado river-valley–delta–shelf system prototype

The underlying assumption of the template in Figure 2.7 is that external sediment supply remains constant. Thus, variation in sediment flux caused by climate change or tectonics can be assessed on grounds of deviations from the template if other external forcing mechanisms are constant or change in (roughly) the same way as they did in our experiments. We illustrate the application of the template on the basis of the Colorado river-shelf system of Texas (Gulf of Mexico), which has been studied extensively in the last decades (Anderson et al., 2004).

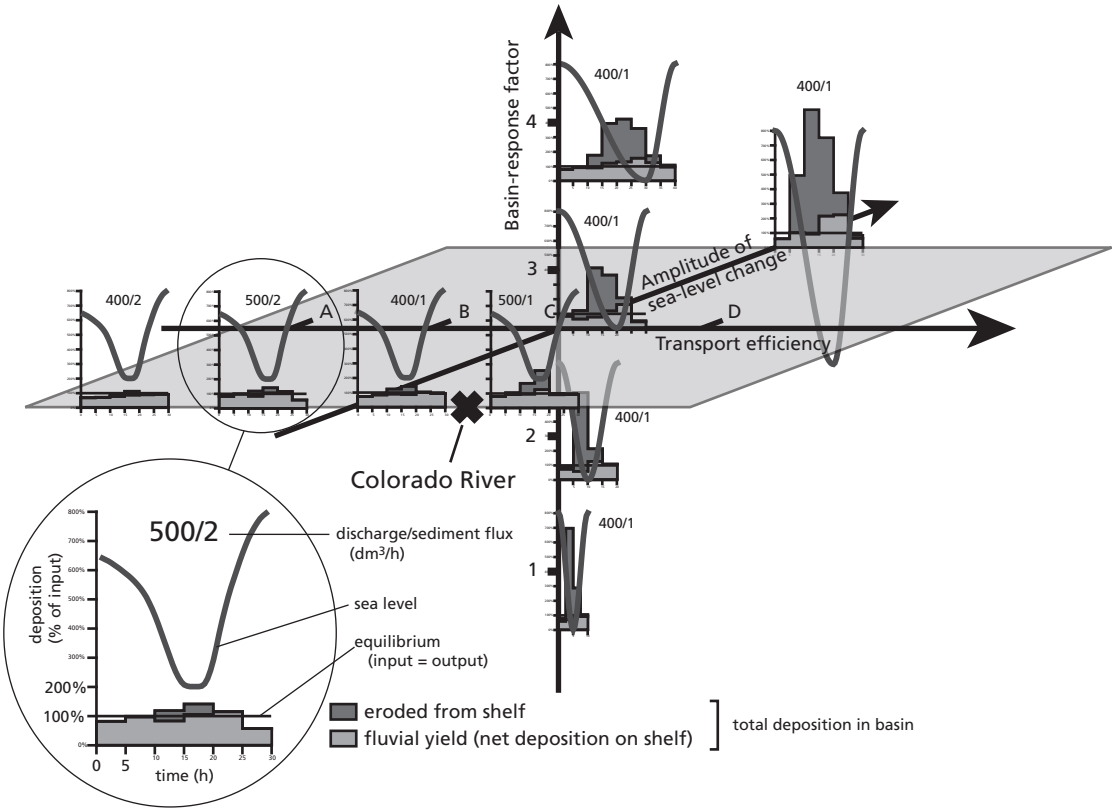

Figure 2.7 Template for sediment flux induced by sea-level change. The sediment flux generated from shelf cannibalization is in dark grey, and the sediment from the fluvial valley is in light grey. Note that the amount of fluvial yield at the valley outlet and the amount of shelf cannibalism follows trends: shelf cannibalism increases with increasing basin-response factor and amplitude of sea-level change (more specifically the degree of sea-level drop below the shelf edge) and transport efficiency. The yield during the transgressive systems tract is enhanced by low basin response values, low transport efficiency, and increasing amplitude of sea-level change, all delaying the timing of connection of shelf canyon and fluvial valley during the transgressive systems tract relative to the sea-level curve (compare with experiment in figure 2.2). Likewise, very wide shelves also promote connection delay.

The Colorado River is fed by a drainage basin of 110.000 km^2 (Fig. 2.8). It is a bed-load dominated system that extends over the shelf during periods of sea-level lowstand feeding shelf and shelf-margin deltas (Anderson *et al*., 1996). The lower Colorado River (downstream of the Balcones escarpment) is characterized by high-gradient fluvial terraces (Fig. 2.8). It was mapped and dated in detail by Blum (1990), Blum & Valastro (1994) and Blum & Price (1998). Deposition during and after the last glacial lowstand (the Eagle Lake Alloformation, 20-14 ka (Blum & Valastro 1994)) has been attributed to a period with high sediment yield that exceeded transport capacity, creating the deposits from which the river could later form fluvial terraces by degradation. If this is true, sediment supply from the drainage basin must have greatly diminished between 14-12 ka BP resulting in abandonment of Eagle Lake Alloformation floodplains and incision of bedrock valleys. Sediment yield from the drainage basin increased again after 5000 BP (Blum & Valastro 1994). Multiple episodes of aggradation, degradation and abandonment of flood plains followed (Columbus Bend Alloformations 1, 2 and 3, respectively). The Colorado River coastal-plain sediments are underlain by a composite basal unconformity that corresponds partly to the lowstand systems tract and in part to the

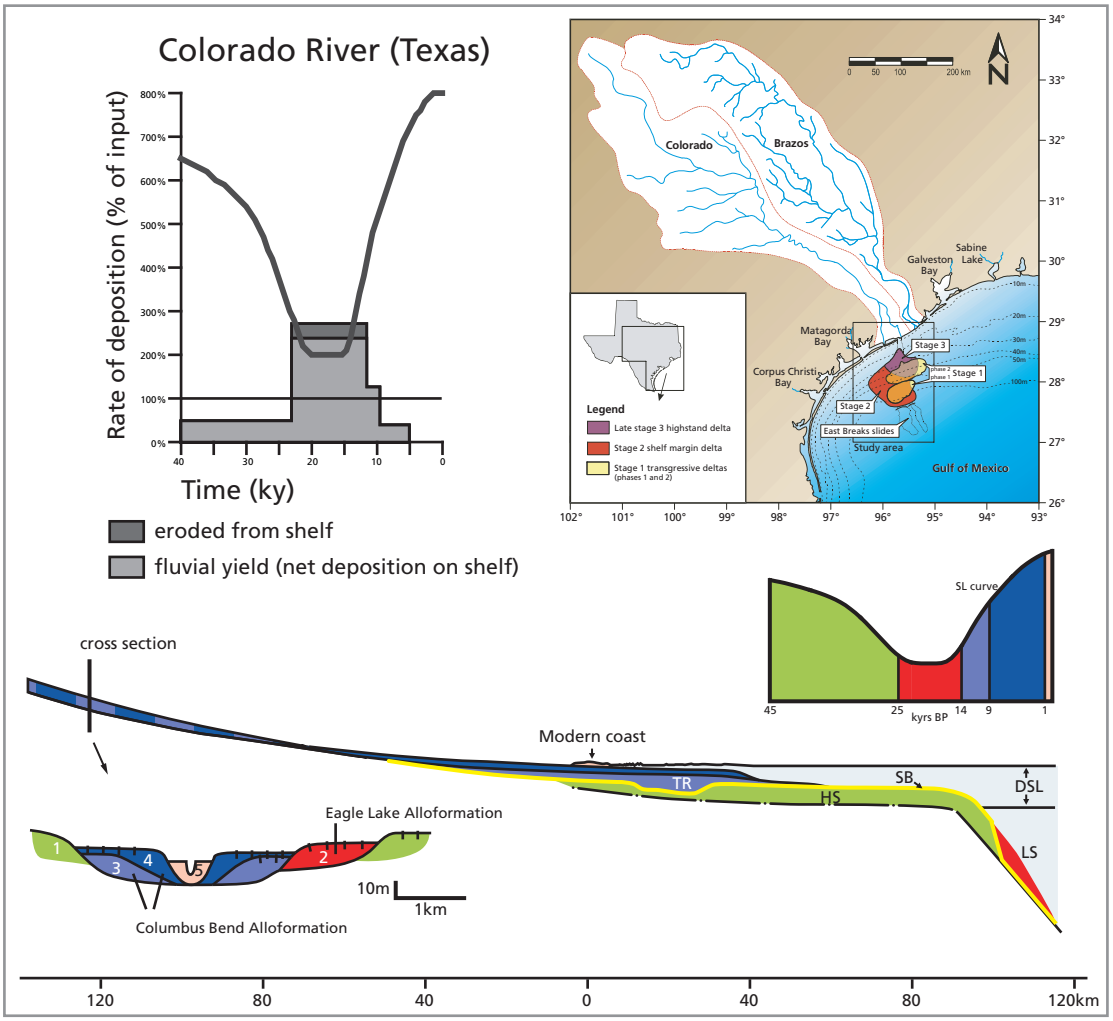

Figure 2.8 Map (Van Heijst et al., 2001), profile (after Blum & Valastro, 1994) and reconstructed sediment flux (based on Blum & Valastro, 1994; Blum & Price, 1998; Van Heijst et al., 2001 and Anderson et al., 2004) of the Colorado River drainage, transfer and shelf basin system. In 2-dimensional view the river profile compares well with profile D in Figure 2.5. Yet, significant preservation of falling stage and lowstand deposits in the form of terraces brings the transport efficiency of the system to a more intermediate position, somewhere in between profiles C and D of fig. 2.5. The light grey in the flux diagram is the reconstructed fluvial yield at the valley outlet and the dark grey the amount added by shelf cannibalism.

transgressive systems tract (Blum & Valastro, 1994). Thus there is a strong diachroneity along the sequence boundary of the Colorado River. The same coastal prism is truncated by an erosive surface (14-11 ka) that merges with the basal unconformity upstream, which shows that the unconformity is strongly time transgressive (Blum & Price, 1998).

The stratigraphy of the Colorado shelf system, created during the last glacial cycle, has also been studied in detail (e.g. Suter & Berryhill, 1985; Berryhill, 1987; Anderson et al., 1996). Gross sediment volume approximations were derived from seismic studies of the shelf (Anderson et al., 1996) and reassessed by Van Heijst et al. (2001), Fig. 2.8). The volume enclosed by the stage-3 and 2 isopach maps is 89 km^3. Subtracting the preserved sand volume of the stage-3

highstand delta (11.5 km^3) from the total volume gives an approximation for the volume of stage 2. This yields a total volume of 77.5 km^3 for the stage-2 deposits on the shelf. The Holocene sea-level rise resulted in two phases of transgressive backstepping of delta lobes on the shelf during stage 1. Phase 1 (11.5 to 9.5 ka) resulted in three fluvially dominated delta lobes with a sand volume of 6.3 km^3. A wave-dominated elongated lobe that contains 4.5 km^3 of sand was formed during phase 2 (9.5 to 5 ka).

Reconstruction of allocyclic forcing in the Colorado River system

To compare the Colorado River system to the template of Figure 2.7 we need to establish the basin response factor of the system and the stratigraphic style to which the Colorado River system corresponds. In addition we need to normalise the sediment flux from the drainage basin.

Determination of the basin response factor (eq. 6) for a dynamically changing system is not straightforward. To calculate the equilibrium time of the system (eq. 5), both the length of the fluvial part of the depositional system, which changes with sea-level change, and the diffusivity of the system, which changes with discharge, need to be established. The shelf width in the Colorado system is about 1/3 of the fluvial depositional system during highstand. As sea-level drops, the width of the shelf increases, leading to an increased response time. Estimations of discharge based on estimations of drainage basin size and rainfall deviate on the order of 20-30%. Using data from Table 2.1, the best estimate of the basin response factor of the Colorado River system is between 0.8 and 2.5.

The stratigraphic style of the Colorado system is intermediate between experiments C and D (figures 2.5, 2.7and 2.8). The falling stage and lowstand deposits in the fluvial valley are

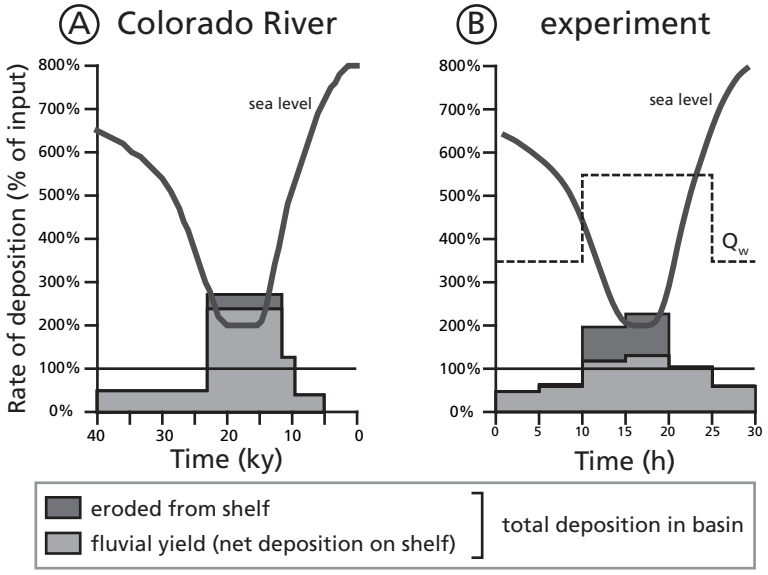

Figure 2.9 A - Time averaged sediment flux from Balcones escarpment to shelf edge (based on Blum & Valastro, 1994, Blum & Price, 1998; Van Heijst et al., 2001; Anderson et al., 2004; climate data from Toomey et al., 1993). **B** - Sediment flux in session 640, where the discharge was temporarily increased coinciding with the lowstand of the Colorado system. The result is an important flux increase that compares well to the reconstructed flux of the Colorado system. See text for further explanation.

poorly preserved. The transgressive deposits are partly preserved. The sequence boundary of the Colorado system can be found up to the catchment area and underlies the Eagle Lake Alloformation (down cutting phase 45-25 ka BP) with a strongly diachronous development (Fig. 2.8). Note that in the longitudinal profile of the Colorado River (Fig. 2.8) the terrace heights are included. These terrace levels converge close to the modern coastline, showing the decrease of the gradient of the river valley during sea-level rise. In our model this reduction of the gradient in the river valley also occurred, but since no terraces are preserved, no remnants are present in the stratigraphy of our experiments (Fig. 2.5).

The reconstructed flux of the Colorado River system can now be compared with the template of Figure 2.7, where we plotted the system for the maximum basin response factor of ~ 2.5 (Table 2.1) to reflect the dry climate setting. During these periods, the sediment influx from the catchment area is assumed to be twice the yield of the river during highstand and early sea-level fall (Fig. 2.9), so keeping this dimensionless value similar to what we generally find in our models. To develop a stratigraphic style intermediate between profiles C and D (Fig. 2.5), the expected flux triggered by the sea-level fall and lowstand should be about 50-100% above its highstand and early fall value as is outlined by the template of Figure 2.7. However, the Colorado system shows a much higher increase. The extra sediment influx must have come from another forcing mechanism, probably climate changing to more humid conditions. Tectonics are likely to be unimportant at these relatively short time scales. On the basis of independent evidence such climate forcing was indeed suggested by Toomey et al. (1993). An extra experiment was done to simulate the increased discharge during stage 2. This shows a much better match with the real-world data (Fig. 2.9B).

Conclusions

Various simple equations for sediment transport over geologically relevant time scales are used by numerical modellers. Many of these depend on slope gradient and on discharge multiplied by a coefficient. None of these equations has been rigorously tested by physical experiment or on the basis of real-world data. Future experimental work in landscape modelling should focus on establishing the best functional relationship for long-term sediment transport in the model, and to test this with real-world examples. Here, a bridge must be built between the classical engineering approach for establishing the physics of sediment transport, valid for short time scales, and the geologist approach, where a need exists for time-averaged sediment transport equations that are relevant for stratigraphical and geological problems (focussing on preservation of sediment instead of the transport itself). The diffusion

Table 2.1 Data used to calculate the equilibrium time of the Colorado River and equivalent data in the model.

	Valley length L (km)	Drainage area (km^2)	Active valley width w (km)	Rainfall (m/yr)	Braided $k = 0.1\ q_w/w$ B-Meandering $k = 0.4\ q_w/w$ (km^2/yr)	$T_{eq} = L^2/k$	T	Br (-)
Colorado River	~350	110 000	4 (humid) 2 (arid)	0.90 0.20	B 2.5 BM 4.4	~49 kyr ~16.5 kyr	40 ky	~0.8 ~2.5
Flume	0.0062	-	0.000011	-		~ 12 h	10 h 40 h	~1 ~4

approach is promising, certainly for base-level induced degradation of landscapes. However, it has not yet been established if the same equation can predict the behaviour resulting from high-frequency climate variability within a fluvial-deltaic system.

Any time-averaged transport equation will open up scaling strategies for modelling landscape evolution on geological timescales in flumes, as shown in this paper by adopting the diffusion equation. An obvious outstanding problem is to verify the value of the equation for real-world prototypes. Values for landscape degradation are for short time scales only (cf. Begin, 1988), while values for sediment transfer over long time scales, caused for instance by climate change, are lacking. Hence, insufficient data are available to verify relaxation (response) times of real-world systems (see further discussion by Castelltort & Van den Driessche, 2003) and to establish reliable Basin Response factors.

The gradient of a natural system depends on the discharge per unit width, sediment input and grain size. Both discharge and grain size are included in the diffusion coefficient, the latter in the form of the drag coefficient. Low discharge and large grains will decrease k (see equation 3), which will increase q/k and the rivers equilibrium gradient. The amount of preservation in the river valley depends on the supply rate that causes progradation of the delta system and thus aggradation in the fluvial system as well. Defining stratigraphic styles (Fig. 2.5), which are easily established from both model and prototype, and reflect the transport efficiency of the system, eliminates the need for a direct functional relationship between the transport efficiency of the model and that of the prototype.

The amount of sea-level induced sediment transport can be estimated if the rough dimensions of the entire source-sink system and the amplitude and frequency of sea-level change are known. This means that the contribution of climate change to sediment transport and stratigraphy can be roughly estimated if a well-dated stratigraphy of the whole system is available. Thus, there is a great need for well-integrated source to sink databases that include changes in slope gradients of river systems and isopach maps of a resolution on the order of 1000's years. The Colorado system is in our opinion one of the best examples to date.

Acknowledgements

We are indebted to Max van Heijst for generating a well-organised database during his PhD research (1996-2000), which was financed by Shell Research, Rijswijk, The Netherlands. The database set up in Pangaea was complemented with later work by the junior author. Without our technicians Tony van der GonNetcher, Hans Bliek and Paul Anten experimental data would not have been generated at all. The manuscript benefited from the critical readings of Poppe L. de Boer and reviewers Juan Pablo Milana and Peter M. Burgess.

Chapter 3

Control of climate change on the yield of river systems

A.P.H. van den Berg van Saparoea and G. Postma

Abstract

Climate and tectonics determine the amount of discharge and sediment delivery to rivers. They also affect the temporary storage of sediment, because gradients of valley floors are adjusted to the amount of bedload and the amount of discharge, and thus control the delivery of sediment to the coast. Can the sediment accumulation history on the coastal plain and shelf help to reconstruct the history of discharge and sediment flux that produced it? Results from both field studies and model studies seem ambiguous and contradictory in that convincing evidence is presented against as well as in favour of distinct, correlatable, climate induced signals in the stratigraphy at river mouths. We have studied the effects of pulses of discharge and sediment influx on the gradient of the river-valley system on different time scales by analogue modeling experiments. Discharge and sediment load were increased and decreased independently and the impact of these changes on the valley gradient and on the sediment flux at the valley mouth were measured. Changes in discharge as well as sediment flux into the system cause predictable increases and decreases in the gradient of the valley floor. However, fundamental differences between the response of the sediment flux at the river mouth to changes in discharge and to changes in sediment flux, and differences between the total mass accumulation history in response to changes in discharge and sediment flux emerge. The first fundamental difference between the response to change of discharge and the response to change of sediment input is the total sediment budget at the valley outlet. The second fundamental difference is that the gradient of the valley floor is positively correlated with sediment influx, and negatively with discharge (Mackin, 1948). Hence, by establishing the total sediment flux history at the valley outlet in combination with a reconstruction of gradients in the river valley (e.g. through reconstruction of terraces) constraints can be put on discharge and sediment flux through time. The third difference is that the response to changes of discharge is very rapid, while the response to sediment flux changes is much slower. Combined with the difference in impact on sediment flux at the outlet of the river system, this causes the small-scale stratigraphy at the river mouth to be controlled by high-frequency changes in discharge and the large-scale stratigraphy at the river mouth to be controlled by low frequency changes in sediment flux.

Introduction

Sea-level, climate and tectonics are considered the primary controls on the stratigraphy of continental margins, both in the fluvial and marine domain. A lot of emphasis has been put on the impact of sea-level fluctuations by the Exxon group (Jervey, 1988; Posamentier et al.,

1988; Posamentier and Vail, 1988; Vail et al., 1977). In shallow-marine, coastal and basin-margin environments, sea-level change indeed is very important, since in these environments sea-level directly controls the creation and destruction of accommodation space, particularly in ice-house conditions, when the frequency and amplitude of sea-level fluctuations are high. However, stratigraphy is the result of not just accommodation space but also of sediment delivery (Schlager, 1993) and processes that control the sediment yield from the river system must also be taken into account (Shanley and McCabe, 1994). Tectonics and climate play an important role in determining the amount of denudation and delivery of sediment to the basin, as well as affecting temporary storage of sediment in the river system. A good understanding of these processes, and the resulting variation in sediment yield at the river mouth is essential for a realistic interpretation of the stratigraphy of both the terrestrial and the marine parts of the system.

Information on fluvial response to climate change and sediment delivery to deltas obtained from both natural systems and model studies seems ambiguous. Metivier and Gaudemer (1999), for example, suggest that the average sediment output of the large rivers of Asia must have been more or less constant over the last 2 million years, despite strong tectonic activity in the hinterland and strong climate fluctuations in the region. This is supported by, for example, Castelltort and Van Den Driessche (2003) who propose that the disturbances caused by high-frequency (20 to 100 ka) climate fluctuations are attenuated to such an extent during transfer through the river system that no correlatable fluctuations in yield can be observed at the river mouth. Goodbred (2003), on the other hand, shows convincingly that the sediment delivery by the Ganges River (one of the rivers discussed by Metivier and Gaudemer, 1999) responds rapidly to 20 ky climate fluctuations without any evidence for attenuation of the signal. Although these studies all investigate response to climate change, there is a striking and crucial difference between them: studies suggesting that the system attenuates the climate signal focus on climate change causing changes in denudation rate in the catchment area (e.g. Castelltort and Van Den Driessche, 2003) and studies suggesting a direct response focus on discharge pulses (e.g. Goodbred, 2003). Could it be that the response of the fluvial system to a change in discharge differs from the response to a change in sediment input?

Changes in water discharge and sediment load cause changes in the profile of a river (Mackin, 1948). An increase in sediment load and/or a decrease in discharge cause the equilibrium slope of the profile to increase and a decrease in sediment load and/or an increase in discharge have the reverse effect (i.e., a lower gradient) (Mackin, 1948). The actual slope of the river system will change to attain this equilibrium gradient. These dynamics cause variations in the accommodation space in the river system (e.g. Quirk, 1996), which results in changes in the total volume of sediment stored in the river valley. The sediment flux from the valley outlet must reflect these changes: a decreasing gradient should cause an increase in sediment flux at the mouth of the river and an increasing gradient should cause a decrease in sediment flux at the mouth of the river. This introduces a complication: an increased sediment flux from the catchment area into the river causes the equilibrium gradient to become steeper, but at the same time this increase in gradient (i.e., accommodation space) results in deposition in the river valley, which decreases the total amount of sediment transported by the river. The opposite happens after a decrease in sediment influx. How is the interaction of these processes reflected in the sediment flux at the mouth of the river? And how does the sediment output of the river differ in the experiments with a change in discharge and constant sediment input?

In natural systems, the complex interaction of forcing processes, the unavailability of direct data on paleo-discharge and paleo-sediment-flux, and a limited amount of field data present an obstacle to answer this question. A model does not have these disadvantages. The effects of different forcing processes can be studied separately and in detail, revealing the first-order behaviour of the system and thus providing a first step in solving the problem.

In this paper we present the results of an analogue modelling study of the response of the profile of a fluvial system to both changes in discharge and sediment flux at different time scales and the impact of these changes on the sediment flux at the outlet of the river valley and the total yield of the river system. We reveal fundamental differences between the impact of changes in discharge and changes in sediment flux into the system on the total yield of the river and the sediment flux at its mouth, even though the response of the river system to both of these processes consists primarily of opposite gradient changes. Furthermore, we show that a careful analysis of the total sediment yield of a river through time can be used, in combination with the stratigraphic architecture of the river system, to put constraints on paleo-discharge and paleo–sediment flux of the river and be used to interpret the stratigraphy of the entire system, from source to sink.

Scaling

Because the spatial and temporal dimensions of the systems we study are too large for conventional Froude scaling (e.g. Peackall et al., 1996) we have applied the scaling approach used by van Heijst et al. (2001) and Postma and Van den Berg van Saparoea (chapter 2). In landscape-sized physical models, changes in topography due to climate or sea-level change are measured in terms of time-averaged sediment transport. Scaling of this time-averaged sediment transport is achieved essentially by assuming purely diffusive behaviour in long-term sediment transport. This gives the possibility to scale the response of the model system (which is the focus of study here) to the equilibrium time (T_{eq}) of the natural prototype. The equilibrium time of a system is defined as the time that is needed for the system to regain its equilibrium profile from the moment that it is disturbed by external forcing processes. A first order approximation of the equilibrium time of a system is given by $T_{eq} = L^2 / k$, where L^2 is the length of the system (drainage basin or deposition area) and k is the sediment diffusivity of the system (Paola et al., 1992). k depends on a number of characteristics of the system, the most important of which (in our experiments) is the discharge. A higher discharge results in a higher diffusivity, and a higher sediment transport rate.

Experimental setup and procedure

Scenarios

We chose two sets of scenarios for our study. First we investigated the response of the fluvial system to changes in discharge and sediment flux into the system with all other parameters kept constant and the freedom of response limited to the adjustment of the gradient only (i.e., no progradation of the delta or change of base-level). The second set of scenarios was used to test the importance of changes in discharge relative to the effect of sea-level fluctuation, and to study the interaction between these external forcing processes.

In the first set of experiments (Table 3.1) the setup consisted of only a rectangular duct with an outlet fixed in both elevation and horizontal location. The setup of the model is described below. In these scenarios, A to F, listed in Table 3.1, only a single parameter was changed

Table 3.1 Experimental scenarios. T_{eq} is approximately 12 hours.

Scenario	Description	Duration of perturbation	Setup
A	discharge +43%	**0.5** × T_{eq}	fixed outlet
B	discharge -43%	**0.5** × T_{eq}	fixed outlet
C	discharge -43%	**0.1** × T_{eq}	fixed outlet
D	sediment input +100%	**0.5** × T_{eq}	fixed outlet
E	sediment input -67%	**0.5** × T_{eq}	fixed outlet
F	sediment input -67%	**0.1** × T_{eq}	fixed outlet
G	No perturbation	-	shelf
H	discharge +25%	~ **1.3** × T_{eq}	shelf
I	discharge + 20%	~ **0.8** × T_{eq}	shelf

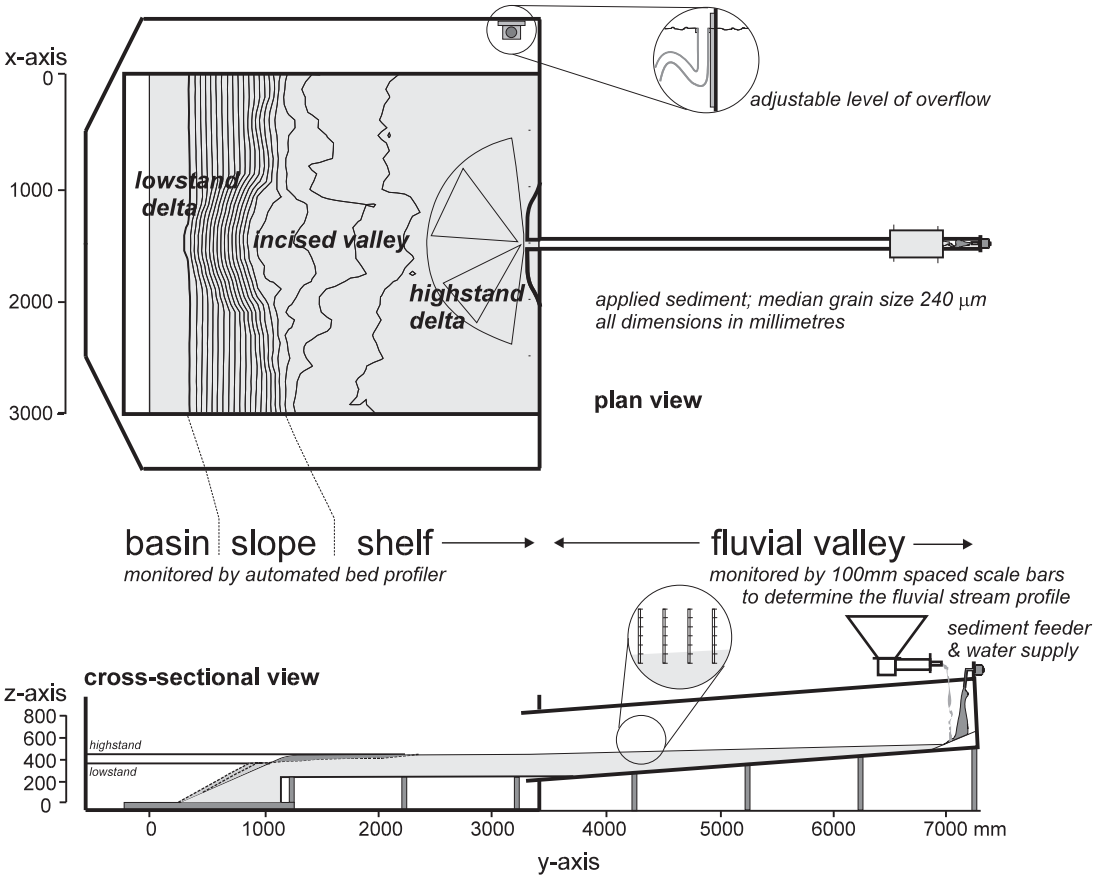

Figure 3.1 Experimental setup in plan view (top) and cross-section (bottom). The catchment area is represented by the sediment feeder and water supply (right side of the figure). The basin, slope and shelf area is monitored with a laser sensor mounted on a computer-controlled automated positioning system. The river valley profile is monitored with rulers attached to one side of the fluvial duct at 10.0 cm intervals.

in each experiment. By definition perturbations lasting longer than T_{eq} produce a shift to equilibrium values for the applied conditions over a period of approximately T_{eq}. Therefore we chose to increase and decrease water discharge and sediment influx over a period of $0.5 \times T_{eq}$ (on the order of T_{eq} of the flume), and secondly to decrease discharge and sediment influx over a period of $0.1 \times T_{eq}$ (significantly shorter than T_{eq} of the flume). Every change started from a state of dynamic equilibrium that was the same for each experiment. The change from the equilibrium state to the disturbed state (i.e., change in discharge or sediment influx) and *vice versa* was instantaneous.

The absolute values chosen for the discharges and sediment fluxes were based on the requirement to keep time-averaged sediment transport rates realistic (see Van Heijst et al., 2001) and the range of slopes allowed by the setup. The upper and lower limits for discharge and sediment influx for the experiments were chosen to be close to the upper and lower limits for discharge and sediment influx of the flume, which have been determined in separate trial runs. The equilibrium state from which the perturbations were started and to which the system recovered after the perturbations was chosen in between these upper and lower limits for discharge and sediment influx. The actual values of the discharge were 200 dm^3/h, 350 dm^3/h and 500 dm^3/h and the values of the sediment flux were 0.50 dm^3/h, 1.50 dm^3/h and 3.0 dm^3/h. Since these absolute values are irrelevant in the further context of this paper, discharge and sediment flux in each experiment are normalised against the average discharge (350 dm^3/h) and sediment flux (1.50 dm^3/h) into the system at the head of the fluvial duct.

The second set of scenarios, in which the impact of discharge fluctuations relative to the impact of sea-level fluctuations and the interaction between these processes was investigated, comprises three experiments carried out with the same setup (Fig. 3.1) used by Van Heijst and Postma (2001) and Postma and Van den Berg van Saparoea (chapter 2). The setup is described in detail below. In all scenarios (G, H and I, Table 3.1), the sea-level curve shown in Figure 3.2 was used. The sea-level curve is based on the curve used by Van Heijst and Postma (2001) (Fig. 3.2), but the amplitude was reduced to better match the maximum depth below the shelf break of the prototype (the Colorado River in Texas). Sediment input was kept relatively low (1.0 dm^3/h) in all scenarios (G, H and I, Table 3.1). A different discharge variation was applied in each scenario in this set. The first scenario, G (Table 3.1), was used as a reference with a fixed discharge of 400 dm^3/h.

The other two scenarios, H and I (Table 3.1), had a variable discharge (Fig. 3.3). In scenario H (Table 3.1 and Fig. 3.3), a discharge pulse was applied with a duration of approximately $1.3 \times T_{eq}$ (15 h). The start is halfway through the base-level fall and the return to the initial discharge is halfway through base-level rise in order to run parallel with the base-level related changes in the system. The timing and shape of the change in discharge in the short scenario (scenario I, Table 3.1 and Fig. 3.3) roughly follows the discharge suggested by Goodbred and Kuehl (2000) for the Ganges River during the Quaternary in response to the intensified monsoon during the Holocene Optimum (e.g. Prins and Postma, 2000; Sirocko et al., 1993). Hence, the increased discharge coincides with the first part of sea-level rise. It should be noted that the equilibrium time of the Ganges system is at least an order of magnitude higher than that of our prototype, the Colorado River in Texas.

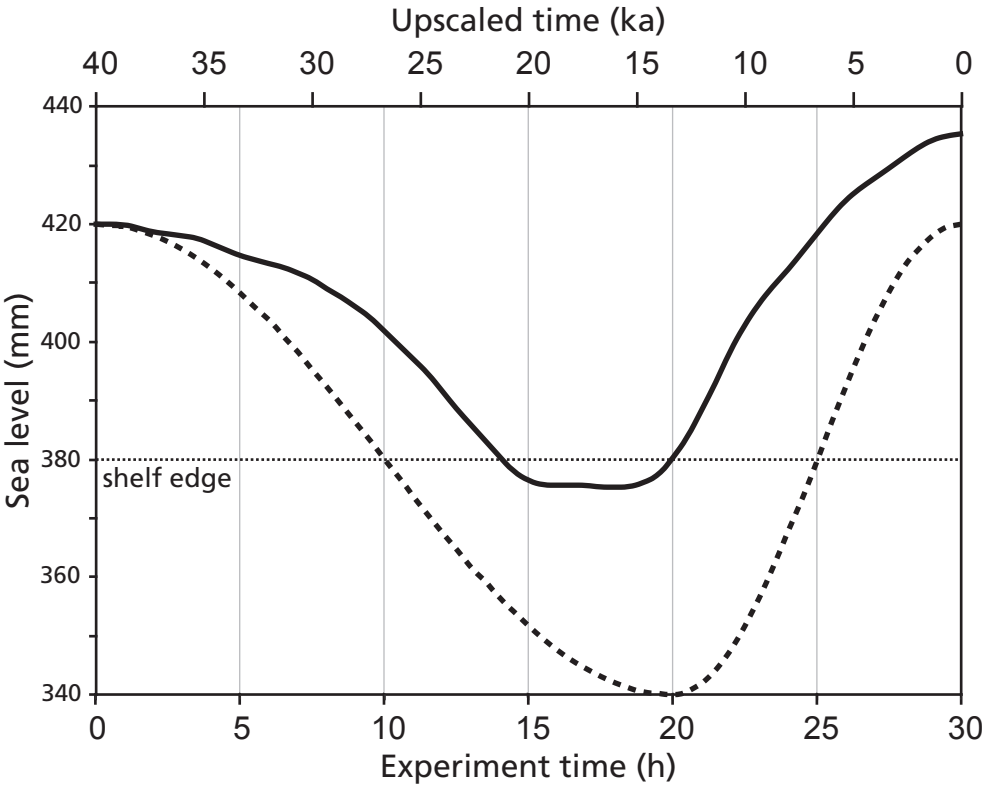

Figure 3.2 Sea-level curve used in scenarios G, H and I. This curve is based on the curve used by Van Heijst et al.(2001), which is indicated by the dashed line. The main difference between the curves is the amplitude. The curve used in our experiments does not drop as far below the shelf edge as the curve used by Van Heijst et al.(2001). This strongly reduces the amount of erosion induced by the sea-level fall and the associated headward erosion rate.

Model setup

The setup of the first set of scenarios (A – F, Table 3.1), used to investigate fluvial response to climate change in isolation from responses to progradation of the system (which creates accommodation space that is (partly) filled and thus reduces sediment flux out of the system) and base-level fluctuations, consisted of a 6.0 m long rectangular duct with an outlet (river mouth) fixed in both elevation and horizontal location.

The second, more complicated setup, used to investigate discharge changes in combination with sea-level fluctuation (scenarios G, H and I, Table 3.1), was identical to that described by (van Heijst et al., 2001) and included a shelf area and basin. The setup (Fig. 3.1) consists of an experimental tank of 4 x 4 x 1 m connected to a rectangular duct (the fluvial valley) of 4 x 0.11 x 0.5 m. Inside the tank a table of 3.0 m x 3.4 m supported a 0.1 m thick cover of sand representing a coastal plain, shelf, slope and basin. The dimensions and initial slopes of the setup are given in Table 3.2.

In both setups the catchment area was represented by the input of water and sediment into the river valley of the system at the top of the fluvial duct. The discharge of the tap was controlled through a flow meter. Sediment was supplied by means of a sediment feeder that delivers a constant sediment volume through a worm gear. The measured deviations

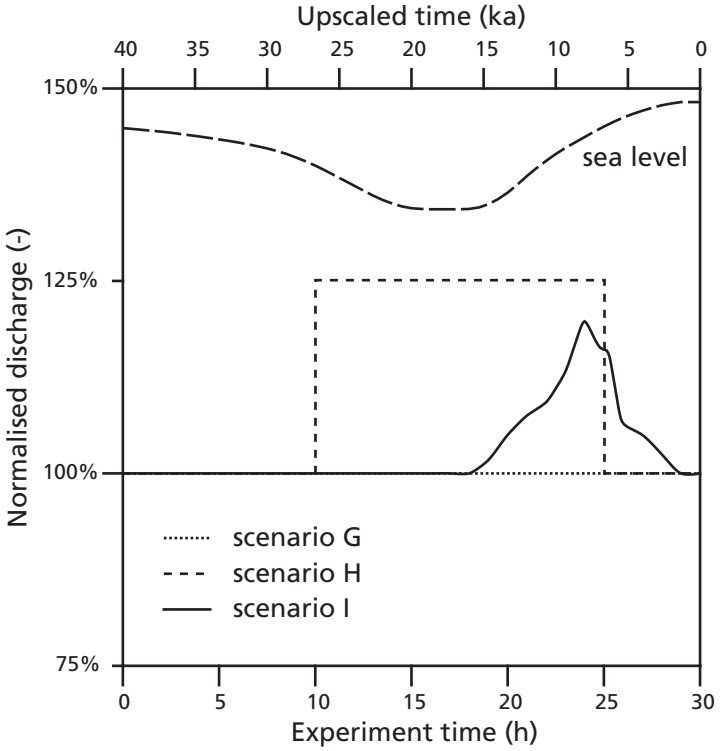

Figure 3.3 Discharge curves used in scenarios G, H and I. Scenario H was the reference scenario, in which no changes were applied. In scenarios H and I the discharge was increased for a relatively long period during sea-level lowstand (scenario H), and a relatively short period during sea-level rise (scenario I).

in sediment delivery by the sediment feeder were less than 1%. We used unimodal medium sand with a median grain diameter of 240 μm as both substrate and as the sediment supplied from the sediment feeder. A precisely adjustable outlet, with a mm scale to measure the water level, controlled the water level (sea-level) in the tank. We recorded the development of the sediment surface in the scenarios with shelf and basin (scenarios G, H and I) by measuring the surface elevation with a laser attached to a computer-controlled positioning system at the ceiling. The elevation of the surface was measured in a 20 x 20 mm grid with a precision of 0.4 mm or better in all three dimensions. In all scenarios the profile of the fluvial valley was measured with rulers attached to the transparent sides of the fluvial duct at 10 cm intervals with a precision of 0.5 mm. The noise in topographical elevation inherent in the model (caused by air trapped in the sediment, temperature fluctuations, etc.) was of the order of 0.5 mm.

Table 3.2 Initial slopes and dimensions of the model.

	Slope (Δy/Δx)	**y-co-ordinates (mm)**	**z-co-ordinates (mm)**
Basin	0	0-300	0-10
Slope & shelf edge	0.42	300-1200	10-385
Shelf	0.03	1200-2400	385-420
Coastal plain	0.02	2400-3400	420-440
Fluvial Valley	0.024 to 0.025	3400-7000	440-530

Procedure

We started each of the experiments with a fixed outlet (labelled scenarios A – F, Table 3.1) by letting the system attain equilibrium by running it for a period in excess of the equilibrium time (approximately 12 hours) of the setup. Equilibrium was taken to be attained when the volume of sediment delivered to the mouth of the flume matched the volume delivered by the sediment feeder without deviations over a period of several hours. This was verified by measuring the changes in the valley profile: when the profile had attained a (dynamic) equilibrium (i.e., the average gradient was stable) the system was considered to be in equilibrium. During the experiments the profile and the sediment flux at the valley mouth were measured at half hour intervals while the system was changing rapidly, and every hour when no significant changes occurred at half hour intervals.

Preparations for the experiments with shelf and basin (scenarios G, H and I) consisted of levelling of the sand according to the fixed initial topography of the setup (Table 3.2). Subsequently we let the experiment run for 15 hours at sea-level highstand to establish a dynamic equilibrium stream profile as uniform starting condition. After this preparation run the experiment was started. Sea-level change was imposed by adjustment of the level of overflow in the main tank at ten minutes intervals. We measured the stream profile in the fluvial valley every hour. At five-hour intervals the topography in the main tank was measured with the automated bed profiler, for which the tank was drained slowly, thereby avoiding disturbances to the sediment bed.

Results

Discharge pulses (scenarios A, B and C)

Impact on valley gradient

Figures 3.4 and 3.5 show that the impact of changes in discharge on the river valley gradient are congruent with the findings of Mackin (1948). In scenario A (Fig. 3.4, Table 3.1) the response of the profile was a uniform decrease of the valley gradient over the whole length of the profile during the period of increased discharge. The decrease of the gradient was induced by a decreased equilibrium gradient, which caused a reduction of accommodation space, leading to erosion. Scenario B (Fig. 3.5, Table 3.1) displayed more complex behaviour. The first order response was as expected: an increase of the gradient in response to the decrease in discharge (the perturbation) followed by a decrease of the gradient in response to the increase in discharge (the return to initial conditions). However, as can be seen in Figure 3.5, the increase of the gradient was not uniform over the length of the profile, but was strongest in the upstream part of the valley. The decrease of the gradient in response to the increase of discharge was not uniform either. The upstream part of the valley, where the gradient was steepest, started eroding rapidly. In the middle part of the valley, where the gradient was lower, a wedge of sediment was rapidly deposited. This wedge was slowly eroded during the remainder of the experiment, without significant downstream or upstream migration. The rapid creation of this sediment wedge was probably the result of the decrease in transport capacity caused by the low gradient in the middle part of the valley relative to the upstream part of the valley. The steep gradient in the upstream part of the valley enabled a relatively large amount of sediment, made available by erosion, to be transported downstream. The lower gradient in the middle part of the valley, and thus the

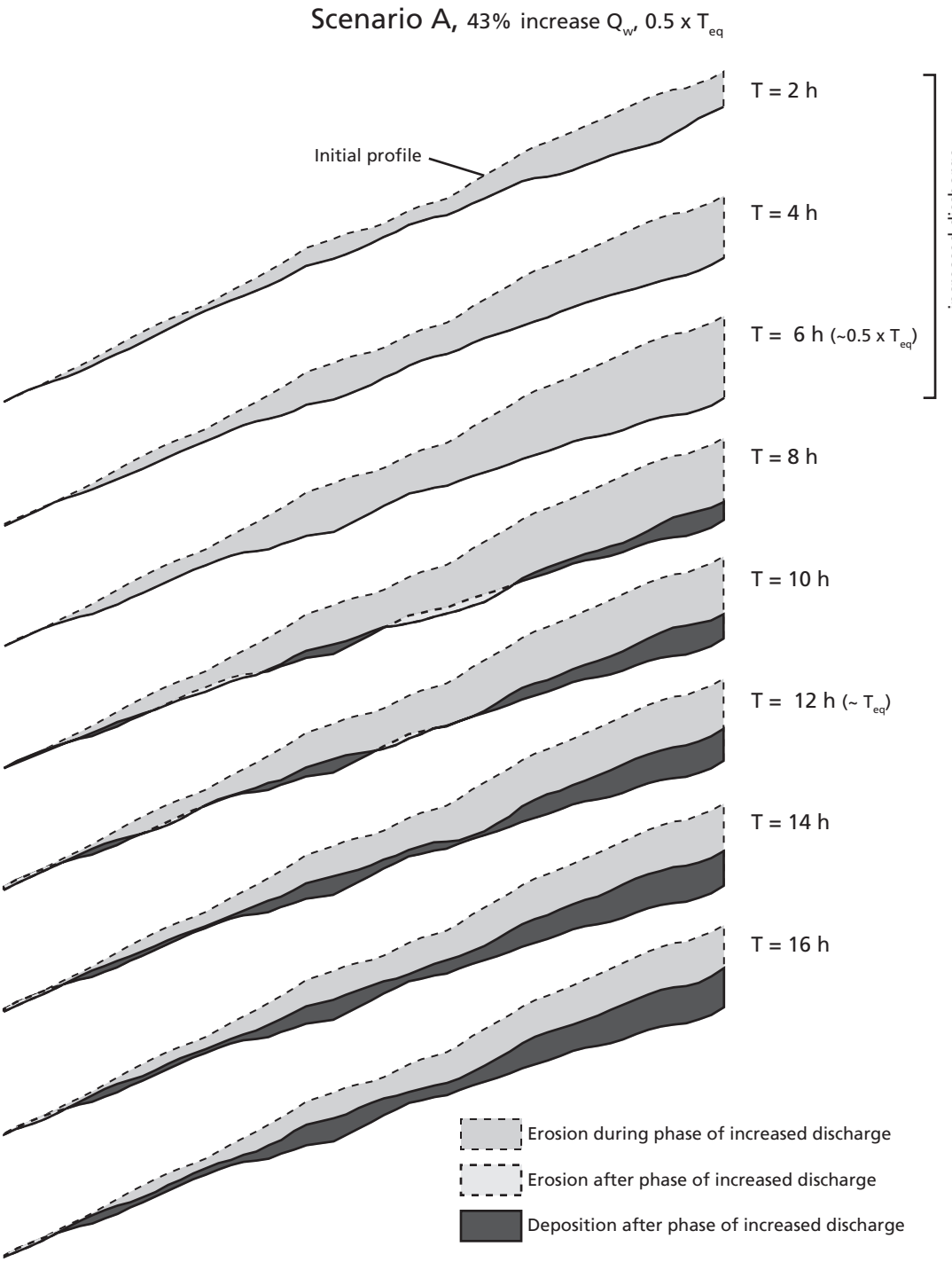

Figure 3.4 Cross section along the flume for scenario A (increase Qw for ~0.5 x Teq (6 hours)). Cumulative erosion during the perturbation (between T = 0 hours and T = 6 hours) is indicated in light grey with dashed borders, cumulative erosion after the perturbation (from T = 6 hours onward) is indicated in very light grey with dashed borders and the deposition after the perturbation is indicated in dark grey.

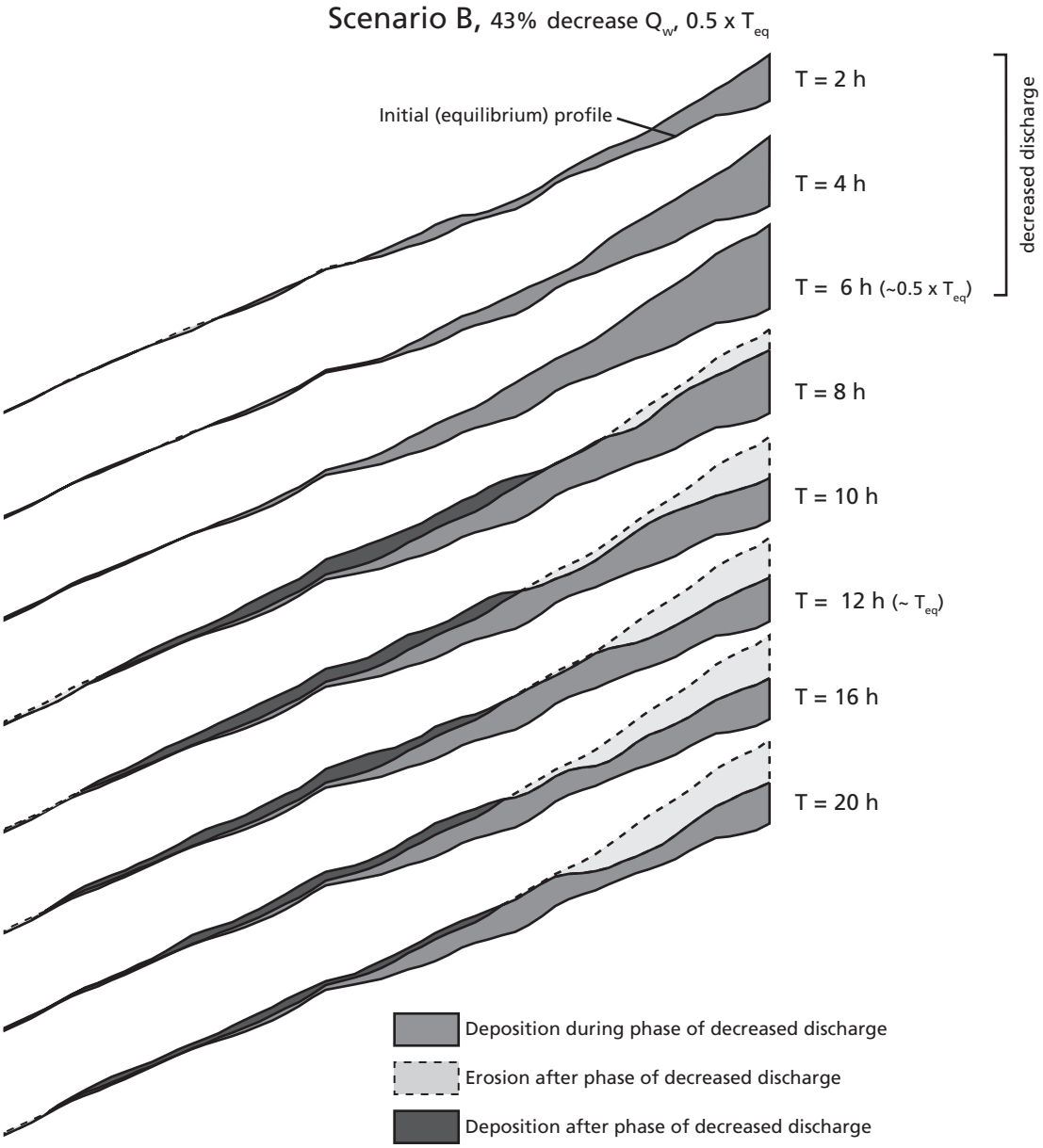

Figure 3.5 Cross section along the flume for scenario B (decrease Qw for ~0.5 x Teq (6 hours)). Cumulative erosion from T = 0 h is indicated in light grey with dashed borders, the cumulative deposition during the perturbation (between T = 0 hours and T = 6 hours) is indicated in medium grey and the deposition after the perturbation (from T = 6 hours onward) is indicated in dark grey. Note the concavity of the profile during the perturbation. After the return to the initial conditions (after T = 6 hours), a wedge of sediment is rapidly created in the middle of the flume (displayed here from T = 8 hours onward, but in existence from at least T = 7 hours onward), and the profile of the flume is nearly straight.

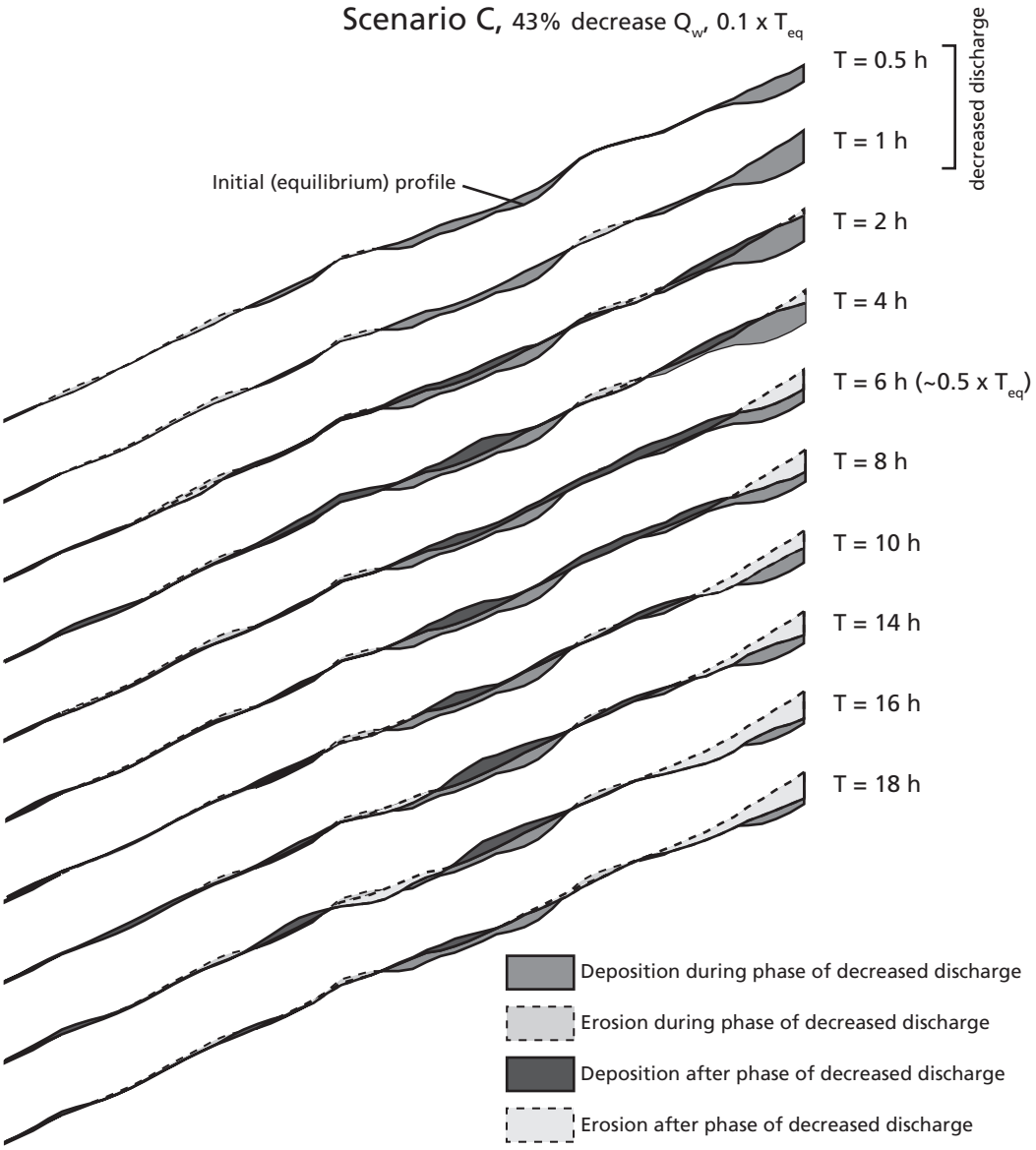

Figure 3.6 Cross section along the flume for scenario C (decrease Qw for ~0.1 x Teq (1.2 hours)). Cumulative erosion from T = 0 h is indicated in light grey with dashed borders, cumulative erosion after the perturbation (from T = 1.2 hours onward) is indicated in very light grey with dashed borders, cumulative deposition during the perturbation (between T = 0 hours and T = 1.2 hours) is indicated in medium grey and the deposition after the perturbation (from T = 1.2 hours onward) is indicated in dark grey. A pattern resembling the pattern observed in scenario B (Fig. 3.5) is visible. Note that the background variations in the systems are relatively large in this scenario because the volumes are smaller, which results in a more cluttered pattern than seen in scenario B (Fig. 3.5).

reduced transport capacity, resulted in deposition in this part of the valley. Because of this rapid upstream erosion and downstream deposition (reducing the steep upstream gradient and increasing the low downstream gradient respectively), the gradient of the valley was made more uniform, which stopped the simultaneous erosion and deposition. Subsequently the gradient was reduced more uniformly along the profile.

Scenario C (Fig. 3.6, Table 3.1) responded to the perturbation in the same way as scenario B (Fig. 3.5, Table 3.1), except that the volume changes were smaller because of the shorter duration of the discharge pulse. As a result the small-scale autocyclic processes that occur in the model even in equilibrium were relatively large, which is why the results have a relatively large amount of background noise. A similar attenuation of signals resulting from external forcing by small-scale autocyclic processes also plays a significant role in the numerical model of Veldkamp and van Dijke (2000).

Impact on yield

In scenarios A and B (Table 3.1) the yield behaved as could be expected from the observed changes in gradients of the river profile: an increased sediment output after an increase in discharge and *vice versa*. In scenario A, after reaching this minimum or maximum rate the sediment flux gradually returned to the rate of sediment input at the upstream end of the river (Fig. 3.7, scenario A). In scenario B the sediment flux from the outlet immediately dropped to about 10% of the sediment input rate from the catchment and remained at this low level until the discharge was changed again (Fig. 3.7, scenario B).

In scenario C, the short discharge pulse scenario (Table 3.1), there was a significant decrease in sediment flux from the outlet of the valley immediately after the onset of the decreased discharge. The response of the sediment output to the ending of the perturbation was a rapid return to the rate of sediment input, but we did not observe a significant increase in output comparable to scenario B (Fig. 3.7, scenarioB). This is probably because the amount of background noise caused by small-scale autocyclic processes was relatively large in this scenario.

Sediment-input pulses (scenarios D, E and F)

Impact on valley gradient

The response of the river valley gradient in scenarios D and E (Figures 3.8 and 3.9, Table 3.1) was in agreement with the findings of Mackin (1948): a uniform decrease of the gradient in response to a decreased sediment influx (scenario E) and a uniform increase of the gradient over the whole length of the profile in response to an increased sediment influx (scenario D). The increase or decrease of the gradient was caused by an increased or decreased equilibrium

Figure 3.7 (opposite) Normalized yield at the mouth of the flume for scenarios A to F. The solid lines represent three point moving averages. The yield is indicated as a percentage of the equilibrium sediment influx from the catchment (i.e., initial conditions). The dashed lines indicate sediment input (scenarios D, E and F) and discharge (scenarios A, B and C), both normalized to the equilibrium sediment influx (1.50 dm3/h) and discharge (350 dm3/h). The rehsponse to a change in sediment influx with a relatively long period (scenarios D and E) is relatively slow. The response to a change in discharge with a relatively long period (scenarios A and B) is rapid. After the return to initial conditions (T = 6 h) the yield shows an opposite response, i.e., a yield below 100% of input after an increased yield during the perturbation (scenario A) and vice versa (scenario B). In the scenario with a relatively short perturbation in the sediment influx (scenario F), no significant response to the perturbation can be recognized in the yield at the mouth of the flume, but the system is clearly disturbed, as the yield fluctuates significantly below and above the sediment influx volume for at least 20 hours after the return to equilibrium conditions (T = 1.2 hours). From T = 24 hours onward fluctuations in the yield are back to the level characteristic for (dynamic) equilibrium conditions. In the scenario with a relatively short perturbation in the discharge (scenario C), there is a rapid significant response in the yield at the mouth of the flume. No significant opposite response after return to initial condition (as in scenarios A and B) is distinguished, but the system is disturbed for about 15 hours after the perturbation, just as in scenario F. In all scenarios, full recovery after the perturbation takes a period on the order of the equilibrium time of the system (~12 hours).

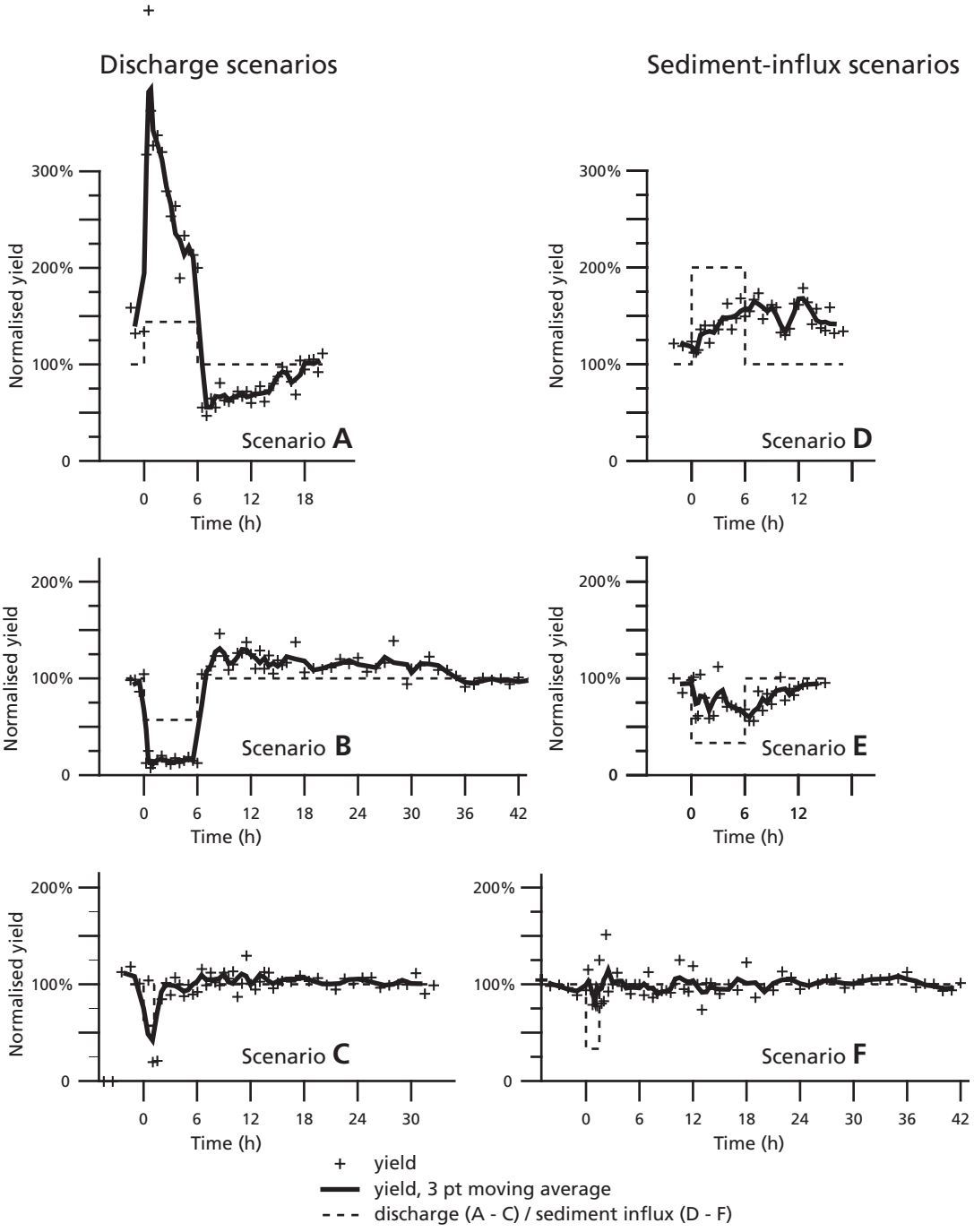
Discharge scenarios
Sediment-influx scenarios
Normalised yield
300%
200%
100%
0
Scenario A
Scenario B
Scenario C
Scenario D
Scenario E
Scenario F
0 6 12 18
0 6 12 18 24 30 36 42
Time (h)
yield
yield, 3 pt moving average
discharge (A - C) / sediment influx (D - F)

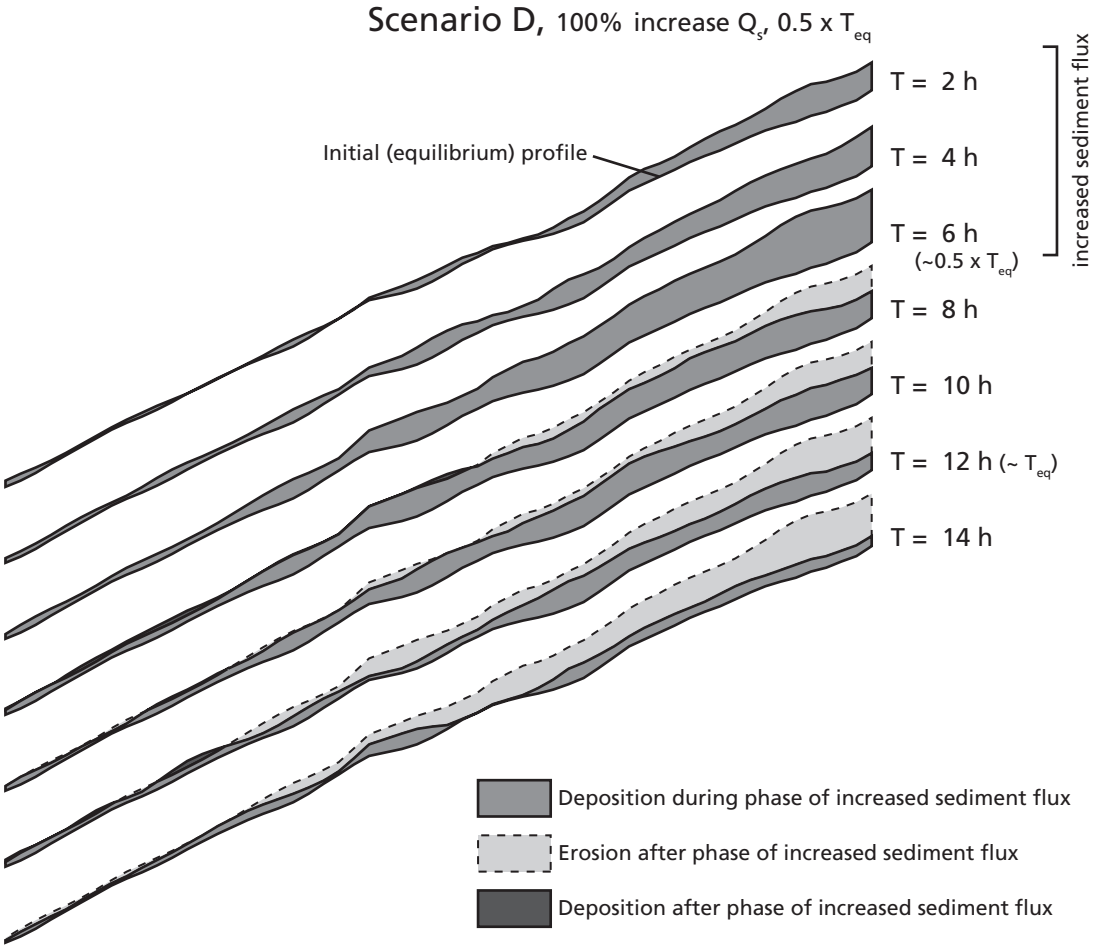

Figure 3.8 Cross section along the flume for scenario D (increase Qs for ~0.5 x Teq (6 hours)). Cumulative erosion from T = 0 h is indicated in light grey with dashed borders, the cumulative deposition during the perturbation (between T = 0 hours and T = 6 hours) is indicated in medium grey and the deposition after the perturbation (from T = 6 hours onward) is indicated in dark grey.

gradient (i.e., accommodation space), which caused deposition or erosion respectively. The response of the gradient in scenario F was not as clear as that of scenarios D and E, because of the relatively high level of background noise in the short pulse experiments, but nevertheless the upstream part of the valley experienced significant erosion.

Impact on yield

The changes in sediment flux from the river mouth in the scenarios with a change in sediment flux (scenarios D and E, Table 3.1) showed a different pattern. Again, the sediment flux from the river mouth started changing immediately after the sediment input from the catchment was changed, but in these scenarios the change was much slower, steadily increasing and reaching a maximum deviation from the sediment input rate at the moment that the perturbation in sediment input was ended, i.e., after 6 hours (Fig. 3.7, scenarios D and E). After this the sediment flux from the river mouth returned to 100% of the sediment input rate

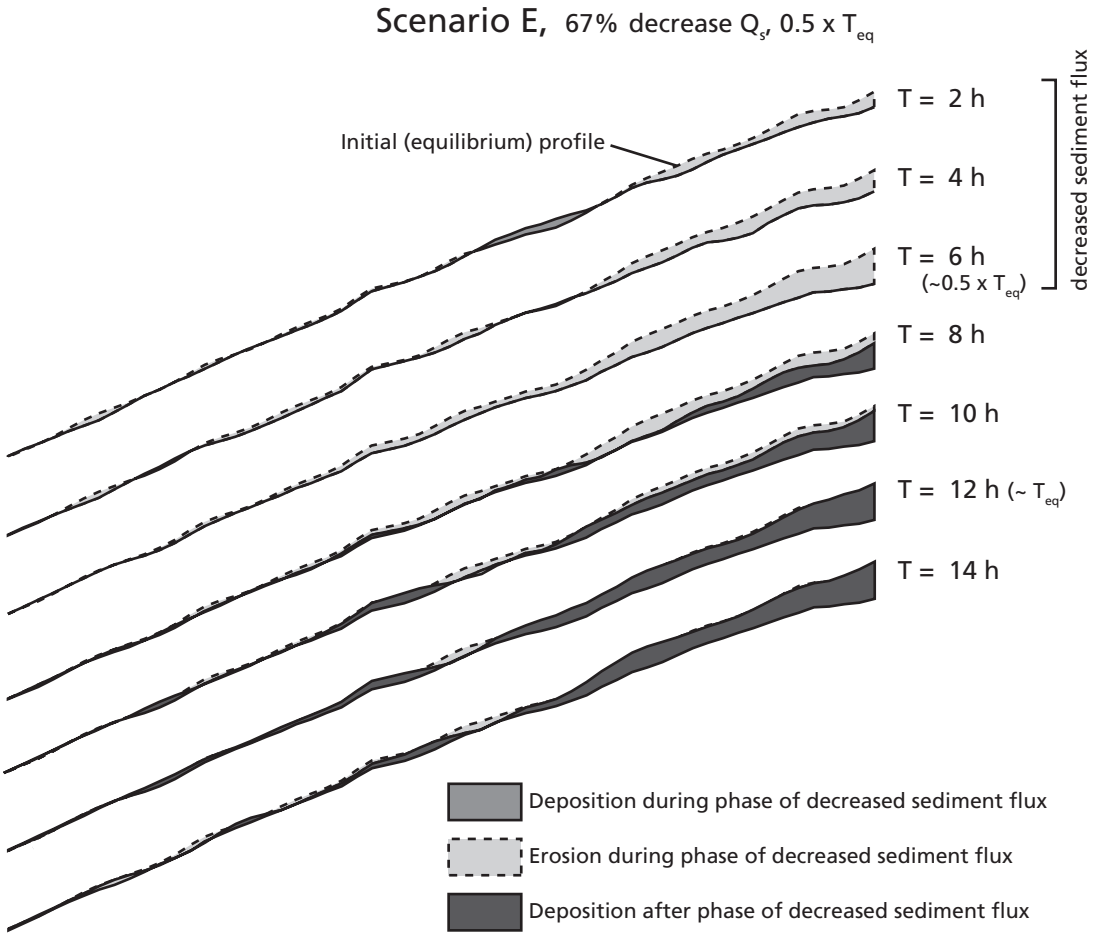

Figure 3.9 Cross section along the flume for scenario E (decrease Qs for ~0.5 x Teq (6 hours)). Cumulative erosion from T = 0 h is indicated in light grey with dashed borders, the cumulative deposition during the perturbation (between T = 0 hours and T = 6 hours) is indicated in medium grey and the deposition after the perturbation (from T = 6 hours onward) is indicated in dark grey.

over a period of roughly T_{eq} (i.e., 12 hours). Scenario D had, in fact, not reached equilibrium yet after 12 hours, but the trend suggests that it would have in another 12 hours (Fig. 3.7), and equilibrium time is a first order approximation (Paola et al., 1992). The relatively slow response in scenario D may result from the higher subsurface water flow that is associated with higher gradients.

The response of the sediment flux from the river outlet was opposite to the volume changes induced by the changes in equilibrium gradient of the river profile (Figures 3.8 and 3.9). Apparently the input of sediment into the river caused a strong response, which was attenuated by the associated changes in equilibrium gradient. This explains the slow response, reduced amplitude of the resulting pulse at the outlet compared to the forcing pulse introduced from the catchment, and the fact that there was no opposite response following the end of the forcing pulse, which might be expected from the volume changes resulting from the changes in gradient (Figures 3.8 and 3.9).

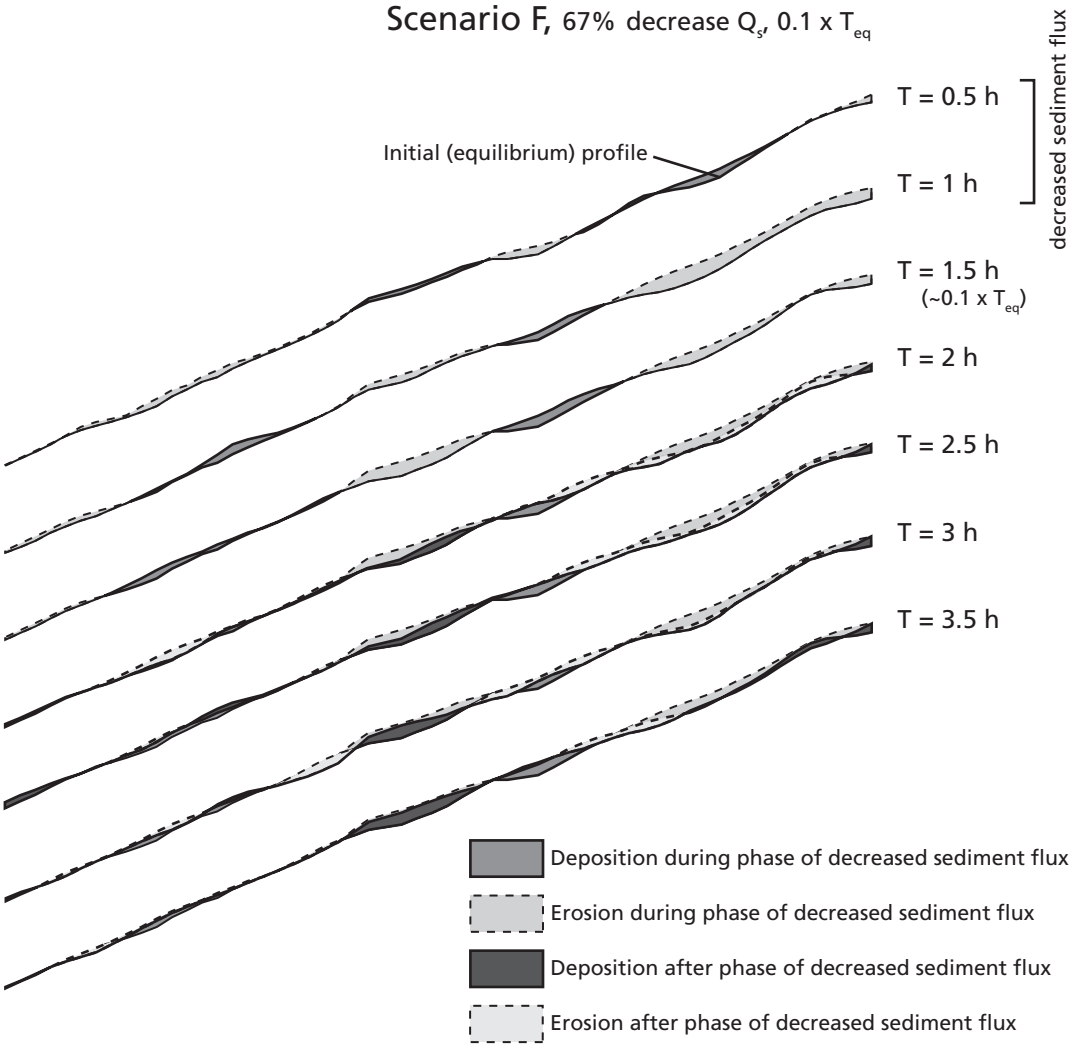

Figure 3.10 Cross section along the flume for scenario F (decrease Qs for ~0.1 x Teq (1.2 hours)). Cumulative erosion from T = 0 h is indicated in light grey with dashed borders, cumulative erosion after the perturbation (from T = 1.2 hours onward) is indicated in very light grey with dashed borders, cumulative deposition during the perturbation (between T = 0 hours and T = 1.2 hours) is indicated in medium grey and the deposition after the perturbation (from T = 1.2 hours onward) is indicated in dark grey. No significant patterns emerge.

In scenario F (Fig. 3.10, Table 3.1) the sediment flux from the outlet fluctuated following the change in sediment input, but the deviations were hardly larger than the variability inherent in the model and it would be impossible to correlate them with certainty to the perturbation. The system is clearly destabilized, however: up to 24 hours into the experiment the yield at the outlet fluctuates more than it does in equilibrium, which is attained at 24 hours into the experiment (Fig. 3.7, scenario F). In a natural river system this might result in changes in, for example, the interconnectedness of the associated fluvial deposits.

Discharge pulse during base-level fluctuation (scenarios G, H and I)

In the scenarios with a fixed outlet (scenarios A-F) the response of the river profile to changes in discharge and sediment input and the resulting changes in sediment output by the river were investigated in isolation. The results did not answer questions about the importance of these processes compared to the impact of base-level change and about the interaction with sea-level change and associated delta progradation. To this end a second set of experiments, with a setup including a shelf and basin (Fig. 3.1) and fluctuating sea-level was done (scenarios G, H and I, Table 3.1).

Constant discharge (scenario G)

A reference experiment in which discharge was fixed (scenario G, Table 3.1) was performed to establish the behaviour of the system under conditions of stable discharge and sediment input.

The progradation of the delta during sea-level fall caused an increase of accommodation space in the valley. Indeed the gradient of the profile did not change (since the discharge and sediment flux into the river system did not change), and the equilibrium profile was translated downstream along with the retreating coastline. Because the slope of the coastal plain was less than the slope of the river valley in our setup (Table 3.2, Fig. 3.1), the accommodation space in the river valley increased until progradation reached the shelf break. As a consequence a continuous succession of sediments was deposited in the valley (Fig. 3.11, scenario G). The deposition of these sediments reduced the sediment flux from the valley onto the coast and shelf area during sea-level fall (Fig. 3.12, scenario G, 0 – 15 h).

After sea-level dropped below the shelf break (14 hours into the experiment), headward erosion commenced. The knick point (furthest extent of headward erosion) migrated over the shelf and connected with the river valley. Knick point migration stopped at 20 hours, after the sea-level rose above the shelf break (Fig. 3.2). At this point erosion had just advanced beyond the mouth of the river valley (Fig. 3.11, scenario G). During sea-level lowstand sedimentation continued in the upstream part of the river (Fig. 3.11, scenario G) and as a consequence the output of sediment from the river remained below the level of input of sediment into the river (Fig. 3.12, scenario G, 14 – 20 h). During the final part of the experiment (20 – 30 hours) limited deposition occurred in the river valley (Fig. 3.11, scenario G), reflected by the level of sediment flux from the river, which was at or just below 100% of sediment input from the catchment area (Fig. 3.12, scenario G, 20 – 30 h). The development described above serves as a reference for two scenarios in which discharge pulses of different lengths were applied (scenarios H and I, Table 3.1).

Long discharge pulse (scenario H)

The scenario with a long discharge pulse, scenario H (Table 3.1, Fig. 3.3), differed from the reference scenario (scenario G, Table 3.1, Fig. 3.3), in that the discharge was increased with 25% during sea-level fall (at the inflexion point of the curve, Fig. 3.3, 10 hours) and decreased again to its initial level during sea-level rise (Fig. 3.3, 25 hours).

During the first ten hours the experiment (scenario H) was identical to the reference experiment (scenario G), and the behaviour was very similar (e.g. Fig. h). This confirms the reproducibility of the experiments.

Immediately after the discharge was increased, after 10 hours of experiment, the sediment flux from the river mouth increased sharply during two hours to about 125% of the initial input into the river (Fig. 3.12, 10 – 12 hours), followed by a decrease in sediment output, similar to the impact of an increase in discharge on sediment output in a fixed outlet experiment (Fig. 3.7, scenario A), but at a lower rate. The response of the sediment flux from the river mouth was expected to be slower, since the reference experiment (scenario G) had shown that in a prograding system the sediment flux from the river was lower than the sediment input flux. So the progradation partly counteracted the effect of the increased discharge. Between 14 hours and 20 hours headward erosion induced by sea-level fall migrated over the shelf into the river valley (as in the reference scenario, scenario G). Because the rate of knick point migration was higher due to the higher discharge, however, the upstream limit

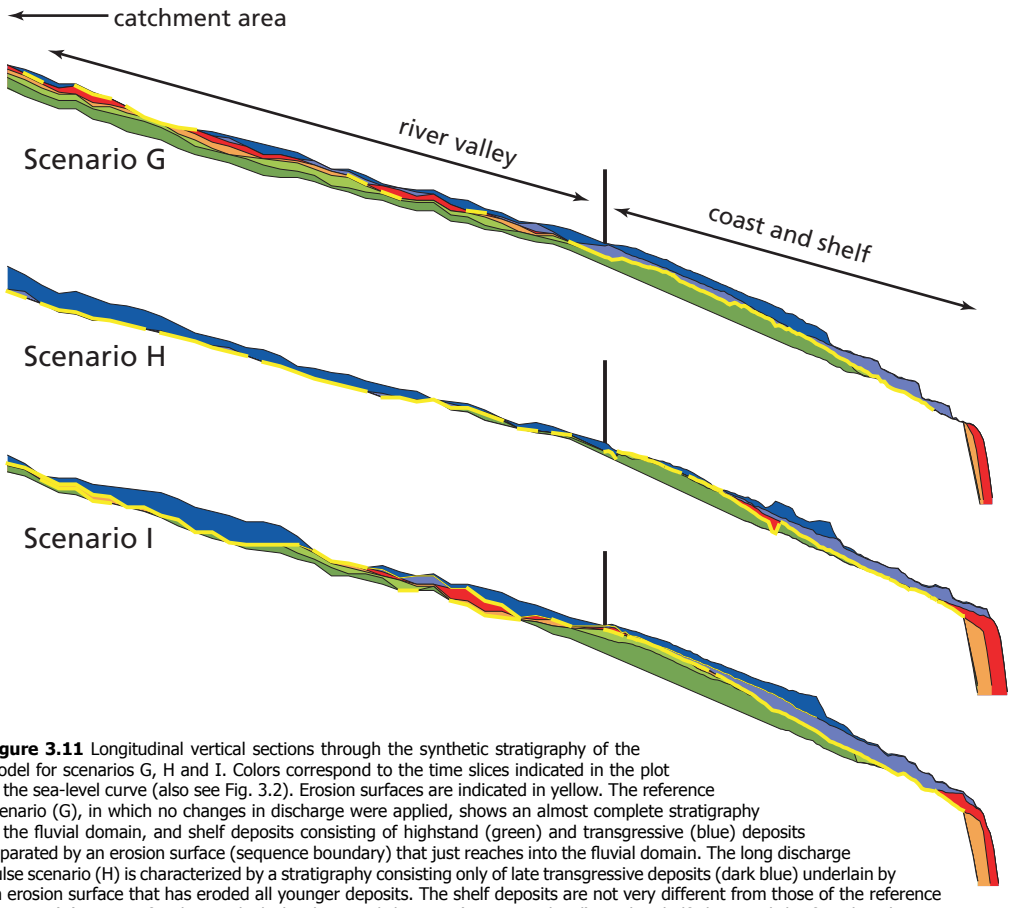

Figure 3.11 Longitudinal vertical sections through the synthetic stratigraphy of the model for scenarios G, H and I. Colors correspond to the time slices indicated in the plot of the sea-level curve (also see Fig. 3.2). Erosion surfaces are indicated in yellow. The reference scenario (G), in which no changes in discharge were applied, shows an almost complete stratigraphy in the fluvial domain, and shelf deposits consisting of highstand (green) and transgressive (blue) deposits separated by an erosion surface (sequence boundary) that just reaches into the fluvial domain. The long discharge pulse scenario (H) is characterized by a stratigraphy consisting only of late transgressive deposits (dark blue) underlain by an erosion surface that has eroded all younger deposits. The shelf deposits are not very different from those of the reference scenario (G), except for the much thicker lowstand deposits (orange and red) on the shelf slope and the fact that the sequence boundary extends all the way up to the catchment area. Also note the lower gradient of the erosion surface compared to the gradient of the overlying deposits, caused by the relatively high discharge during its formation. The short discharge pulse scenario (I) is characterized by an incomplete stratigraphy in the upstream part of the fluvial valley, overlain by a thick wedge of young sediment (dark blue), and a more or less complete stratigraphy in the downstream part of the valley. In this scenario the sequence boundary does not extend into the fluvial valley, just as in the reference scenario (G). The deep erosion in the upstream part of the valley is purely climate (discharge) induced. The stratigraphy of the deposits on the shelf is not much different from those in scenario G, except that the late lowstand deposits (red) are thicker, which is a consequence of the pulse in discharge, which started late in the lowstand phase (Fig. 3.3). The early lowstand deposits (orange) also appear to be thicker, but this is a consequence of lateral variation in thicknesses.

of headward erosion lay further upstream than in the reference scenario (scenario G), more than three quarters up the river valley. During this interval (14 – 20 hours) the sediment flux from the river mouth rose back to 125% of the sediment input rate (Fig. 3.12, 14 – 20 hours). After 20 hours the sediment flux from the river dropped again, reaching 100% of the sediment input rate at 23 hours (which is about 1 × T_{eq} after the start of the discharge pulse). From 23 hours to 25 hours (the end of the discharge pulse, Fig. 3.3) the sediment output exactly matches the output observed in the reference scenario (scenario G, Fig. 3.12), indicating equilibrium conditions (sediment volume in = sediment volume out). After 25 hours, when the discharge was decreased to its initial value (Fig. 3.3), the sediment flux from the river continued to drop (Fig. 3.12), while the gradient of the river profile increased again in response to the lower discharge.

The combination of decreased equilibrium gradients (during the discharge pulse) and further knick point migration, caused by the higher discharge, resulted in marked differences between the stratigraphy of this scenario (H) and the reference scenario (G, Fig. 3.11). Almost all of the sediments deposited in the river valley prior to the onset of sea-level rise were eroded due to the increased discharge combined with rapid headward erosion and almost no sediments were deposited on top of the resulting erosion surface before the return to the initial discharge

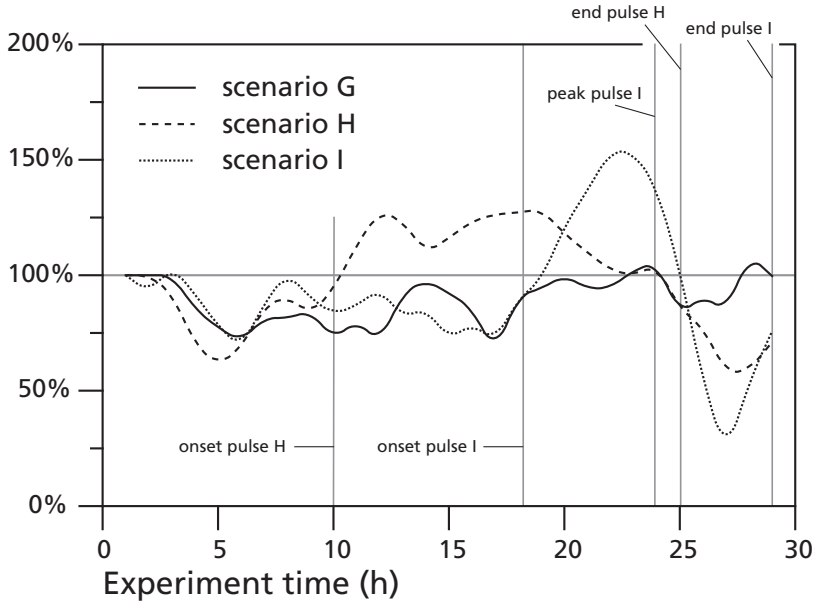

Figure 3.12 Normalized yield (% of influx from catchment area) at the river valley mouth for scenarios G, H and I. For the first ten hours of all three scenarios, during which the scenarios are identical, the sediment output is very similar. This shows the reproducibility of results. At T = 10 h the discharge of scenario H is increased instantly with 25% (Fig. 3.3), resulting in a lower equilibrium gradient and consequent rapid increase in yield at the valley outlet to ~125% of input due to erosion of sediment stored in the river valley. The return to initial the discharge level, at T = 25 hours, is reflected as a sharp decrease in yield relative to the reference scenario (G). The lower discharge results in a steeper equilibrium gradient, thus creating accommodation space, which is filled with sediment from the catchment area. The short discharge pulse scenario (I) is similar to the reference scenario (G) up to T = 19 hours. In scenario I the discharge starts to increase at T = 19 hours (Fig. 3.3). At this moment yield has started to increase already in both scenario G and I because of headward erosion induce by sea-level lowstand. The headward erosion process combined with erosion in the fluvial valley caused by the reduction of accommodation space in the fluvial valley (resulting from a lower equilibrium gradient because of the higher discharge) causes a strong increase in yield at the valley outlet. The return to initial discharge levels combined with termination of headward erosion (after sea-level rises above the shelf break) results in a strong decrease of the yield. The concurrence of the discharge changes with the headward erosion process causes the high amplitude of the yield fluctuations at the river valley outlet in comparison to the long discharge pulse scenario (H). The final increase in yield (present in all three scenarios) is the result of the reduction of accommodation space by transgression.

at 25 hours (Fig. 3.3). The gradient of the river profile at the end of the experiment clearly was steeper than the underlying erosion surface created under conditions of relatively high discharge (Fig. 3.11). In the reference scenario (G), the stratigraphy showed that the gradient of the river profile was the same throughout the experiment (Fig. 3.11). The stratigraphy of the shelf in scenario H was not significantly different from scenario G, but the volume of the lowstand deposits in scenario H was much larger than in scenario G (Fig. 3.11).

Short discharge pulse (scenario I)

The scenario with a short discharge pulse, scenario I (Table 3.1, Fig. 3.3), differed from the reference scenario (scenario G, Table 3.1, Fig. 3.3), in that the discharge was increased with 20% during early sea-level rise and decreased again to its initial level during late sea-level rise (Fig. 3.3). Since in this scenario the discharge increase occurred during transgression (Fig. 3.3), i.e., after knick point migration (which stopped after sea-level rose above the shelf break at 20 hours), and the sediment flux from the river in the reference scenario (G) did not show a significant response to sea-level rise (Fig. 3.12), we expected that the sediment output of the river would be affected primarily by the effect of the increased discharge on the gradient of the valley profile and not by increased headward erosion rates, as in the long discharge pulse scenario (H).

Again the experiment produced similar results under similar conditions, and up to the increase of discharge at, 19 hours, the sediment flux from the mouth of the river matched the results for the reference scenario (H) well (Fig. 3.12). The maximum extent of headward erosion at the moment that knick point migration was terminated (at 20 hours) was just beyond the mouth of the river valley, i.e., very similar to that in the reference scenario (G).

After the onset the increase in discharge, the gradient of the river profile immediately started to decrease, just as in the long discharge pulse scenario (H), causing erosion and an increase in the sediment flux from the river. The sediment output peaked at 150% of the sediment input, significantly higher than the 25% increase in the long discharge pulse scenario (G) (Fig. 3.12). This difference was the result of the timing of the increase in discharge relative to the sea-level fall. As explained for the reference scenario (G), progradation in this setup causes an increase in accommodation space (and a decrease in sediment output from the river caused by sedimentation in the river valley) and transgression a decrease in accommodation space in the river valley (and an associated increase in sediment output from the river). Therefore the increase in sediment output from the river in response to increased discharge was strengthened in this scenario (I). Immediately after the discharge started decreasing, the sediment flux from the river mouth also started to decrease as the accommodation space created in the river valley was filled. After 25 hours the sediment output dropped below 100% of the sediment input and continued to drop until 27 hours. Subsequently the sediment flux from the river started to increase again until the end of the experiment (Fig. 3.12). This pattern was found in all three scenarios in this set (Fig. 3.12). The stratigraphy resulting from scenario I (Fig. 3.11) contained elements of both other scenarios (H and I). In the upstream part of the valley most of the sediments deposited before the discharge pulse were eroded. The erosion surface was covered by relatively thick deposits of the youngest stratigraphical unit. The stratigraphy of this part of the system was similar to the stratigraphy of the river valley in the long discharge pulse scenario (H). The downstream half of the river valley contained a more or less continuous sequence of sediments very similar to the stratigraphy of the river valley of the reference scenario (G). The stratigraphy of the coastal and shelf

zones was mostly similar to both other scenarios (G and H). The lowstand deposits were intermediate in thickness between the reference scenario (G) and the long discharge pulse scenario (H).

Sensitivity of the system to forcing at different frequencies

Our results confirm the findings of Paola et al. (1992). They conclude from numerical modelling experiments that slow (i.e., $T >> T_{eq}$) variations in sediment flux (i.e. variation in sediment production) strongly influence basin stratigraphy, while rapid (i.e. $T << T_{eq}$) sediment flux changes show strong proximal effects that diminish into the basin. On the other hand, slow variations in discharge produce hardly any visible or measurable effect, while rapid variations in discharge produce abrupt, asymmetrical progradational cycles (cf. Figures 2 and 4 in Paola et al., 1992). Intermediate frequency changes (i.e. $T \approx T_{eq}$) show intermediate behaviour. The most important difference between their and our results is that our intermediate frequency results are more like their high frequency results. This can be explained by the fact that in our model no subsidence is applied. Subsidence increases the elevation of the equilibrium profile of the river system relative to a chronostratigraphic datum (e.g the basement of the basin) (Quirk, 1996). An increased sediment flux or a decreased discharge have a similar impact on the equilibrium profile (an increase in the gradient of the equilibrium profile), while a decreased sediment flux or an increased discharge decrease the gradient of the equilibrium profile (Quirk, 1996). Subsidence should therefore enhance the impact of increased sediment flux or a decreased discharge on the equilibrium profile and counteract the impact of decreased sediment flux or increased discharge. This enhanced forcing over a relatively short period should produce results similar to weaker forcing over a longer period.

The lack of response in the basin to high-frequency sediment flux variations, which is clearly shown in our experiments, is predicted for real-world systems by Castelltort and Van Den Driessche (2003) based on calculations of response times. They estimate the mean slope of the river system by dividing the maximum elevation of the drainage basin by the stream length. This is without doubt an overestimation for the transfer subsystem (the depositional part), since the slope of this part of the system is much lower and an underestimation for the catchment area, where slopes are higher. This means that the diffusivity for the river valley is higher, making response times shorter. Although this implies that relatively short rivers may not be as effective as buffers as Castelltort and Van Den Driessche (2003) conclude (or, in other words, a river must be longer than predicted to be an effective buffer), it does not mean that the basic principle of buffering of sediment pulses by rivers is not sound. Similar behaviour is displayed by our experimental systems. Our experiments suggest that high-frequency sediment flux pulses from the catchment area have no significant impact on the yield at the river mouth. The same is predicted by Castelltort and Van Den Driessche (2003). Our experiments, however, do suggest that discharge-induced high-frequency pulses are very likely to cause high frequency sediment pulses at the mouth of a river system. This supports the idea that the sediment delivery form the river mouth can vary in response to climate change with Milankovitch periodicities. The rapid response to discharge pulses by the river system in our experiments suggests that the occurrence of these yield pulses at the mouth of the river in response to discharge pulses do not depend on the size of the river system. This is supported by data from the Ganges River (see below).

Timing of climate pulses relative to sea-level fluctuation

The timing of a change in discharge relative to the change in sea-level has important consequences for the response of the system. It can slow down or accelerate headward erosion (knickpoint migration), and cause significant differences in stratigraphic architecture. A relatively small pulse can have greater impact in terms of yield at the valley mouth than a longer pulse of a higher magnitude if the timing relative to sea-level fall is right, as can be seen in scenarios H and I (Fig. 3.12).

The impact of intermediate to high-frequency discharge fluctuations is largest in the fluvial domain because the volume of the valley is much smaller than potential volumes on the shelf. This can clearly be seen in the longitudinal profiles through the stratigraphy (Fig. 3.11). The impact on volumes deposited on the shelf is very limited, which is demonstrated in the total mass accumulation curves for scenarios G, H and I in Figure 3.13. The impact on erosion processes on the shelf, on the other hand, is pronounced (Fig. 3.11), since headward erosion rates increase with increasing discharge. This in turn influences both the internal redistribution of sediments within the basin and the geometry, extent and diachroneity of

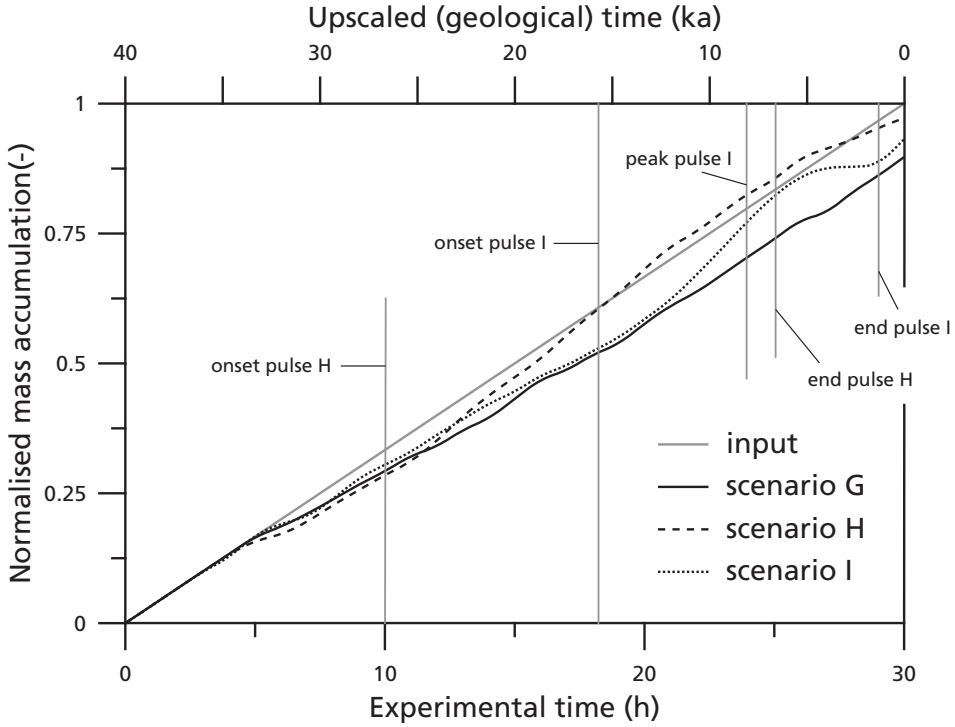

Figure 3.13 Total mass accumulation at the river valley mouth through time of scenarios G, H and I. The straight line indicates the input from the catchment area into the river valley. The position of the mass accumulation curve of scenarios G drops steadily below the cumulative sediment influx line throughout the experiment, indicating steady net deposition in the river valley. In scenario H the mass accumulation curve rises above the cumulative sediment influx line around 20 hours. This indicates that most, if not all, deposits older than 20 hours have been eroded from the river valley. The position of the mass accumulation curve of scenarios I is below the cumulative sediment influx line, but approaches it very closely around 25 hours, and subsequently drops below it significantly. This means that most deposits in the valley older than 25 hours have been eroded, followed by significant deposition between 25 and 30 hours. These observations match the stratigraphy of the scenarios (Fig. 3.11). Note that for the period during which the scenarios are identical (the first 10 hours for all three scenarios, and the first 20 hours for scenarios G and I, Figure 3.3) the mass accumulation curves are almost identical, illustrating the reproducibility of the experiments.

erosion surfaces over timescales of the order of T_{eq}. These aspects of the system are central to the concept of sequence stratigraphy. Sea-level change is in itself the dominant external forcing process in passive margin settings; the impact of climate change (i.e., discharge and sediment flux) can strongly modify the resulting stratigraphy.

The use of mass-accumulation curves

The results of our experiments reveal fundamental differences in the responses of the sediment flux from the valley outlet to changes in discharge and changes in sediment flux from the catchment. These differences should also be reflected in the total sediment yield at the valley outlet. In the discharge pulse scenarios (A, B and C, Table 3.1), the amount of sediment put into the system does not change. In the sediment flux change scenarios (D, E and F, Table 3.1), the amount of sediment put into the river system was varied. In all scenarios the amount of sediment delivered to the mouth of the river should be the same as the amount of sediment delivered by the sediment feeder (i.e., the catchment area) after the system has returned to the equilibrium state following the termination of the perturbation and the return of the river valley profile (and thus the total volume) to its initial state. Since the sediment input through time is different, the development of the accumulation of sediment at the outlet must be different as well. Finally, after the river system has returned to equilibrium, sediment output from the river should match sediment input from the catchment again. In other words, the slope of the sediment accumulation curve (i.e., the sediment flux from the outlet) should be equal (parallel) to the of the total sediment input curve (i.e., the sediment flux into the river system). Because the mass accumulation history is often preserved in natural systems, it is important to see if such patterns are recognisable in our results, and, if so, how mass accumulation curves can be used to reconstruct the development of the river systems that produced them.

Fixed base level

Figure 3.14 shows the sediment accumulation at the valley mouth (solid lines) and the total sediment input (dashed lines) through time for scenarios A – F (Table 3.1). The sediment accumulation curves for the long pulse scenarios (A, B, D and E) reveal the major differences between the total sediment accumulation histories of the sediment flux pulse scenarios, and those of the discharge pulse scenarios. The sediment accumulation histories of the sediment flux pulse scenarios are characterised by very gradual changes in slope (Fig. 3.14, scenarios D and E), while the total sediment accumulation histories of the discharge pulse scenarios show abrupt changes in slope (Fig. 3.14, scenarios A and B). Since the slope of the sediment delivery curve is defined by the sediment flux from the outlet, these changes in slope match the changes in sediment delivery rates observed in the experiments (Fig. 3.7).

The shape of the sediment accumulation curves for the long sediment flux pulses (Fig. 3.14, scenarios D and E) is different from the shape of the sediment accumulation curves for the discharge pulses (Fig. 3.14, scenarios A and B). Assuming that the curves can be extrapolated parallel to the total sediment input curves (i.e., under equilibrium conditions), the sediment flux changes (scenarios D and E) cause a permanent shift in the trend of the mass accumulation curve, while the discharge changes (scenarios A and B) cause a temporary deviation from the overall trend. The mass accumulation history of scenario A (Fig. 3.14) does not match this pattern. Although the sediment accumulation curve runs parallel to the sediment input curve towards the end of the experiment, indicating that the system is in equilibrium (flux in equals

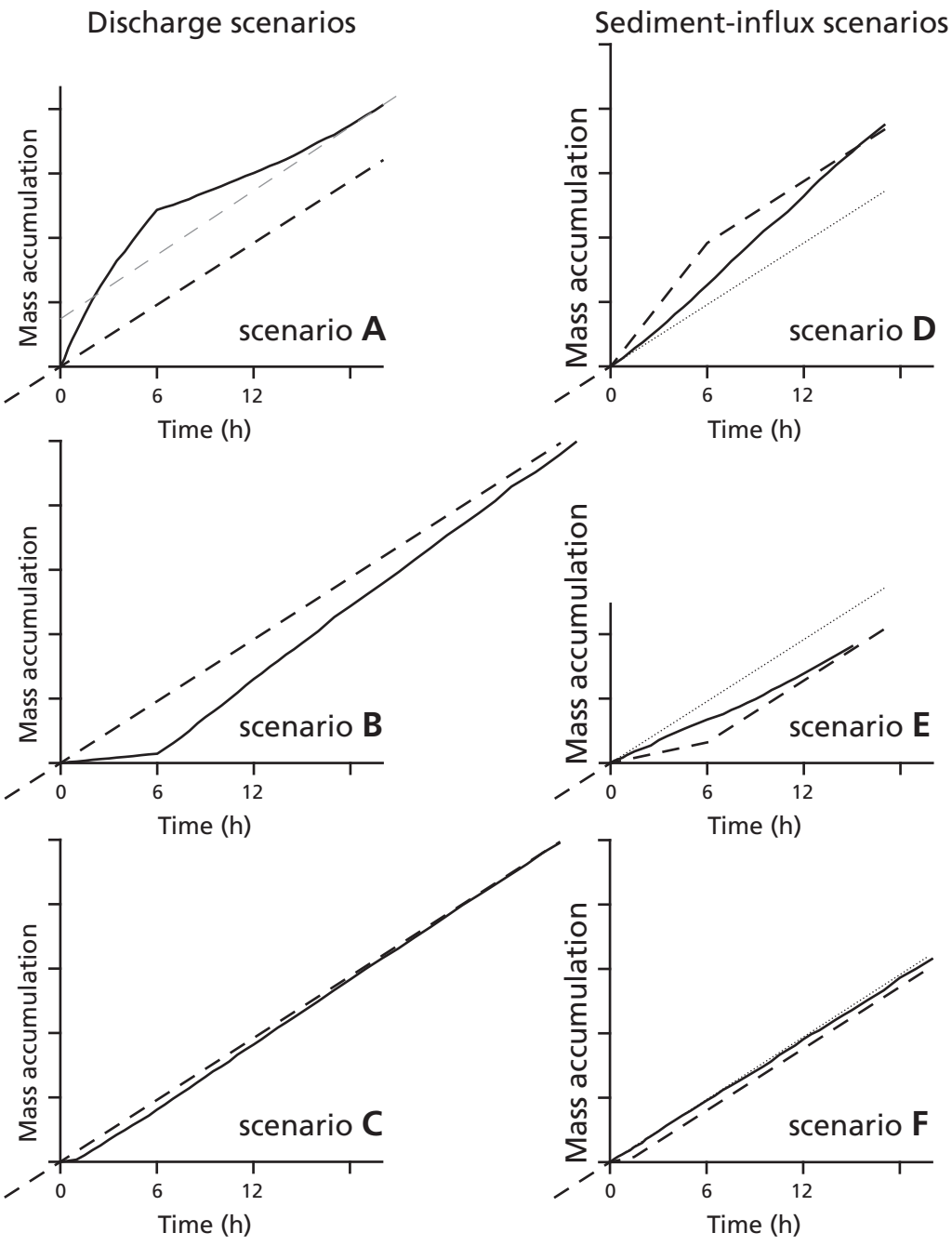
Discharge scenarios
Sediment-influx scenarios
Mass accumulation
scenario A
scenario B
scenario C
scenario D
scenario E
scenario F
0
6
12
Time (h)
mass accumulation
sediment input
hypothetical mass accumulation under constant sediment influx

flux out), and the volume of the experiment cannot have deviated from the sediment input, which was constant, the amount of sediment accumulated at the outlet is significantly higher than the amount of sediment input. Thus, additional sediment was released from the river valley. Figure 3.4 suggests that a relatively large volume of sediment was eroded during the discharge pulse. This is confirmed by the final state of the river profile. As explained above, the system was in equilibrium at the end of the experiment. The gradient of the final profile is much lower than the initial profile. Apparently the experiment was not in equilibrium at the start of the perturbation. The difference between the initial volume and the final volume of the river valley actually matches the discrepancy between the sediment input curve and the sediment accumulation curve for scenario A (Fig. 3.14, scenario A) exactly. This discrepancy is not as readily apparent from the plot of the sediment flux from the valley mouth for scenario A (Fig. 3.7).

The sediment accumulation curves for the short pulse scenarios (Fig. 3.7, scenarios C and F) have the same features as described above for the long pulse scenarios (Fig. 3.7, scenarios A, B, D and E) on a much smaller scale. Without knowing the pulses in sediment input and discharge, the difference between sediment input and sediment output would not be sufficient to associate the deviations with perturbations at the upstream end of the river.

Discharge pulses during base-level fluctuations

The second set of experiments (scenarios G, H an I, Fig. 3.3), in which the response to changes in discharge interacted with the responses to sea-level change and progradation, was more complicated. Therefore, interpretation of the mass accumulation history of these experiments (Fig. 3.13, scenarios G, H and I) is less straightforward. The response of the yield at the valley outlet to the changes in discharge (described in the results section, Figure 3.12) was less direct than in the experiments with a fixed outlet. The mass accumulation curves reflect this as more gradual responses than in the fixed outlet experiments that lag behind the discharge changes.

The mass accumulation curve for scenario G (Fig. 3.13), i.e., the reference scenario in which the discharge was constant (Fig. 3.3 and Table 3.1), shows a very clear pattern: the slope of the mass accumulation curve is systematically lower than the slope of the input line (Fig. 3.13), indicating deposition in the river valley. In the final three hours of the experiment the slope of the mass accumulation curve runs parallel to the sediment input line (Fig. 3.13). This means that no sediment should have been deposited in the valley during this period and that the system was in equilibrium again. The stratigraphy of the model (Fig. 3.11, scenario G), indeed shows more or less continuous deposition in the valley throughout the experiment. The chronostratigraphic resolution is insufficient to determine if sediments were deposited in the valley during the final three hours of the experiment. The mass accumulation

Figure 3.14 (opposite) Mass accumulation at the river valley mouth for scenarios A-F. The dashed lines indicate the input from the catchment area into thhe valley. The dotted lines indicate the rate of sediment influx at the start of the experiments, which represents equilibrium conditions, and thus the mass accumulation pattern that would have emerged if discharge and/or sediment flux would not have been changed. In scenario A this line is elevated because the experiment did not start under equilibrium conditions by accident. The resulting additional volume of eroded sediment (i.e., the vertical separation between the dashed and the dotted lines in this graph) matches the difference in volume between the initial valley profile and the final valley profile. In scenarios B and C the dotted line coincides with the dashed line, and is therefore not plotted. In all scenarios the output (solid lines) deviates from the input (dashed lines) in response to the applied perturbation (at T = 0 h). In all scenarios the cumulative outputs as well as the output rate (slope of the curves) eventually match the input, which indicates equilibrium conditions. (Scenario A is an exception, since the experiment did not start from equilibrium conditions. In this case the output returns to the level corrected for the additional input from erosion of the non-equilibrium profile.) In all scenarios this occurs at approximately 1 x T_{eq} after the return to initial conditions (at T = 6 h in scenarios A, B, D and E, and at T = 1.2 h in scenarios C and F). Scenario B is an exception: after 2 x T_{eq} the system has still not attained equilibrium conditions. While this is still within the same order of magnitude as the other experiments (T_{eq} is an indication of the order of magnitude on which the system can attain equilibrium), it is nevertheless a striking difference with the other experiments.

curve (Fig. 3.13) resembles the mass accumulation curve for scenario E (Fig. 3.14). If the actual sediment input was not known (as is likely to be the case in natural systems), it would be impossible to determine whether the mass accumulation pattern had been caused by a decrease in sediment flux into the system or progradation of the system. Using the stratigraphy of the river valley, however, the distinction can be made. A reduction of sediment flux would have caused a reduction of the equilibrium gradient of the river profile, which would have reduced accommodation space and thus caused erosion. It is clear from the stratigraphy of the river valley (Fig. 3.11, scenario G), that this did not happen. This demonstrates clearly that the stratigraphy of the river valley provides additional information that is crucial for the interpretation of the mass accumulation history.

The mass accumulation curve for the long discharge pulse scenario (scenario H, Fig. 3.13) is nearly identical to that for the reference scenario (scenario G, Fig. 3.13) up to about two hours after the onset of increased discharge (after 10 hours). Besides this lag in response, the response is not as sharp as in the equivalent fixed outlet scenario (scenario A, Fig. 3.14). As has been explained in the results section for the response of the sediment flux at the river mouth, this is caused by the interaction with the response to progradation of the system over the shelf. Between 12 hours and 20 hours into the experiment, the slope of the mass accumulation curve is steeper than the total sediment input line (Fig. 3.13, scenario H). This indicates a reduction of the total volume of the sediments in the river valley, i.e. erosion in the river valley. At about 19 hours the total accumulation curve crosses the total sediment input curve. Thus the volume of sediment in the river valley now is lower than the volume of sediment put into the system. A least in some parts of the valley deposits already present at the start of the experiment ('basement') have been eroded and preservation of sediments deposited in the valley during the experiment is very limited, if any at all. This is confirmed by the stratigraphy of this model (Fig. 3.11, scenario H), that shows a large erosion surface directly on top of the 'basement' sediments and almost no preservation of sediments younger than 20 hours. Between 20 hours and 26 hours, the mass accumulation curve runs parallel to the total sediment input line (Fig. 3.13, scenario H). As in the reference scenario this indicates that no deposition occurred in the river valley (confirmed by the stratigraphy, Figure 3.11, scenario H) and that the system must have been in equilibrium. Finally, from 26 hours to the end of the experiment, the slope of the mass accumulation curve was lower than that of the total sediment input line (Fig. 3.13, scenario H), indicating deposition in the river valley (confirmed by the stratigraphy, Figure 3.11, scenario H). Again, as at the start of the discharge change, there is a short time lag between the forcing discharge change an the response of the mass accumulation.

The mass accumulation curve of scenario I (Fig. 3.13) basically shows the same pattern as the total mass accumulation curve of scenario H (Fig. 3.13): no major deviations from the reference experiment until the discharge is changed, a short time lag between the onset of discharge change and response by the total mass accumulation, a steeper slope than the sediment input line after the discharge has been increased and a lower slope than the sediment input line after the discharge has been decreased. There are some differences with scenario H, however. The mass accumulation curve does not cross the total sediment input line, although it approaches it closely. This suggests that almost all sediment deposited in the valley up to this point in time must have been eroded, but not to the extent of scenario H. The stratigraphy of scenarios H and I confirms this (Fig. 3.11, scenario H and I). Another difference is the slope of the mass accumulation curve of scenario I during increased

discharge (Fig. 3.13, scenario I, 21 - 26 hours), which is significantly steeper than the equivalent slope of scenario H (Fig. 3.13, scenario H, 12 - 20 hours). This indicates that the total erosion in the river valley must have been higher in scenario I.

Mass accumulation histories clearly contain much information on the discharge and sediment flux conditions during the development of a river system. As demonstrated by scenarios E and G, however, different forcing conditions may result in very similar mass accumulation curves. To provide a definite answer the stratigraphy of the river system, specifically the history of the gradient of the river profile, is essential additional information. Application of the use of mass accumulation in combination with fluvial stratigraphic architecture in a natural system is demonstrated below.

Geological applications

Total mass accumulation Colorado River, Texas

In the previous section the use of mass accumulation curves in combination with profile gradients was demonstrated for our model data. We will now discuss a similar analysis for a natural river system: the Colorado River in Texas. The most important difference between our model data and natural river systems is that for natural systems the input of sediment into the system is often poorly known. This makes interpretation less straightforward. However, much can still be deduced from the available data, as we will demonstrate below.

As in the analysis of the model data, two types of data are required: the total mass accumulation history of the river system and the development of the gradient of the river valley for the same period. Figure 3.15 shows the normalised total mass accumulation for the Colorado River, based on volume estimates by Van Heijst et al. (2001) from isopach maps of the deposits of the Colorado River on the Texas shelf by Morton and Price (1987) and Snow (1998). An estimate of valley-floor gradients was made from river terraces in the Colorado River. These are characterised by a progressive decrease in slope from 20 ka (sea-level lowstand) to present (Fig. 3.16). The terraces intersect a short distance upstream from the present coastline (Blum and Valastro, 1994). In addition an indication of the discharge of the river system over the last 20 ky is provided by climate reconstructions for the catchment area (Toomey et al., 1993). These indicate a relatively wet climate up to 14 ka, followed by a relatively dry and stable climate up to modern times (Toomey et al., 1993), i.e., during sea-level rise.

Using this information we now can put some constraints on sediment input into the river system. The actual sediment input from the catchment area is unknown. Therefore an assumption of the sediment input must be made. An obvious choice is the average recent yield of the river system. An estimate of the yield of the Colorado River over the last 10 ky is indicated in Figure 3.15 with the dotted line. Since the total mass accumulation is higher than the hypothetical input (i.e., lies above the input line in Figure 3.15) for the entire period, more sediment would have been delivered by the river than it received from the catchment area over the past 40 ky. This means that no significant volume of sediments of this age would have been preserved in the river system, which is not the case, and that the river system has been in equilibrium for the last 10 ky (since the slope of the total mass accumulation curve and the total input curve would be parallel). This is in contradiction with the lowering of the actual river profile during this period. Sediment input from the catchment area must therefore have been higher.

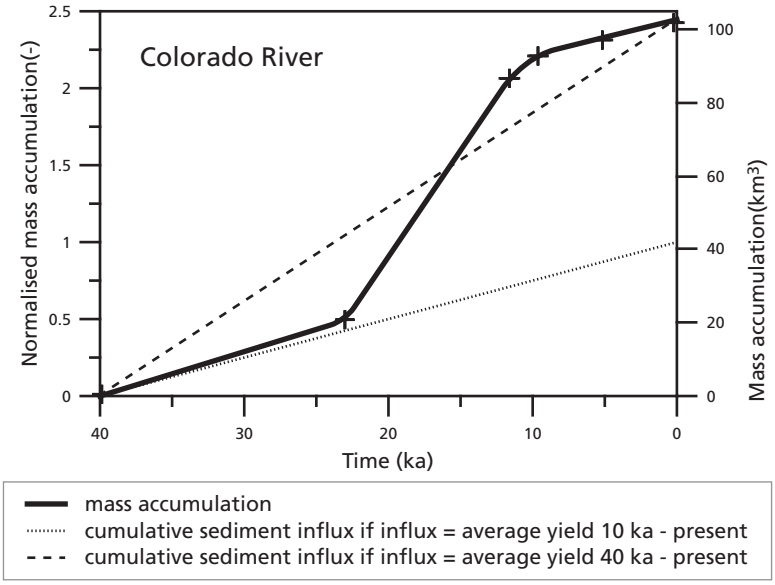

Figure 3.15 Estimated total mass accumulation curve for the Colorado River (solid line), based on volume estimates by Van Heijst et al. (2001) from isopach maps of the deposits of the Colorado River on the Texas shelf by Morton and Price (1987) and Snow (1998). The interpretation of this graph is similar to the interpretation of Figure 3.13. In this case, however, the sediment influx into the river system from the catchment is unknown. It must therefore be based on assumptions. In combination with the stratigraphy of the river valley of the Colorado River (Fig. 3.16), however, the likelihood of various sediment influx scenarios can be assessed. Two possible sediment influx scenarios are displayed: the average yield of the river system over the last 10 ky (dotted line) and the average yield of the river system over the last 40 ky (dashed line). A detailed interpretation can be found in the text.

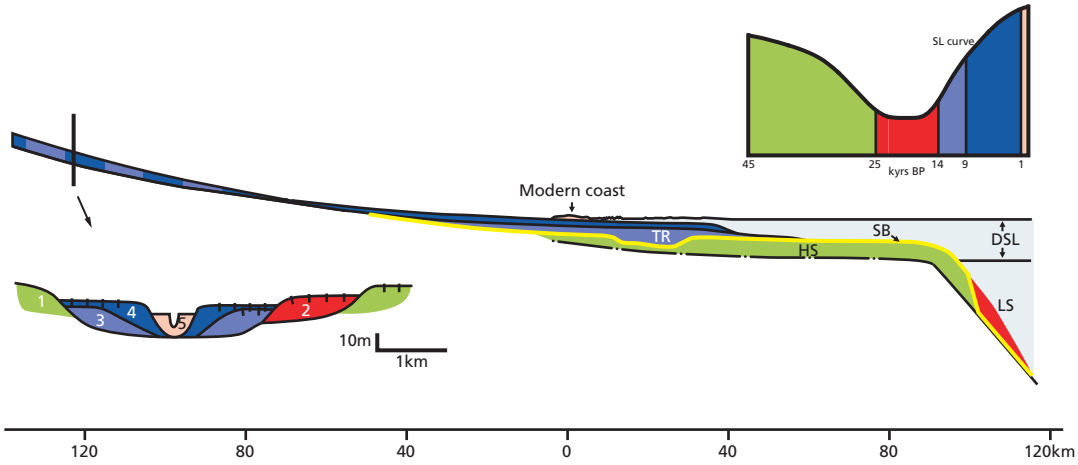

Figure 3.16 Longitudinal profiles of the Colorado River, Texas, from 20 ka to present. (After Blum and Valastro (1994).) The colours indicated below the sea-level curve indicate the ages of the stratigraphic units in the longitudinal and cross sections. Erosion surfaces are indicated in yellow. All of the river terraces in the system intersect near the modern coastline. The terrace levels in the cross section (in the upstream end of the river valley) show that the gradient of the river profile has an overall decreasing trend, with the exception of unit 4. This is probably the result of a decrease in discharge in this period, caused by a change in climate (Toomey et al. 1993), which could have caused deposition in response to a steeper equilibrium gradient under these conditions. Note that the stratigraphic architecture of our scenario H is most similar to the stratigraphic architecture of Colorado River, and that the discharge curve (Fig. 3.3) imposed in scenario H is most similar to the actual discharge pattern of the Colorado River, deduced from climate changes observed by Toomey et al. (1993). LS = lowstand systems tract, SB = sequence boundary, HS = highstand systems tract, TR = transgressive systems tract.

As an alternative hypothesis we assume the average yield of the Colorado River over the last 40 ky as the sediment input rate (indicated by the dashed line in Figure 3.15). Between 40 ka and 23 ka, less sediment was delivered to the shelf than entered it from the catchment area. This can be ascribed to infilling of accommodation space created by progradation over the low-angle shelf, as in our scenarios G, H and I. Between 23 ka and 11.5 ka sediment delivery to the shelf increased sharply. At the same time a relatively high discharge is predicted (Toomey et al., 1993). The increase in sediment delivery is congruent with the notion of an increase in discharge. After 11.5 ka the sediment delivery rate dropped, which approximately coincided with a switch to a relatively dry climate in the catchment area. This decrease in discharge could explain the presence of high terrace levels in the river valley suggesting a relatively steep river profile, comparable to our scenario H (Fig. 3.11). The final part of the development is characterised by flattening of the river gradient and associated erosion, which cannot be explained by changes in discharge (climate was relatively stable (Toomey et al., 1993)), nor by delayed response to sea-level fluctuation, because neither would cause a flattening of the river gradient. This leaves a decrease in sediment flux from the catchment area as the most likely explanation.

This analysis illustrates how our method can be applied to natural systems to provide clues to the sediment flux and discharge history.

Sediment delivery from the Ganges River

The difference in response of the yield of a river system to changes in discharge and sediment flux also sheds light on the question if river systems can act as a filter for responses to climate change. The Ganges River offers an excellent illustration. Metivier and Gaudemer (1999) proposed that output fluxes of large Asian rivers, including the Ganges River, have been stable over the last 2 million years. They attributed this to either long-term tectonic control or buffering of high frequency pulses by the trunk rivers, which is supported by Castelltort and Van Den Driessche (2003). The main argument for this conclusion is the match between the present-day sediment flux from the large Asian rivers and the mean yield from these rivers. Goodbred (2003), however, concludes convincingly that the sediment delivery by the Ganges River responds rapidly to 20 ky climate fluctuations without evidence for attenuation of the signal. If this is correct the match between present-day yield and the long-term yield over the past two million years must be a coincidence.

These apparently contradictory results can be reconciled by the results from our experiments. Our results indicate that it is crucial to make a distinction between pulses in discharge and pulses in sediment flux. High-frequency pulses in sediment flux from the catchment area (our scenario F, Figures 3.7 and 3.10) are not recognisable as pulses at the river mouth, as is also predicted by Castelltort and Van Den Driessche (2003). High-frequency discharge pulses, on the other hand, do have an immediate and recognizable impact on the yield at the river mouth (our scenario F, Figures 3.6 and 3.7). This is in agreement with the observations of Goodbred (2003). It should be noted that the sediment flux from the catchment area of the Ganges River increased in response to the increase in discharge (Goodbred, 2003). In our experiments only discharge was increased. Increased discharge in the Ganges River in combination with an increase of sediment supply from the catchment thus must have caused extra increase in yield at the river mouth.

Low-frequency variations in sediment flux from the catchment area have a clear impact on total sediment delivery to the basin. Pulses in sediment delivery to the river system over such long timescales (i.e., larger than the equilibrium time of the river system), should therefore be clearly recognisable at the river mouth. The same is concluded from numerical modelling by Paola et al. (1992). If the sediment flux from the river is more or less constant over a long period, long-term sediment input must have been constant as well. In contrast, discharge pulses of any frequency that are not accompanied by a major change in sediment flux from the catchment area cannot have a significant impact on the total delivery of sediment by rivers over long periods. They do have a significant short-term effect, however. This is clearly demonstrated by our scenarios A, B and C (Fig. 3.14) and observed in the Ganges River (Goodbred, 2003).

If mass accumulation has been constant over the last two million years (Metivier et al., 1999), this means that the delivery of sediment from the source area must have been stable. The river system cannot have buffered sediment pulses over such long time scales, i.e., larger than the equilibrium time of the river system. Instead the alternative explanation of tectonic forcing (Metivier et al., 1999) seems more plausible.

Modelling studies of response of catchments areas to climatic and tectonic forcing by Bonnet and Crave (2003) suggest that climate (runoff) change can only produce short term deviations from an equilibrium sediment flux. The equilibrium sediment flux is controlled by the uplift rate. Changes in uplift rate, on the other hand, produce a relatively slow shift towards a different equilibrium sediment flux. If uplift is steady for periods of the order of the equilibrium time of the associated river system or longer, this is reflected in the long-term sediment delivery by the river system. In other words, the input of material into the system affects the long-term behaviour of the system, while the amount of water coming into the system only affects the short-term response. Exactly the same pattern we observe in our experiments. Changes tectonic activity (i.e., on a relatively long time scale) would thus be reflected in the mass accumulation rate at the mouth of the river. This would justify the hypothesis of Metivier and Gaudemer (1999), who proposed that uplift of the Ganges source area has been stable over the last two million years.

Finally, high-frequency changes in sediment input from the catchment are not reflected by the yield at the mouth of the river system. Therefore, the impact of vegetation changes in the catchment area caused by high-frequency climate change (such as the 20 ky intensified monsoon cycles in the Ganges system) on the stratigraphy at the mouth of the river system must be insignificant.

Ice-house versus greenhouse

The discussion above has focussed on river systems in ice-house conditions, in which fourth order sea-level fluctuations play an essential role. In greenhouse conditions, where high-frequency, large amplitude sea-level fluctuations are absent and river systems can be expected to be in equilibrium with base-level, only the other external forcing processes (tectonics and climate) remain important. This reduces the complexity of the system with regard to high frequency ($T << T_{eq}$) changes. At these frequencies only changes in discharge, causing, for example, avulsions and changes in overall delta progradation, are likely to be reflected in the stratigraphic record produced by river systems. This does not necessarily mean that interpretation of the stratigraphy is straightforward. Autocyclic processes, such

as progradation, must also play a role. Even if they occur on time scales significantly shorter than the equilibrium time of the river system, they can still have local impact, and/or produce uncorrelatable pulses on a larger scale.

Conclusions

There is a fundamental difference between the response in terms of the sediment yield at the river mouth of a river system to discharge changes and the response to sediment flux changes, even though the changes in river valley gradient are basically identical (though opposite).

As a result of these different responses, high-frequency ($T << T_{eq}$) changes in discharge control the small-scale stratigraphy at the river mouth and low frequency ($T > T_{eq}$) changes in sediment flux control the large-scale stratigraphy at the river mouth. Thus, low resolution mass accumulation rates and low resolution stratigraphy tell much about tectonics and little about climate, while high resolution mass accumulation rates and high resolution stratigraphy tell little about tectonics, but much about climate.

Careful study of mass accumulation through time and the development of the valley gradient of the river system, from source to sink, can be used to put constraints on paleo-discharge and paleo-sediment flux. Well dated and correlated river terraces are of particular importance in this context.

Chapter 4

Intersecting river terraces as the result of complex response to simple climate forcing

A.P.H. van den Berg van Saparoea and G. Postma

Introduction

Changes in river dynamics cause aggradation and entrenching of river channels, resulting in the formation of river terraces. Relating the creation and preservation of river terraces to external forcing parameters can help the correct interpretation of the fluvial stratigraphic record, as has been illustrated in the previous chapters.

The importance of climate change in the creation of river terraces is well established. Studies covering a wide range of different time scales (ranging from the order of 10 ky to 10 My) and spatial scales (ranging from very local, km scale, to global patterns) all point towards the important role of climate change in the creation of river terrace sequences (e.g. Molnar and England, 1990; Huisink, 2000; Mol et al., 2000; Maddy et al., 2001; Vandenberghe, 2001; Zhang et al., 2001; Gibbard and Lewin, 2002). The other major external forcing processes, tectonics and sea-level change, also clearly affect for the formation of river terraces (e.g. Blum and Price, 1998; Bridgland, 2000; Maddy et al., 2001).

Usually a combination of climate change, tectonics and base-level change is inferred to explain the architecture of river terraces. In some cases, however, base-level change and tectonic activity can be ruled out as significant parameters affecting the system. An example of such a system is the Rhine-Meuse River in the Late Weichselian. In the Rhine-Meuse River, two terrace levels are recognised, intersecting hundreds of kilometres upstream of the Weichselian coastline (Törnqvist, 1998; Berendsen and Stouthamer, 2000). Regional subsidence and collapse of the glacial forebulge (Cohen et al., 2002) rule out incision by uplift, leaving climate and base-level change as possible candidates.

Here we propose a mechanism for the creation of intersecting terrace levels far upstream of base level by climate change alone. Results from the modelling study discussed in chapter 3 show that fluvial response to very simple scenarios of climate change may be surprisingly complex. Here we show that a rapid increase in discharge in an analogue model of a river system in a state of disequilibrium can cause nearly instantaneous erosion and simultaneous deposition in different parts of a river valley, thus creating the equivalent of intersecting river terraces. Climate change alone may be capable of creating river terrace levels that intersect at locations far removed from base level.

Chapter 4

Experimental setup and procedure

Scaling

Since the spatial and temporal dimensions of the systems we study are too large for conventional Froude scaling (e.g. Peackall et al. 1996), we have applied the scaling approach used by van Heijst et al. (2001) and used in the previous chapters. In landscape-sized physical models, changes in topography due to climate or sea-level change are measured in terms of time-averaged sediment transport. Scaling of this time-averaged sediment transport is achieved essentially by assuming purely diffusive behaviour in long term sediment transport. This offers the possibility to scale the response of the model system (which is the focus of study here) relative to the equilibrium time (T_{eq}) of the natural prototype. The equilibrium time of a system is defined as the time that is needed for the system to regain its equilibrium profile from the moment that it has been disturbed by external forcing processes. A first order approximation of the equilibrium time of a system is given by $T_{eq} = L^2 / k$, where L^2 is the length of the depositional basin and k is the sediment diffusivity of the system (Paola et al., 1992). k depends on a number of characteristics of the system, including grain properties and discharge. A higher discharge results in a higher diffusivity, and thus in shorter equilibrium times. Temporal scaling of our experiments is achieved by scaling the equilibrium time of the model to equilibrium time of the prototype: the equilibrium time of the model is equivalent to the equilibrium time of the prototype, and all changes applied to the system should be scaled accordingly.

Model setup

The purpose of the model is to represent a river valley in a first order approximation. The setup of the experiments consisted of a 6.0 m long rectangular duct with an outlet (river mouth) fixed in both elevation and horizontal location (Fig. 4.1). The catchment area was simplified to input of water and sediment into the trunk river part of the system at the top of the fluvial duct to reduce the complexity of the model. The discharge of the tap was controlled through a flow meter. Sediment was supplied by means of a sediment feeder that delivers a constant

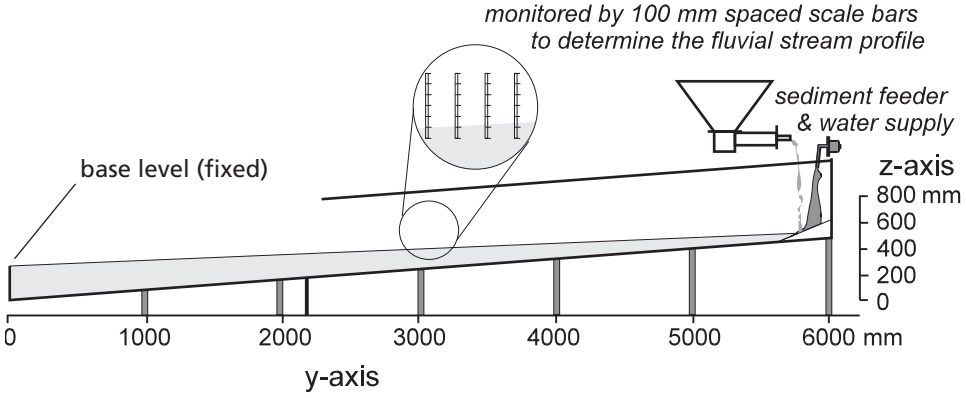

Figure 4.1 Experimental setup in cross section. The catchment area is represented by the sediment feeder and water supply (right side of the figure). The lower part of the valley (0 – 2200 mm) is monitored with a laser sensor mounted on a computer-controlled automated positioning system. The upper part of the valley (2200 – 6000 mm) is monitored with rulers attached to one side of the fluvial duct at 10.0 cm intervals.

sediment volume through a worm gear. The measured deviations in sediment delivery by the sediment feeder were less than 1%. We used unimodal medium sand with a median grain diameter of 250 μm as the sediment supplied by the sediment feeder. We recorded the development of the sediment surface by measuring the surface elevation with a laser (with a precision of 0.4 mm or better in all three dimensions) attached to a computer-controlled positioning system suspended from the ceiling in the downstream half of the duct and with rulers attached to the transparent sides of the fluvial duct at 10 cm intervals in the upstream half of the duct (with a precision of 0.5 mm).

Procedure

We started the experiments by letting the system attain equilibrium by running it for a period in excess of the equilibrium time of the setup (which is approximately 12 hours). Equilibrium was taken to be attained when the volume of sediment delivered to the mouth of the flume matched the volume delivered by the sediment feeder without significant deviations over a period of several hours. This was verified independently by measuring the changes in the valley profile: when the profile had attained a (dynamic) equilibrium (i.e., the average gradient was stable) the system was considered to be in equilibrium. During the experiment the profile and the sediment flux at the valley mouth were measured at intervals of half an hour while the system was changing rapidly and at one hour intervals when changes were becoming that slow that no significant changes were observed over half hour intervals.

Scenarios

The rationale behind the choice of scenarios and the experimental procedure was to study the impact on a river valley of changes that are too rapid for the system to attain equilibrium, in this case over an interval of $0.5 \times T_{eq}$ and $0.1 \times T_{eq}$.

The scenarios of the experiments consist of a decrease in discharge (Q_w) of 43% (350 dm^3/h to 200 dm^3/h) for a duration of $0.5 \times T_{eq}$ of the flume and a decrease of 43% in discharge (350 dm^3/h to 200 dm^3/h) for a duration of $0.1 \times T_{eq}$ of the flume, both under a constant sediment influx of 1.5 dm^3/h (Fig. 4.2). The absolute values chosen for the discharges and sediment

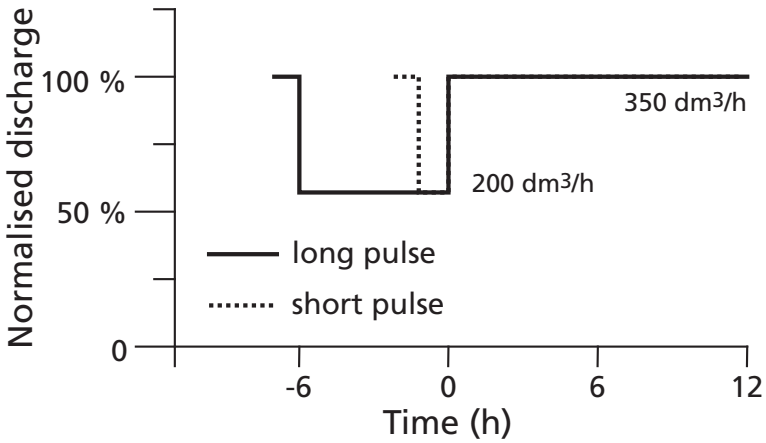

Figure 4.2 Scenarios used in the experiments. Discharge was reduced by 43% during a period of 0.5 × Teq of the model (6 hours), and during a period of 0.1 × Teq of the model (1.2 hours). Sediment influx was constant, at 1.5 dm3 / h. After the restoration of initial conditions the experiments were continued for 3 × Teq (36 hours).

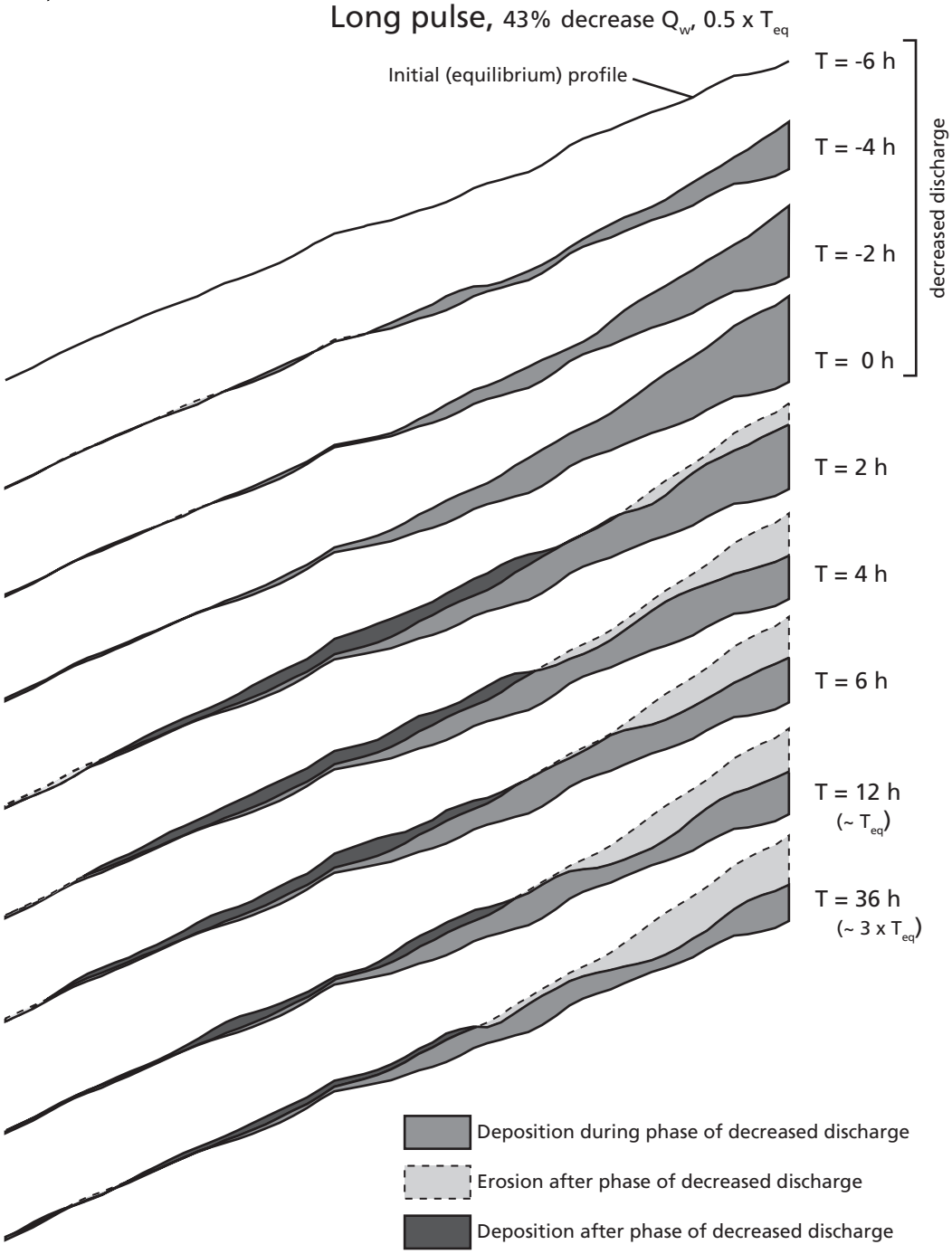

Figure 4.3 Development of the longitudinal profile during the experiment with a long discharge pulse. In this experiment discharge was reduced by 43% during a period of 0.5 × Teq of the model, i.e., 6 hours. Erosion is indicated in light gray and deposition in dark gray. Medium gray indicates the sediment deposited on top of the equilibrium surface between T = -6 h and T = 0 h. The pattern is described and explained in detail in Fig. 4.5.

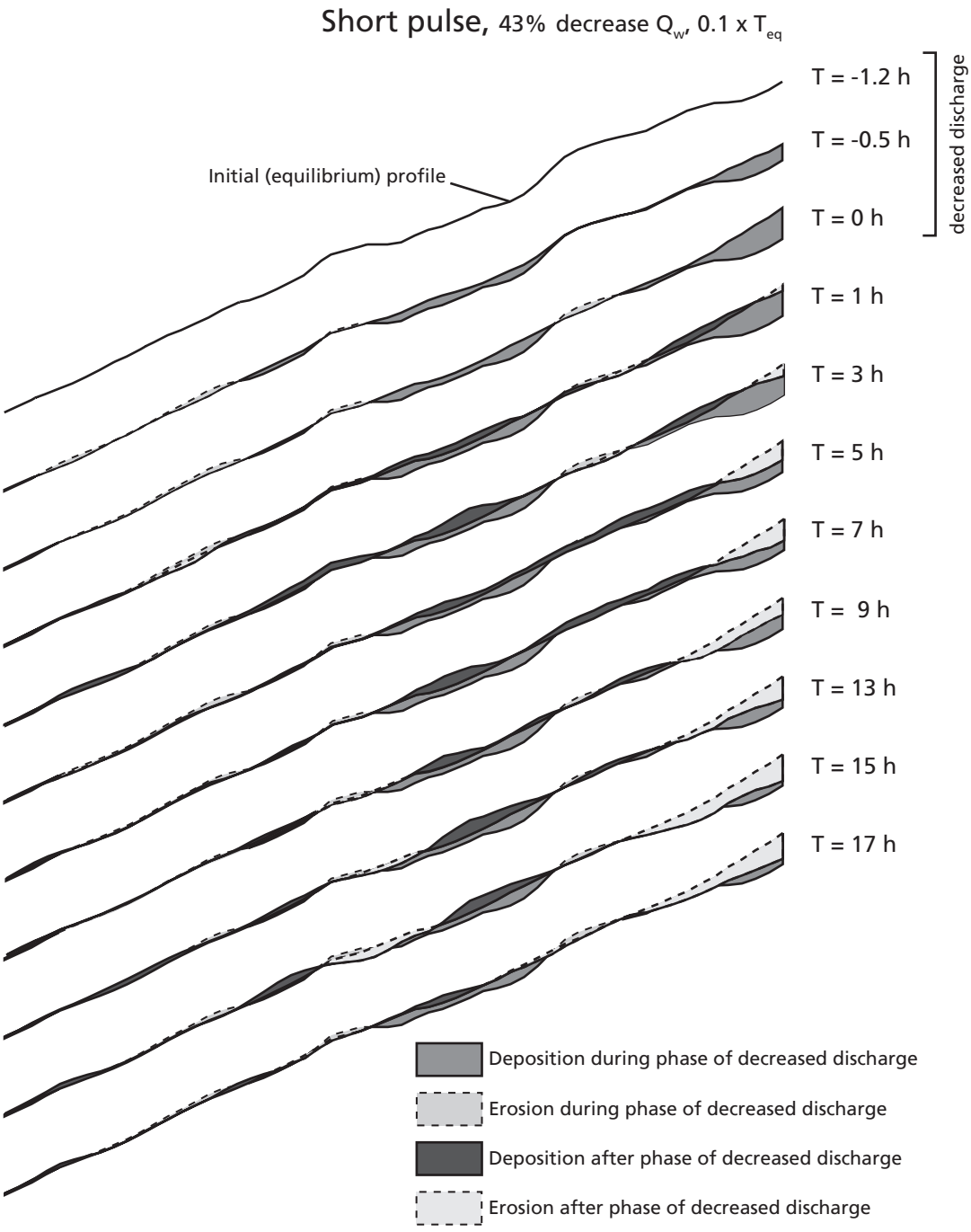

Figure 4.4 Development of the longitudinal profile of the experiment with a short discharge pulse. In this experiment discharge was reduced with 43% during a period of 0.1 × Teq of the model, i.e., 1.2 hours. Erosion is indicated in light gray and deposition in dark gray. Medium gray indicates the sediment deposited on top of the equilibrium surface at the start of the experiment. The pattern is described and explained in detail in Fig. 4.5.

fluxes were based on the requirement to keep time-averaged sediment transport rates realistic (a full explanation can be found in Van Heijst et al., 2001) and the range of slopes allowed by the setup. The equilibrium conditions (the 'normal' discharge and the sediment influx) from which the perturbations were started and to which the system recovered after the perturbations were chosen to be in between the practical upper and lower limits for discharge and sediment flux in our model. Since the absolute values of discharge and sediment flux are irrelevant in the context of this paper, discharge and sediment flux are normalised against the discharge and sediment flux going into the system at the head of the fluvial duct.

We expected both these scenarios to result in an increase of the gradient of the river valley in response to the decrease in discharge, followed by a decrease of the gradient in response to the return to initial conditions. Changes in discharge and sediment load cause changes in the profile of a river (Mackin, 1948). An increase in sediment load or a decrease in discharge cause the slope of the profile to increase, and a decrease in sediment load or an increase in discharge have the reverse effect, i.e., a lower gradient (Mackin, 1948).

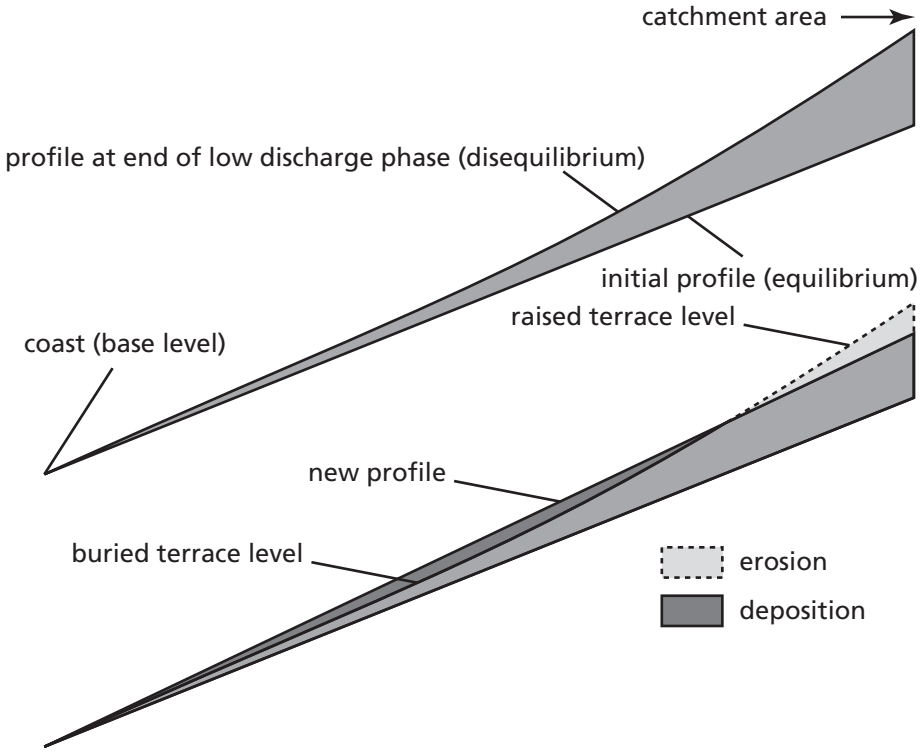

Figure 4.5 Schematic profile development and creation of terrace intersection in our experiments. The upper part of the figure shows the situation just before the discharge is restored to its initial level, 6 hours ($0.5 \times T_{eq}$) after the onset of the perturbation in the discharge, in a state of disequilibrium. The lower part of the figure schematically shows the system one hour after the return to the higher initial discharge level. In the upstream, previously steepest part of the valley deep erosion has reduced the gradient. Downstream of this zone, sediment has been deposited in a wedge on top of the previous surface. The result is that in the upstream part the new valley profile has a lower gradient than the profile just prior to the increase in discharge. After this geometry has developed, it remains more or less stable during the rest of the experiment, while the profile is gradually decreased evenly over the entire valley towards the equilibrium profile for the new discharge level.

Results

The response of the system to the changes in discharge is shown in Figure 4.3 (long pulse) and Figure 4.4 (short pulse). The changes in the short pulse experiment (Fig. 4.4) are smaller because of the shorter duration of the pulse, and are relatively small compared to changes resulting from autocyclic processes in the flume (even in equilibrium, the system is dynamic). Although the pattern that emerges is less clear, it shows the same trend as the pattern displayed by the long pulse scenario (Fig. 4.3). For clarity only the results of the long pulse experiment will be discussed.

The gradient of the river valley did indeed show an increase of the gradient in response to the decrease in discharge and a decrease of the gradient in response to the subsequent increase in discharge (Fig. 4.3). The increase of the gradient was not uniform over the length of the profile, however, but was strongest in the upstream part of the valley, resulting in a concave profile (Fig. 4.3, T = 0 h, and Fig. 4.5). Since the equilibrium profile of the model is straight (as a consequence of the unimodal size distribution of the sand that is used and the lack of tributaries) this is a clear indication of disequilibrium.

The decrease of the gradient in response to the increase of discharge was not uniform either. As is illustrated by Figure 4.3 (T = 1 h) and Figure 4.5, the upstream part of the valley, where the gradient was steepest, started eroding rapidly, and a wedge of sediment was deposited rapidly in the middle part of the valley, where the gradient was lower. The sediment deposited

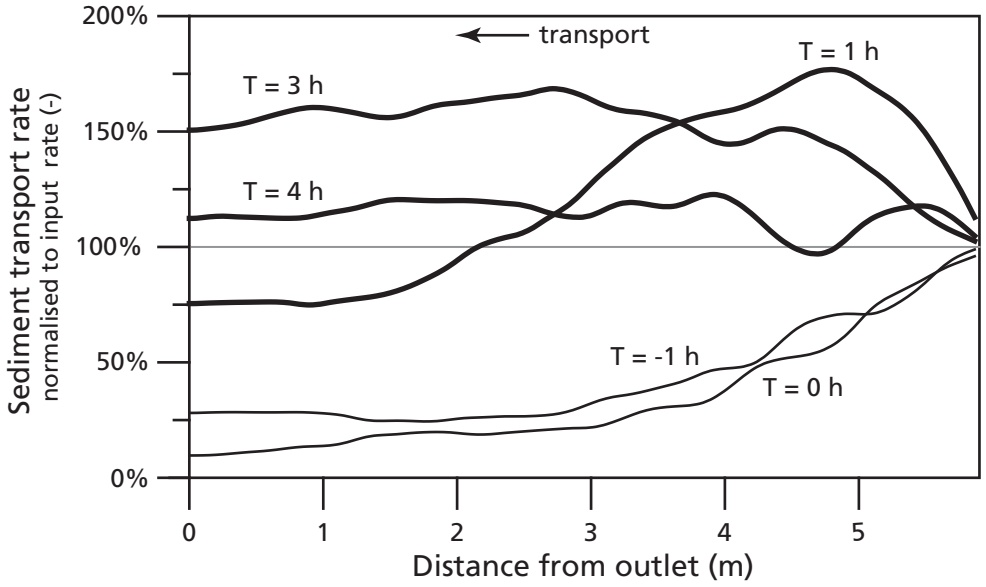

Figure 4.6 Sediment transport rate normalized to the sediment input rate along the profile for the long discharge pulse experiment. When the sediment transport rate is approximately 100% of the input rate over the entire profile, there is no net change in the profile, which means that the system is in equilibrium (none of the curves shown here meets this criterion). The slope of the curves indicates erosion or deposition at the particular location along the profile. A positive slope indicates that the transport rate is increasing at that point, which implies that sediment must be eroded at that point. A negative slope indicates that the sediment transport rate is decreasing, which implies that sediment must be deposited at that point. A more or less horizontal sediment transport curve indicates that the sediment transport rate at that point does not change, which implies that the profile is in equilibrium at that point. The transport rate at the outlet of the valley (at 0 m) represents the yield of the system.

in the wedge consists of both sediment derived from upstream erosion and sediment from the catchment area (Fig. 4.6, T = 1 h). The yield at the valley outlet initially remained below 100% of the input from the catchment area (Fig. 4.6, T = 1 h). The simultaneous upstream erosion and downstream deposition occurred rapidly in comparison to the equilibrium time of the model. . We relate this phenomenon to the decrease in transport capacity caused by the decrease in gradient in the middle part of the valley. The steep gradient in the upstream part of the valley enabled a large amount of sediment, made available by erosion, to be transported downstream. This is shown in Figure 4.6 (T = 1 h): the sediment transport along the river profile in our experiment increases sharply in the upstream part of the model, indicating erosion. In the downstream direction the gradient decreased (Fig. 4.3), and herewith the transport capacity of the system, resulting in deposition, reflected in Figure 4.6 (T = 1 h) as a decrease in sediment transport in the downstream part (~4.5 m) of the valley. The point at which sediment transport shifts from increasing (i.e., erosion) to decreasing (i.e., deposition) defines the potential location of the river terrace intersection. The erosion and deposition processes reduced the steep upstream gradient and increased the low downstream gradient (Figures 4.3 and 4.5), thereby reducing the contrast in stream power between the upstream and downstream parts of the system and causing slower and more uniform decrease of the gradient along the profile (Fig. 4.3).

Discussion

Terrace formation in the Rhine-Meuse River

The Late Weichselian onshore deposits of the Rhine-Meuse River show several terrace levels. The Lower Terrace was created during the Late Pleniglacial (at the Last Glacial Maximum, 18 ka) under conditions of high sediment supply, which resulted in a relatively high gradient (Törnqvist, 1998) (Fig. 4.7). The so-called 'Terrace X' is of Younger Dryas age (11-10 ka). It was created under conditions of relatively high discharge and low sediment load, and is characterised by a relatively low gradient (Törnqvist, 1998) (Fig. 4.7). Both these terraces can be traced and correlated from locations close to the present coastline up to 200 km upstream along both the Rhine and Meuse rivers (Huisink, 1997; Törnqvist, 1998; Berendsen and Stouthamer, 2000). The Lower Terrace and Terrace X intersect close to the present coastline and progressively divert upstream (Törnqvist, 1998) (Fig. 4.7). Apparently the relatively

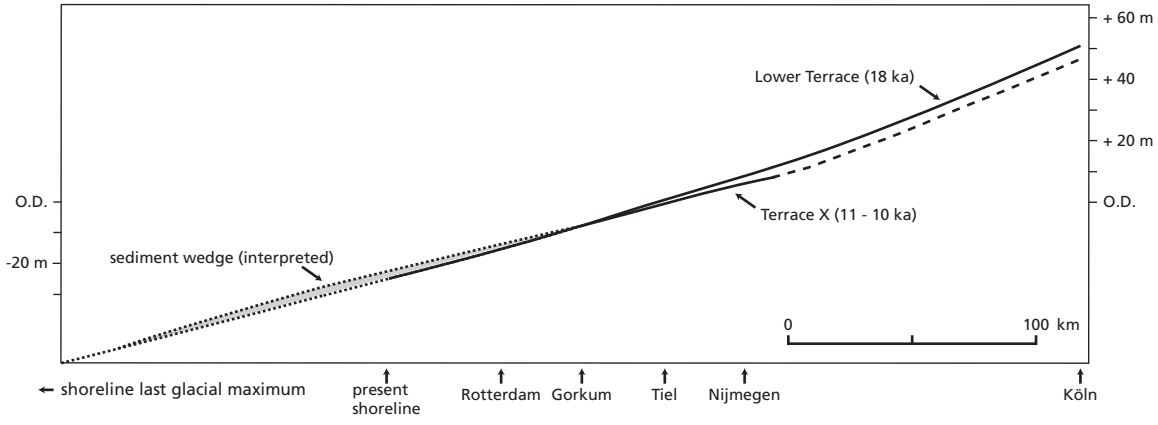

Figure 4.7 Lower Terrace and Terrace X intersection in the Rhine-Meuse River (after Törnqvist, 1998), and schematic depiction of the associated sediment wedge, based on the extent of the Kreftenheye Formation (see Fig. 4.8).

high-gradient river valleys of the Last Glacial Maximum (represented by the Lower Terrace) were incised during the Younger Dryas due to relatively high discharge, causing the creation of relatively low-gradient river valleys, represented by Terrace X. This primary role of climate change in the creation of these terrace levels is undisputed (e.g. Huisink, 1997; Törnqvist, 1998). However, the longitudinal equilibrium profile of a river is graded to base level, which was probably located in the Strait of Dover at the time of the formation of the youngest terrace (Cohen et al., 2002). The location of the intersection point, about 200 kilometres upstream of base level, requires an additional explanation.

Tectonics

Regional tectonics and glacial isostasycan be ruled out as a primary factor in the creation of these intersecting terraces and the location of the intersection point. Uplift could cause incision of the river system. However, the area is characterised by subsidence and aggradation since the Late Weichselian (Cohen et al., 2002). If subsidence would have been a significant factor in the creation of the terraces, the opposite pattern would have been found: a younger terrace level above an older terrace level, intersecting near the hinge line. If subsidence played a role, it can only have counteracted the observed pattern.

Sea level

Törnqvist (1998) suggested that backfilling during early sea-level rise created a coastal prism, thus creating the terrace intersection near the present coastline. Since the Rhine-Meuse River probably drained through the Strait of Dover during the Weichselian (Bridgland and D'Orlier, 1995) (Fig. 4.8) and base level was fixed at 40-50 m below present sea level due to a resistant sill in the Strait of Dover (Cohen et al., 2002), this is unlikely. Even if base level would have been controlled by sea level, it would require that a coastal prism were created with an extent of more than 200 kilometres, between the coast and the point of terrace intersection. The Late Pleistocene channel deposits of which the Lower Terrace and Terrace X are part do not extend more than 80 km beyond the present coastline, however (Laban and Rijsdijk, 1993). Furthermore, the hypothesis of Törnqvist (1998) requires the river system to be graded to base-level. Assuming a river length of 300 km between catchment area and shoreline, the equilibrium time of the Rhine-Meuse system is of the order of 200 ky (Paola et al., 1992; Castelltort and Van Den Driessche, 2003). This implies that it is impossible for the river system to have been graded to the rapidly changing base-level over hundreds of kilometres during the 3 ky period between formation of the Lower Terrace and Terrace X.

Climate change

This leaves climate as the only forcing process that can reasonably account for the intersection between the Lower Terrace and Terrace X (Fig. 4.7).

The first order geometry of the model matches that of the natural system. Our experiment starts with a buildup of sediment (in response to decreased discharge), mainly in the proximal reaches, but does not have the time to reach an equilibrium profile (Fig. 4.5). In the Rhine-Meuse River aggradation prevailed in the upper reaches of the river system during the Pleniglacial (Törnqvist, 1998). This episode of aggradation did not last long enough (approximately 50 ky) for the system to attain an equilibrium profile. Both the model and the natural system start from a situation of strong aggradation in the proximal reaches under disequilibrium conditions. This initial situation is followed by a rapid (relative to the

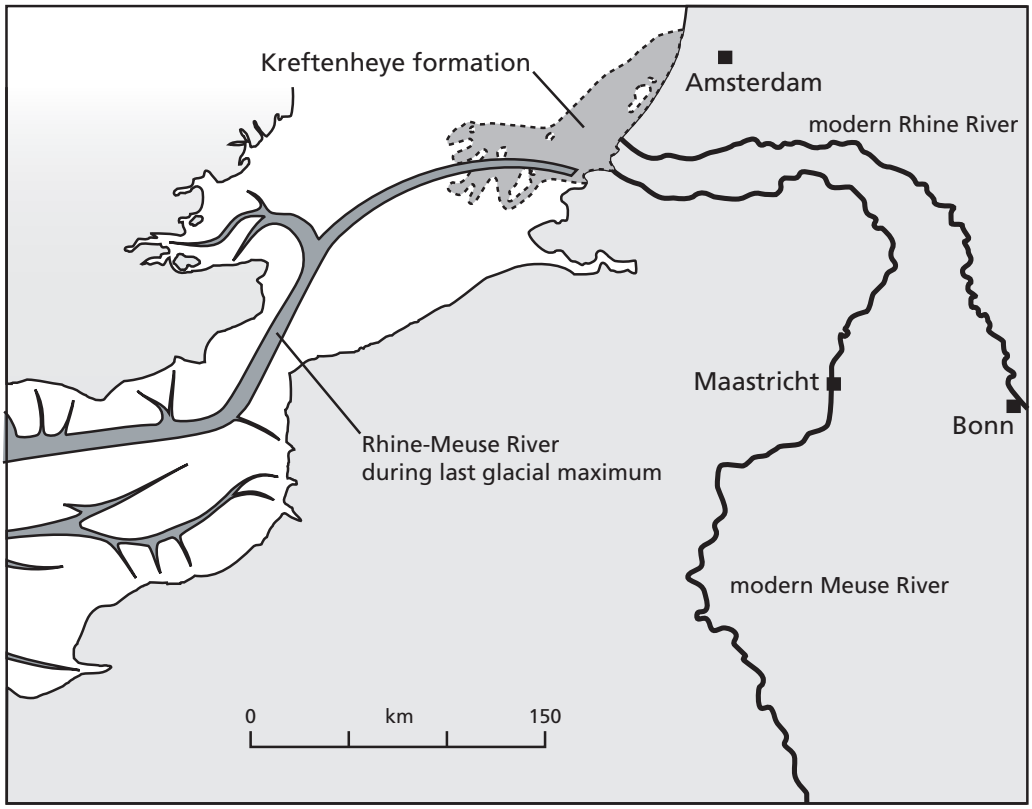

Figure 4.8 Probable location of the Rhine-Meuse River during the last sea-level lowstand (after Bridgland, 2002), and offshore extent of the Kreftenheye formation (after Laban and Rijsdijk, 1993).

equilibrium time of the system) increase in discharge (transport capacity), both in the model and in the natural prototype. In the model this results in very rapid erosion in the proximal part of the system and deposition in the middle reaches of the river system, as described in detail in the results section (Fig. 4.5). At the point where the zone of erosion meets the zone of deposition, the new, lower river valley gradient intersects the old, higher river valley gradient. The change in river valley gradient in the model is very similar to the pattern of terrace intersection found in the Rhine-Meuse River (Fig. 4.7). Downstream of the terrace intersection point, in the model, a wedge of sediments is deposited (Fig. 4.5). This sediment wedge tapered off downstream and did not reach the location that represents the coastline during the experiment (Fig. 4.5). In the Rhine-Meuse system, the extent of the Late Pleistocene deposits downstream of the intersection between the Lower Terrace and Terrace X is limited to a location roughly 300 kilometres upstream of the Late Pleistocene coastline (Laban and Rijsdijk, 1993; Bridgland and D'Olier, 1995).

Complex response

The relevance of the results of the experiments is not the duration of the period of decreased discharge in the experiments, but the rapid and complex response of the system to the rapid increase in discharge while the model system was in a state of disequilibrium. The experiments

show that climate change alone is capable of creating a complex stratigraphic architecture. Interpretation of the intersecting terrace levels in the Rhine-Meuse River in terms of forcing by climate change alone, deserves serious consideration.

Conclusions

The results of these experiments show that the stratigraphic architecture found in the Rhine-Meuse River, i.e., intersecting river terraces, could have been caused, in a state of disequilibrium, by an increase in discharge alone. No other external forcing mechanisms are required to explain the geometry. A relatively low discharge, combined with a relatively high sediment load, causes a steep buildup of sediments in the upstream segment of the river valley, while the downstream part maintains the relatively gentle gradient of the pre-existing river profile. As soon as discharge is increased, rapid erosion in the upstream part combined with rapid, simultaneous deposition in the downstream part creates a terrace intersection and a wedge of sediment with limited extent immediately downstream of the intersection. This geometry is created rapidly, and remains relatively stable thereafter.

Chapter 5

Matlab tool for constructing synthetic stratigraphy from sequential DEMs

A.P.H. van den Berg van Saparoea

Introduction

Physical modelling is widely used in the earth sciences, for example in modelling studies in geomorphology (e.g. Metivier et al., 2005), landscape evolution (e.g. Bonnet and Crave, 2003), stratigraphy (e.g. Milana and Tietze, 2002 and van Heijst et al., 2002) and tectonics (e.g. Persson et al., 2004). Various methods are used to measure and record the results of these experiments, ranging from simple photographs to laser altimetry and X-ray-computed tomography (CT) images (e.g. Ellis et al., 2004). The latter technique provides 3D images of the interior geometric evolution of an experiment, which is, at least in terms of geometry, the most complete data set attainable.

However, for most model setups computed tomography is not feasible, because the setups are too large. Instead, a common method of gathering data is making scans of the elevation of the surface of the model at intervals (Digital Elevation Models, DEMs) using laser altimetry or similar techniques. This method does not provide direct information on the subsurface geometry of the model, however, and it is therefore usually combined with the making of vertical sections of the final product of the experiment, of which peels (e.g. van Heijst et al., 2002)) and/or digitally processed photographs (e.g. Paola, 2000) are made, which can then be analysed. Since this method is destructive, it can only be used after an experiment has been finished, and it reveals only the final state of the experiment. Furthermore, it is time-consuming and the reconstruction of true chronostratigraphic surfaces can be problematic, as it is in natural systems. Although the usefulness of making these sections is undisputed, additional information on the 3D buildup of the model and especially its development during an experiment would be a great asset.

We present a Matlab tool designed to reconstruct the 3D geometric evolution of modelling experiments from series of DEMs. The DEMs of the surface of a model represent the chronostratigraphic surfaces mentioned above. These DEMs constitute a perfect stratigraphic data set: not only is every surface a true chronostratigraphic surface of which the exact age is known, the entire development of each surface through time can, in principle, be reconstructed. The ability to generate complete three-dimensional stratigraphic data sets and their evolution has hardly been utilized until now. Analysis of this type of experimental data is usually limited to comparisons of the surface of the model at different moments in the experiment. Besides this the presentation of the data is often in a format that is not immediately recognizable and intuitive to a geologist, which complicates interpretation and communication of results.

In this paper we describe a set of algorithms used to make a reconstruction of the stratigraphy of a model, and to obtain geologically relevant information based on a set of successive DEMs. Furthermore, the manner in which this information can be presented in a useful format is illustrated and opportunities for further development are discussed.

Algorithms

The basic principles behind the algorithm are very straightforward. By calculating the difference in elevation between successive DEMs, deposition, erosion, and non-deposition during the time slice between the two DEMs can be determined. By storing the elevation of the chronostratigraphic surface for each time slice and correcting for erosion after each next step, the complete history of the experiment can be assembled. Information on the amount of deposition or erosion for each location can be calculated and stored for each time slice.

Before describing the algorithms, the use of a number of geological concepts in the context of our model should be explained. The term stratigraphic unit in our model applies to the body of sediment deposited between two successive DEMs. A stratigraphic unit is delimited by true chronostratigraphic surfaces. The lower boundary of all erosion occurring between two DEMs forms one erosion surface, which means that an erosion surface is not necessarily continuous. In the current version of our tool, composite (diachronous) erosion surfaces (i.e., amalgamated or connected erosion surfaces of different ages) are not recognised as distinct entities.

```
//
// deposition
// this code is applied to every point on the grid
//

if currentSurfaceElevation > previousSurfaceElevation then
// if deposition has occurred

   lowerBoundingsurfaceElevation := previousSurfaceElevation


else
// if no deposition (or erosion) has occurred

   lowerBoundingSurfaceElevation := currentSurfaceElevation;

// the upper bounding surface of the youngest stratigraphic unit
// is always the youngest DEM
upperBoundingSurfaceElevation := currentSurfaceElevation;

// calculate thickness of deposit
deposition := upperBoundingSurfaceElevation
                          - lowerBoundingsurfaceElevation;
```

Figure 5.1 Pseudocode describing the algorithm used to determine the boundaries of a new stratigraphic unit.

Creating stratigraphic units

For calculating the amount of deposition and finding the upper and lower boundaries of stratigraphic units deposited between successive scans the logic presented in Figure 5.1 is used. With this procedure a new stratigraphic unit is created by determining its boundaries and thickness. The stratigraphic unit has an upper and lower bounding surface at every location, but its thickness can be nil, which represents non-deposition. This is different from the situation in which the stratigraphic unit has been entirely eroded at a certain location, in which case it no longer exists at this location. Since the thickness of the deposit is implicit in the difference between the elevation of the chronostratigraphic surfaces it is not strictly necessary to store it. However, if a cut-off value is introduced to reduce clutter caused by measurement errors and noise instead of determining the actual existence of the stratigraphic unit by checking for a thickness of zero, it is easier to check it against the stored thickness than to calculate the thickness at that moment. Therefore the thickness is calculated and stored explicitly. With a simple if-statement within the calculation procedure all values below the cut-off level can then be set to zero, eliminating the necessity to make this decision elsewhere in the code, which would be more complicated and thus increase overhead.

```
//
// total erosion
// this code is applied to every point on the grid
//

if currentSurfaceElevation < previousSurfaceElevation then
// if erosion has occurred

  begin
  depthOfErosion := previousSurfaceElevation -
  currentSurfaceElevation;
  erosionSurfaceElevation := currentSurfaceElevation;
  end;

else
// if no erosion has occurred

  begin
  depthOfErosion := 0;
  erosionSurfaceElevation := currentSurfaceElevation;
  end;
```

Figure 5.2 Pseudocode describing the algorithm used to determine the surface of a new erosion surface and the total volume of

Erosion

Calculating erosion is slightly more complicated because it involves the modification of existing stratigraphy. The process can be split into two logical parts: creation of the new erosion surface, which is essentially the opposite procedure of calculating deposition, and modification of existing deposits.

Figure 5.2 shows the algorithm used to evaluate erosion. In analogy to stratigraphic units, erosion surfaces also have an elevation and a depth of erosion for every point on the grid. If no erosion has occurred, erosion depth is set to zero and the elevation is set to the surface elevation, signifying that the surface does exist, but is a correlative non-deposition surface instead of a true erosion surface, as opposed to being non-existent at that point, which happens if the erosion surface is eroded by subsequent phases of erosion. Again, a cut-off value can be introduced to reduce noise in the manner described for the creation of stratigraphic units.

```
//
// erosion of existing stratigraphic units
// this code is applied to every point on the grid
// for every stratigraphic unit
//

if unit.lowerBoundaryElevation >= currentSurfaceElevation then
// if stratigraphic unit has been completely eroded at these coordinates

   begin
   unit.lowerBoundaryElevation := 0;
   unit.upperBoundaryElevation := 0;
   unit.thickness := 0;
   end;

else if unit.upperBoundaryElevation > currentSurfaceElevation then
// if stratigraphic unit has been partially eroded at these coordinates

   begin
   // lower boundary elevation is unchanged
   // upper boundary elevation is corrected for erosion
   unit.upperBoundaryElevation := currentSurfaceElevation;
   // thickness is corrected for erosion
   unit.thickness := lowerBoundaryElevation -
                                    upperBoundaryElevation;
   end;

// if no erosion has occurred, the stratigraphic unit remains unchanged
// at these coordinates,so there is no need for a final else statement
```

Figure 5.3 Pseudocode describing the algorithm used to evaluate modifications to existing stratigraphic

```
//
// erosion of existing erosion surfaces
// this code is applied to every point on the grid for every erosion surface
//


if erosionSurfaceElevation > currentSurfaceElevation then
// if stratigraphic unit has been eroded at these coordinates

   erosionSurfaceElevation:= 0;
```

Figure 5.4 Pseudocode describing the algorithm used to evaluate modifications to existing erosion surfaces.

The algorithms used to correct existing stratigraphic units and erosion surfaces for erosion are shown in Figure 5.3 and Figure 5.4 respectively. The algorithm evaluates whether erosion has occurred and, if so, how much of the stratigraphic unit has been removed. Erosion of surfaces, which have no thickness, consists only of evaluation of the occurrence of erosion. Stratigraphic units and erosion surfaces that have been completely eroded at a particular location are assigned an elevation of zero for that location to indicate that they do not exist there, as opposed to having no thickness, which specifies non-deposition.

Implementation

The algorithms used to evaluate deposition and erosion are straightforward and require little code. Most of the code in our tool performs elementary tasks such as supplying the algorithms with data and storing the results. ASCII format text files are used for input and permanent storage of the output. This assures compatibility with almost any other program that could be used in this context.

Since the algorithms only apply to elevation data, they are identical for one-, two- and three-dimensional data sets. The supporting code implemented in our tool handles three-dimensional data. It can be used to process one- or two-dimensional data simply by restricting the horizontal coordinates of input data to lines or points. Cross sections are constructed by processing two-dimensional subsets taken from our raw input data. This is described further below. This approach eliminates the need for additional code to analyse the complicated three-dimensional stratigraphy data after processing. The much smaller size of a two-dimensional data set compared to a three-dimensional data set strongly reduces computation time, so that the overhead caused by repeating the analysis is minimal. The same principles apply to the construction of logs through the stratigraphy.

Performance

For our current application of the tool, however, performance is excellent. A typical data set consists of approximately ten DEMs containing 25 000 data points each. Using MATLAB on a desktop computer with an AMD Athlon 1.6 GHz processor running Windows XP processing takes no more than ten minutes. Analysis of a vertical section through ten DEMs containing 200 data points takes approximately ten seconds. Since the DEMs obtained from our experiments are produced at a rate of no more than one or two per day, performance far exceeds our current requirements.

Automation

A completely different aspect of the software is the visualization of the results. Doing this by hand is very time-consuming. Since much of the work is simple and repetitive it is well suited for automation. It speeds up the process enormously, and eliminates errors made while doing repetitive tasks.

A good example of automation is the construction of sections. Selecting the location can only be done by hand. We use the digitisation function of Golden Software Surfer to select points along a line of interest by hand. The slice function can then be used to extract the required data from the DEMs. This operation needs to be performed on each of the DEMs in a series without any further decision making. Automating this procedure makes it a very simple task that can be executed quickly for any number of DEMs.

Application

We use the prototype of our analysis software in our research to test it in operational conditions. Flexibility and ease of use of the prototype are limited, but despite this drawback it offers a huge improvement in the quantity and quality of the information obtained from our experiments. Representation of the information in a format that is familiar to a geologist makes understanding an interpretation of the results much easier.

We currently use three basic types of representation. The first is the geological map. This is constructed by overlaying contour maps of the thickness of stratigraphic units, in which only two levels are displayed: thickness equals nil and thickness is greater than nil. The map can then be combined with a 3D wireframe or surface map (Fig. 5.5). Since the complete development of the stratigraphy through time is known, successive geological maps can be made, as is illustrated in Figure 5.6. Net erosion and deposition between successive maps is also indicated in Figure 5.6. The erosion/deposition maps can be extended to erosion per stratigraphic unit during this interval, as this information is also contained in the three-dimensional stratigraphy.

The second type of geological representation, already mentioned above, is vertical sections through the stratigraphy. Figure 5.7 shows a series of such sections through the stratigraphy. In this particular scenario an extensive erosion surface can be seen to develop. The final erosion surface is made up of sections of widely varying ages (indicated under the sea level curve in Figure 5.6).

The final type of visualisation is the Wheeler diagram, i.e., the distribution of deposition (and in this case also erosion) in space plotted versus time. Figure 5.8 shows two Wheeler diagrams for contrasting experiments, one in which deposition is widespread an erosion nearly absent and one in which deposition is more localised and erosion plays an important role. Because the development of the system as well as the final result is available, our Wheeler diagrams contain more information than Wheeler diagrams constructed from field data (which are necessarily derived from the final product only). In these Wheeler diagrams not only erosion is indicated, but also the original extent of deposition. Wheeler diagrams can be constructed for every time slice, which allows further specification of information such as the timing of erosion. Construction of these diagrams involves relatively complex,

Figure 5.5 Creation of a geological map. Contour plots of individual stratigraphic units are overlaid on a wireframe map of the model. We use Golden Software Surfer for this purpose.

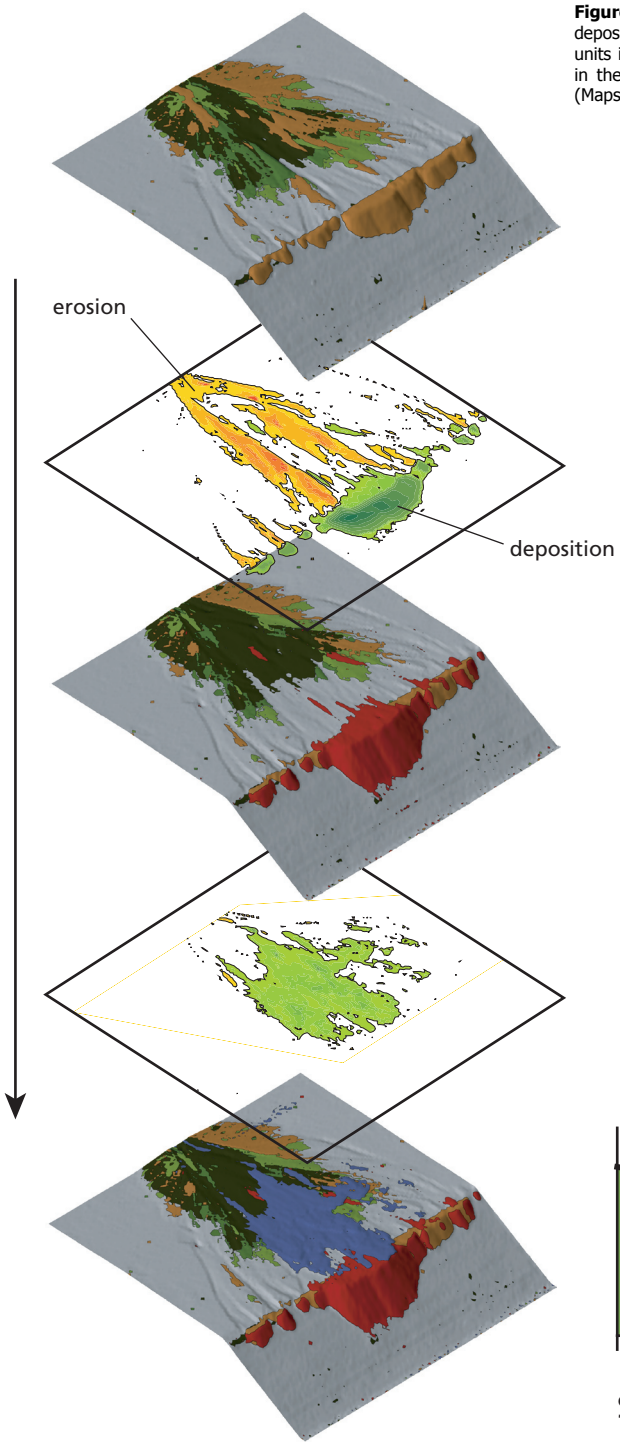

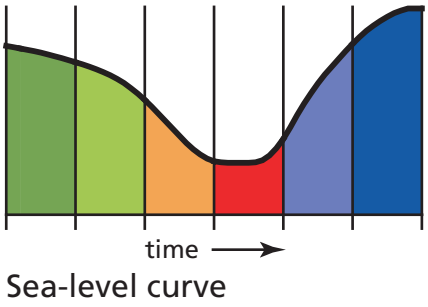

Figure 5.6 Successive geological maps and total erosion and deposition between each step. The colors of the stratigraphic units in the geological maps correspond with the time slices in the graph of the sea level curve used in this scenario. (Maps made with Golden Software Surfer.)

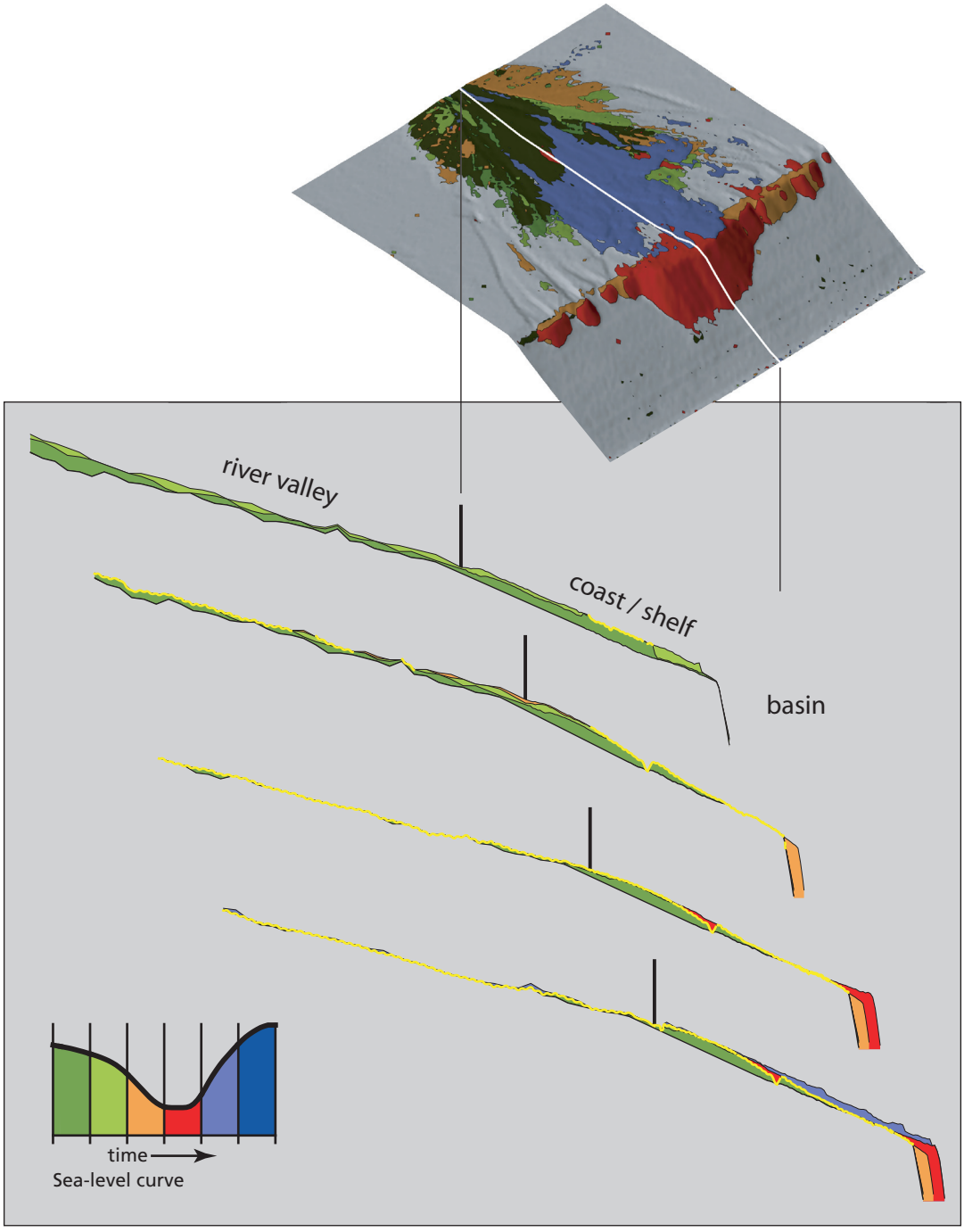

Figure 5.7 Successive vertical cross sections through the stratigraphy along the section line indicated in the geological map. Erosions surfaces are indicated in yellow. In this particular scenario the erosion surface in the final section is continuous and might be interpreted to be isochronous from the end result. The preceding cross sections show that it is in fact strongly diachronous. The sections in this figure consist of overlaid line graphs made with Golden Software Grapher.

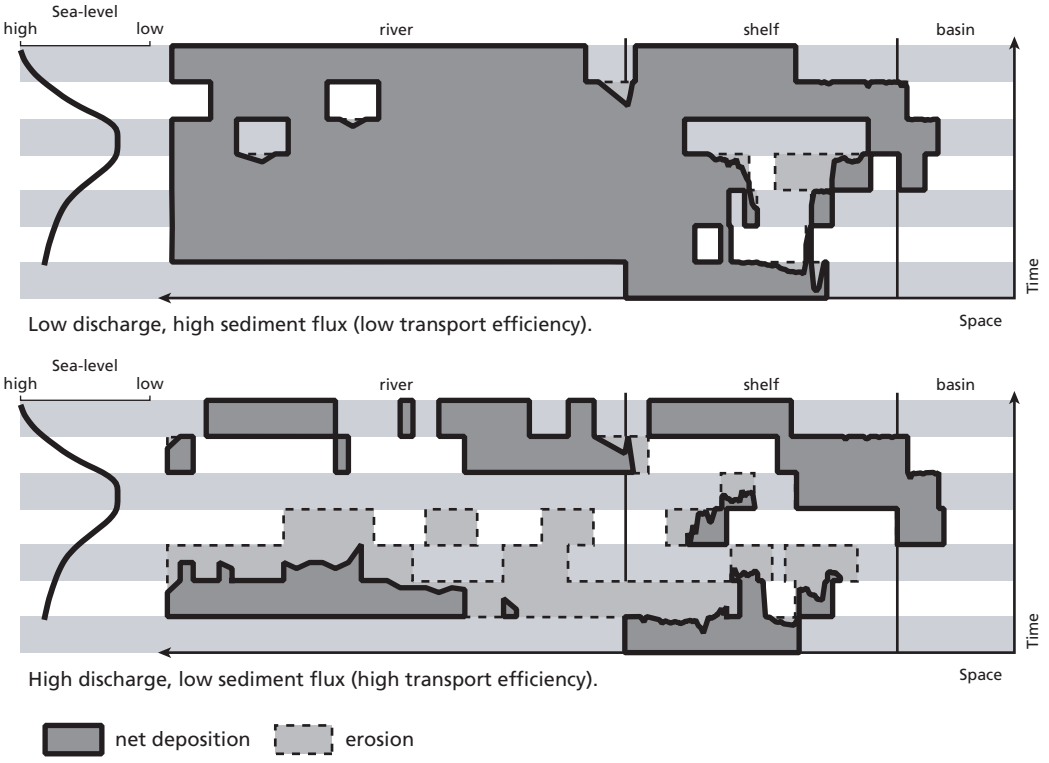

Figure 5.8 Wheeler diagrams (deposition / erosion through time). Solid lines indicate the situation at the end of each experiment (the equivalent of a Wheeler diagram for natural systems), dashed lines indicate eroded deposits.

subjective decision making to simplify them. Therefore they are not produced by the current version of our tool, but are constructed by hand instead. All input data for the diagrams are generated by the tool, however.

Future extension and opportunities

The prototype version of our tool is currently in use in active research, where it proves to be most useful in practice. Chapters 2, 3 and 4 contain examples of its practical use. The tool greatly increases the amount of information obtained from experiments and aids in interpretation of the results by presenting the model results in a geological framework. It also enables better tracking of the development of an experiment while it is running. The tool is very flexible because the input and output of data are very simple, requiring only ASCII format text files with coordinate sets and some additional information such as the age of the DEMs and the sea level associated with these ages. Any series of sequential DEMs in ASCII format can be analysed by the software.

We have plans to make a fully operational version of the software with a user-friendly (graphic) interface and a better design to enable easy future extension and addition of functionality. An important feature that will be incorporated in the full version of the tool is an object-oriented design. This will make maintenance and extension of the tool much easier and will simplify internal data management and data integrity. A simplified class diagram of

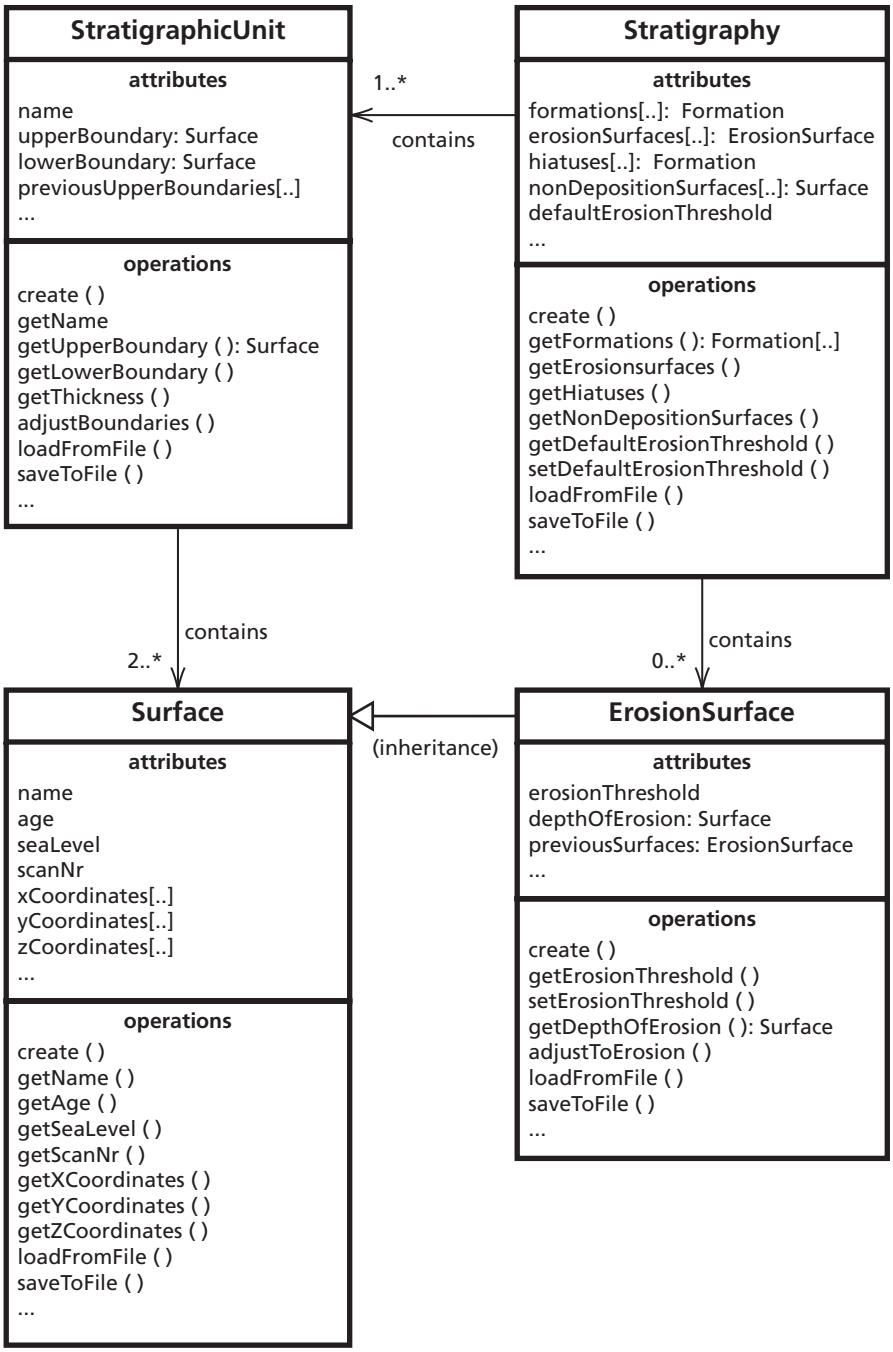

Figure 5.9 Simplified and incomplete UML (Unified Modeling Language) class diagram illustrating what the basic object oriented design of our tool might look like. The deposition algorithm is part of the constructor (create operation) of the StratigraphicUnit class, the erosion of existing strata algorithm is used by the adjustBoundaries operation of the StratigraphicUnit class, the total erosion algorithm is part of the constructor of the ErosionSurface class, and the erosion of erosion surfaces algorithm is used by the adjustToErosion operation of the ErosionSurface class. (A complete specification of UML and additional information can be found at www.uml.org.)

the design is shown in Figure 5.9. The diagram is incomplete, but it does illustrate essential elements of the design. The algorithms presented here are integrated into this design. The algorithm for determining the boundaries of a new stratigraphic unit (Fig. 5.1) is part of the constructor (procedure named 'create' in Figure 5.9) of the Stratigraphic unit class, the 'adjustBoundaries' procedure of the same class contains the algorithm for evaluating modifications to existing stratigraphic units by erosion (Fig. 5.3), the algorithm used to find the elevation of a new erosion surface and the total volume of erosion (Fig. 5.2) is located in the code of the constructor of the ErosionSurface class (Fig. 5.9) and the adjustToErosion procedure of this class uses the algorithm described in Figure 5.4, which is responsible for evaluating the state of erosion surfaces after subsequent erosion events.

This design enables easy extension of the tool. Fence diagrams and the explicit inclusion of hiatuses and composite erosion surfaces are examples of straightforward additions. More complicated features such as determination of sediment composition and maturity require the design of additional algorithms based on carefully thought-out assumptions and simplifications. Finally, calculation of the effects of tectonics may be incorporated as well. Providing that the applied subsidence or uplift are known precisely for every point on the DEMs, this is a straightforward operation as well.

In summary, this new way of analysing DEM data obtained from physical modelling experiments provides a significant improvement in the type and quantity of information produced from these experiments, which eases interpretation of the results and opens up new opportunities. In addition it reduces the time required for data processing and producing results. The possibilities for adding new features to the tool promise further gains.

Chapter 6

Epilogue

The nature of geological models is such that they can never provide undisputable conclusions, or prove or refute hypotheses with certainty. They can be very useful, however, if applied to the right problems and used with appropriate caution. Geological models, especially analogue models, can be used for the development of conceptual models and to explore solution spaces, constraining the probability of interpretations of natural systems. A big advantage of analogue models is that they largely prevent the inclusion of preconceived notions about the results: if a carefully thought-out and correctly executed experiment yields unexpected results, one is forced to come up with an explanation that may not fit existing concepts, thus gaining new insights. It is hardly possible to tune such models as to fit expectations or to 'correct' results, as can be very easy in numerical modelling. Chapter 3 serves as a good example: unexpected results suggested a fundamental and, in hindsight, very obvious difference between the control of discharge and the control of sediment flux on the yield of our model river systems. This explains why current literature contains both convincing evidence in favour of as well as convincing evidence against the attenuation by river systems of stratigraphic signals induced by climate change. The term climate change is not specific enough. Changes in discharge must be distinguished from changes in sediment flux. A further lesson is that surprising complexity can result from the simplest experiments, as is illustrated in chapter 4. An increase in discharge in a state of disequilibrium can cause rapid, simultaneous upstream erosion and downstream deposition, creating a complex geometry of intersecting terrace levels. Thus, even in a simple setup, the response of a system to very simple changes can be very complex. Even the most elementary large-scale / long-term behaviour is not completely understood. This implies that the interpretation of the stratigraphy of natural systems should include evidence from as many independent sources as possible to be anywhere near reliable. Furthermore, the first-order behaviour of fluvial systems in response to individual internal and external forcing processes must be understood much better before attempts can be made at understanding complicated scenarios involving various interacting external forcing processes. Finally, before a thorough understanding of the system dynamics and parameter sensitivity is attained, the value of true quantification of model results (if possible at all) is of very limited use: quantifying a process that is not understood does not improve comprehension of that process.

A good strategy for further advance in the understanding of the behaviour of fluvial systems on geological time scales deems combining analogue and numerical modelling studies with field studies of complete river systems, from source to sink, focussed on the large-scale stratigraphic architecture and sediment budget. Conceptual models developed on the basis of modelling studies will provide important insights into the first-order behaviour of river systems in response to changing external forcing processes, and enhance the quality of sequence-stratigraphic models (including the development of useful fluvial sequence-stratigraphic models). It may even allow an interpretation of the stratigraphic record in terms of discharge and sediment flux. Existing studies of the Rhine-Meuse (chapter 4), Ganges (chapter 3) and Colorado (chapters 2 and 3) Rivers are good examples of the kind

of data necessary for solving the puzzle of fluvial response to climate and tectonic change. New methods, in modelling (e.g. the generation of synthetic stratigraphy, described in detail in chapter 5) as well as in field studies, show great promise. Fluvial stratigraphy may never be predictable or unambiguously interpretable, but a much better understanding of the system dynamics can certainly be attained.

References

Anderson, J.B., Abdulah, K.C., Sarzaleojo, S., Siringan, F.P., and Thomas, M.A., 1996, Late Quaternary sedimentation and high-resolution sequence stratigraphy of the east Texas shelf, *in* De Batist, M., and Jacobs, P., eds., Geology of Siliciclastic Shelf Seas, Volume **117**: *Geological Society of London Special Publication*, p. 95-124.

Anderson, J.B., Rodriquez, A., Abdulah, K.C., Fillon, R.H., Banfield, L.A., McKeown, H.A., and Wellner, J.S., 2004, Late Quaternary stratigraphic evolution of the northern Gulf of Mexico margin: a synthesis., *in* Anderson, J.B., and Fillon, R.H., eds., Late Quaternary Stratigraphic Evolution of the Northern Gulf of Mexico Margin, Volume **79**: *SEPM Spec Publication*, p. 1-23.

Andrews, D.J., and Bucknam, R.C., 1987, Fitting degradation of shoreline scarps by a non-linear diffusion model: *Journal of Geophysical Research*, **v. 92**, p. 12857-12867.

Begin, Z.B., 1988, Application of a diffusion-erosion model to alluvial channels which degrade due to base-level lowering: *Earth Surface Processes and Landforms*, **v. 13**, p. 487-500.

Begin, Z.B., Meyer, D.F., and Schumm, S.A., 1981, Development of longitudinal profiles of alluvial channels in response to base-level lowering: *Earth Surface Processes and Landforms*, **v. 6**, p. 49-68.

Berendsen, H.J.A., and Stouthamer, E., 2000, Late Weichselian and Holocene palaeogeography of the Rhine-Meuse delta, The Netherlands: *Palaeogeography Palaeoclimatology Palaeoecology*, **v. 161**, p. 311-335.

Berryhill, H.L., 1987, The Continental Shelf off South Texas, *in* Berryhill, H.L., Suter, J.R., and Hardin, N.S., eds., Late Quaternary Facies and Structure, Northern Gulf of Mexico, Volume **23**: *AAPG Studies in Geology*, p. 11-80.

Blum, M.D., and Price, D.M., 1998, Quaternary alluvial plain construction in response to glacio-eustatic and climatic controls, Texas Gulf coastal plain, *in* Shanley, K.W., and McCabe, P.J., eds., Relative Role of Eustasy, Climate, and Tectonism in Continental Rocks, Volume **59**: *Society of Economic Paleontologists and Mineralogists Special Publication*, p. 31-48.

Blum, M.D., Toomey, I., Rickard S., and Valastro, J., Salvatore, 1994, Fluvial response to Late Quaternary climatic and environmental change, Edwards Plateau, Texas: *Palaeogeography, Palaeoclimatology, Palaeoecology*, **v. 108**, p. 1-21.

Blum, M.D., and Valastro, S., 1994, Late Quaternary Sedimentation, Lower Colorado River, Gulf Coastal-Plain of Texas: *Geological Society of America Bulletin*, **v. 106**, p. 1002-1016.

Bonnet, S., and Crave, A., 2003, Landscape response to climate change: Insights from experimental modeling and implications for tectonic versus climatic uplift of topography: *Geology*, **v. 31**, p. 123-126.

Bridgland, D., and D'Olier, B., 1995, The Pleistocene evolution of the Thames and Rhine drainage systems in the southern North Sea Basin., *in* Preece, R.C., ed., Island Britain: a Quaternary Perspective., Volume **96**: *Geological Society of London Special Publication*, Geological Society of London, p. 27–45.

Bridgland, D., Maddy, D., and Bates, M., 2004, River terrace sequences: templates for Quaternary geochronology and marine-terrestrial correlation: *Journal of Quaternary Science*, **v. 19**, p. 203-218.

Bridgland, D.R., 2000, River terrace systems in north-west Europe: an archive of environmental change, uplift and early human occupation: *Quaternary Science Reviews*, **v. 19**, p. 1293-1303.

Bridgland, D.R., 2002, Fluvial deposition on periodically emergent shelves in the Quaternary: example records from the shelf around Britain: *Quaternary International*, **v. 92**, p. 25-34.

References

Bridgland, D.R., and D'Orlier, B., 1995, The Pleistocene evolution of the Thames and Rhine drainage systems in the Southern North Sea Basin, *in* Preece, R.C., ed., Island Britain: a Quaternary perspective, Volume **96**: *Geological Society of London Special Publication*, p. 27-45.

Burgess, P.M., and Allen, P.A., 1996, A forward-modelling analysis of the controls on sequence stratigraphical geometries, *in* Hesselbo, S.P., and Parkinson, D.N., eds., Sequence Stratigraphy in British Geology, Volume **103**: *Geological Society of London Special Publication*, p. 9-24.

Burgess, P.M., and Hovius, N., 1998, Rates of delta progradation during highstands: consequences for timing of deposition in deep-marine systems: *Journal of the Geological Society*, **v. 155**, p. 217-222.

Castelltort, S., and Van Den Driessche, J., 2003, How plausible are high-frequency sediment supply-driven cycles in the stratigraphic record?: *Sedimentary Geology*, **v. 157**, p. 3-13.

Cohen, K.M., Stouthamer, E., and Berendsen, H.J.A., 2002, Fluvial deposits as a record for Late Quaternary neotectonic activity in the Rhine-Meuse delta, The Netherlands: *Geologie En Mijnbouw-Netherlands Journal of Geosciences*, **v. 81**, p. 389-405.

Curray, J.R., 1964, Transgressions and regressions, *in* Miller, R.L., ed., Papers in Marine Geology, Shepard commemorative volume: New York, MacMilland, p. 175-203.

Ellis, S., Schreurs, G., and Panien, M., 2004, Comparisons between analogue and numerical models of thrust wedge development: *Journal of Structural Geology*, **v. 26**, p. 1659-1675.

Galloway, W.E., 1989, Genetic Stratigraphic Sequences in Basin Analysis .1. Architecture and Genesis of Flooding-Surface Bounded Depositional Units: *Aapg Bulletin-American Association of Petroleum Geologists*, **v. 73**, p. 125-142.

Gibbard, P.L., and Lewin, J., 2002, Climate and related controls on interglacial fluvial sedimentation in lowland Britain: *Sedimentary Geology*, **v. 151**, p. 187-210.

Goodbred, J., Steven L., 2003, Response of the Ganges dispersal system to climate change: a source-to-sink view since the last interstade: *Sedimentary Geology*, **v. 162**, p. 83-104.

Goodbred, S.L., and Kuehl, S.A., 2000, Enormous Ganges-Brahmaputra sediment discharge during strengthened early Holocene monsoon: *Geology*, **v. 28**, p. 1083-1086.

Hay, W.W., 1998, Detrital sediment fluxes from continents to oceans: *Chemical Geology*, **v. 145**, p. 287-323.

Heller, P.L., and Paola, C., 1992, The large-scale dynamics of grain-size variation in alluvial basins, 2: Application to syntectonic conglomerate: *Basin Research*, **v. 4**, p. 91-102.

Heller, P.L., Paola, C., Hwang, I.G., John, B., and Steel, R., 2001, Geomorphology and sequence stratigraphy due to slow and rapid base-level changes in an experimental subsiding basin (XES 96-1): *Aapg Bulletin*, **v. 85**, p. 817-838.

Hooke, R.L., 1968, Model Geology: Prototype and Laboratory Streams: Discussion: *Geological Society of America Bulletin*, **v. 79**, p. 391-394.

Huisink, M., 1997, Late-glacial sedimentological and morphological changes in a lowland river in response to climatic change: The Maas, southern Netherlands: *Journal of Quaternary Science*, **v. 12**, p. 209-223.

Huisink, M., 2000, Changing river styles in response to Weichselian climate changes in the Vecht valley, eastern Netherlands: *Sedimentary Geology*, **v. 133**, p. 115-134.

Jervey, M.T., 1988, Quantitative geological modelling of siliciclastic rock sequences and their seismic expression, *in* Wilgus, C.K., Hastings, B.S., St Kendall, C.G., Posamentier, H.W., Ross, C.A., and Van Wagoner, J.C., eds., Sea-level changes: an integrated approach, Volume **42**: *Society of Economic Paleontologists and Mineralogists Special Publication*: Tulsa, p. 47-69.

Kooi, H., and Beaumont, C., 1996, Large-scale geomorphology: Classical concepts reconciled and integrated with contemporary ideas via a surface processes model: *Journal of Geophysical Research-Solid Earth*, **v. 101**, p. 3361-3386.

Koss, J.E., Ethridge, F.G., and Schumm, S.A., 1994, An Experimental-Study of the Effects of Base-Level Change on Fluvial, Coastal-Plain and Shelf Systems: *Journal of Sedimentary Research Section B-Stratigraphy and Global Studies*, **v. 64**, p. 90-98.

Laban, C., and Rijsdijk, K.F., 1993, General map of top Pleistocene geology in the Dutch sector of the North Sea: Haarlem, Geological Survey of The Netherlands.

Mackin, J.H., 1948, Concept of the graded river: *Bulletin of the Geological Society of America*, **v. 59**, p. 463-511.

Maddy, D., Bridgland, D., and Westaway, R., 2001, Uplift-driven valley incision and climate-controlled river terrace development in the Thames Valley, UK: *Quaternary International*, **v. 79**, p. 23-36.

Martin, Y., and Church, M., 1997, Diffusion in landscape development models: On the nature of basic transport relations: *Earth Surface Processes and Landforms*, **v. 22**, p. 273-279.

Meijer, X.D., 2002, Modelling the drainage evolution of a river-shelf system forced by Quaternary glacio-eustasy: *Basin Research*, **v. 14**, p. 361-377.

Metivier, and Gaudemer, 1999, Stability of output fluxes of large rivers in South and East Asia during the last 2 million years: implications on floodplain processes: *Basin Research*, **v. 11**, p. 293-303.

Metivier, F., Gaudemer, Y., Tapponnier, P., and Klein, M., 1999, Mass accumulation rates in Asia during the Cenozoic: *Geophysical Journal International*, **v. 137**, p. 280-318.

Metivier, F., Lajeunesse, E., and Cacas, M.C., 2005, Submarine canyons in the bathtub: *Journal of Sedimentary Research*, **v. 75**, p. 6-11.

Milana, J.P., 1998, Sequence stratigraphy in alluvial settings: A flume-based model with applications to outcrop and seismic data: *Aapg Bulletin*, **v. 82**, p. 1736-1753.

Milana, J.P., and Tietze, K.W., 2002, Three-dimensional analogue modelling of an alluvial basin margin affected by hydrological cycles: processes and resulting depositional sequences: *Basin Research*, **v. 14**, p. 237-264.

Mol, J., Vandenberghe, J., and Kasse, C., 2000, River response to variations of periglacial climate in mid-latitude Europe: *Geomorphology*, **v. 33**, p. 131-148.

Molnar, P., and England, P., 1990, Late Cenozoic Uplift of Mountain-Ranges and Global Climate Change - Chicken or Egg: *Nature*, **v. 346**, p. 29-34.

Moreton, D.J., Ashworth, P.J., and Best, J.L., 2002, The physical scale modelling of braided alluvial architecture and estimation of subsurface permeability: *Basin Research*, **v. 14**, p. 265-285.

Morton, R.A., and Price, A.W., 1987, Late Quaternary sea-level fluctuations and sedimentary phases of the Texas coastal plain and shelf, *in* Nummedal, D., Pilkey, O.H., and Howard, J.D., eds., Sea-level Fluctuation and Coastal Evolution, Volume **41**: *Society of Economic Paleontologists and Mineralogists Special Publication*: Tulsa, p. 181-189.

Paola, C., 2000, Quantitative models of sedimentary basin filling: *Sedimentology*, **v. 47**, p. 121-178.

Paola, C., Heller, P.L., and Angevine, C.L., 1992, The large-scale dynamics of grain-size variation in alluvial basins, 1: Theory: *Basin Research*, **v. 4**, p. 73-90.

Peakall, J., Ashworth, P.J., and Best, J.L., 1996, Physical modelling in fluvial geomorphology: principles, applications and unresolved issues, *in* Rhoads, B.L., and Thorn, C.E., eds., The scientific nature of geomorphology, proceedings of the 27th Binghamton symposium in geomorphology: Chichester, John Wiley & Sons, p. 221-254.

References

Persson, K.S., Garcia-Castellanos, D., and Sokoutis, D., 2004, River transport effects on compressional belts: First results from an integrated analogue-numerical model: *Journal of Geophysical Research-Solid Earth*, **v. 109**.

Posamentier, H.W., Jervey, M.T., and Vail, P.R., 1988, Eustatic controls on clastic deposition I - Conceptual framework, *in* Wilgus, C.K., Hastings, B.S., St Kendall, C.G., Posamentier, H.W., Ross, C.A., and Van Wagoner, J.C., eds., Sea-level changes: an integrated approach, Volume **42**: *Society of Economic Paleontologists and Mineralogists Special Publication*: Tulsa, p. 109-124.

Posamentier, H.W., and Vail, P.R., 1988, Eustatic controls on clastic deposition II - Sequence and Systems Tract Models, *in* Wilgus, C.K., Hastings, B.S., St Kendall, C.G., Posamentier, H.W., Ross, C.A., and Van Wagoner, J.C., eds., Sea-level changes: an integrated approach, Volume **42**: *Society of Economic Paleontologists and Mineralogists Special Publication*: Tulsa, p. 125-154.

Postma, G., and Van den Berg van Saparoea, A.P.H., in press, Flume modelling of river-delta-shelf systems at geological relevant time scales: Templates for sea-level induced flux, IAS Special Publication.

Prins, M.A., and Postma, G., 2000, Effects of climate, sea level, and tectonics unraveled for last deglaciation turbidite records of the Arabian Sea: *Geology*, **v. 28**, p. 375-378.

Quirk, D.G., 1996, Base profile: a unifying concept in alluvial sequence stratigraphy, *in* Howell, J.A., and Aitken, J.F., eds., High resolution sequence stratigraphy: Innovations and applications, Volume **104**: *Geological Society of London Special Publication*, p. 37-49.

Schlager, W., 1993, Accommodation and Supply - a Dual Control on Stratigraphic Sequences: *Sedimentary Geology*, **v. 86**, p. 111-136.

Schumm, S.A., 1998, To interpret the Earth; ten ways to be wrong: Cambridge, Cambridge University Press, 131 p.

Shanley, K.W., and McCabe, P.J., 1994, Perspectives on the Sequence Stratigraphy of Continental Strata: *Aapg Bulletin-American Association of Petroleum Geologists*, **v. 78**, p. 544-568.

Sirocko, F., Sarnthein, M., Erlenkeuser, H., Lange, H., Arnold, M., and Duplessy, J.C., 1993, Century-Scale Events in Monsoonal Climate over the Past 24,000 Years: *Nature*, **v. 364**, p. 322-324.

Snow, J.N., 1998, Late Quaternary highstand and transgressive deltas of the ancestral Colorado River: eustatic and climatic controls on deposition: Houston, Texas, Unpublished Ph.D. thesis, Rice University, 138 p.

Steel, R.J., Rasmussen, H., Eide, S., Neuman, B., and Siggerud, E. (2000) Anatomy of high-sediment supply, transgressive systems tracts in the Vilomara composite sequence, Sant Llorenç del Munt , Ebro Basin, NE Spain. In: M. Marzo & R.J. Steel (eds), High-resolution sequence stratigraphy and sedimentology of syntectonic clastic wedges (SE Ebro Basin, NE Spain), *Sedimentary Geology*, **v. 138**, 125-142.

Suter, J.R., Berryhill, H.L., and Penland, S., 1987, Late Quaternary sea-level fluctuations and depositional sequences, Southwest Louisiana continental shelf, *in* Nummedal, D., Pilkey, O.H., and Howard, J.D., eds., Sea-Level Fluctuation and Coastal Evolution, Volume **41**: *Society of Economic Paleontologists and Mineralogists Special Publication*: Tulsa, p. 199-219.

Toomey, I., Rickard S., Blum, M.D., and Valastro, J., Salvatore, 1993, Late Quaternary climates and environments of the Edwards Plateau, Texas: *Global and Planetary Change*, **v. 7**, p. 299-320.

Törnqvist, T.E., 1998, Longitudinal profile evolution of the Rhine-Meuse system during the last deglaciation: interplay of climate change and glacio-eustasy?: *Terra Nova*, **v. 10**, p. 11-15.

Vail, P.R., Mitchum, R.M., Todd, R.G., Widmier, J.M., Thompson, S.I., Sangree, J.B., Bubb, J.N., and Hatelid, W.G., 1977, Seismic Stratigraphy - applications to hydrocarbon exploration, *in* Payton, C.E., ed., Seismic Stratigraphy - applications to hydrocarbon exploration, Volume **26**: *American Association of Petroleum Geologists Memoir*, p. 49-212.

van Heijst, M., and Postma, G., 2001, Fluvial response to sea-level changes: a quantitative analogue, experimental approach: *Basin Research*, **v. 13**, p. 269-292.

van Heijst, M., Postma, G., Meijer, X.D., Snow, J.N., and Anderson, J.B., 2001, Quantitative analogue flume-model study of river-shelf systems: principles and verification exemplified by the Late Quaternary Colorado river-delta evolution: *Basin Research*, **v. 13**, p. 243-268.

van Heijst, M., Postma, G., van Kesteren, W.P., and de Jongh, R.G., 2002, Control of syndepositional faulting on systems tract evolution across growth faulted shelf margins: An analog experimental model of the Miocene Imo River field, Nigeria: *Aapg Bulletin*, **v. 86**, p. 1335-1366.

Van Heijst, M.W.I.M., and Postma, G., 2001, Fluvial response to sea-level changes: a quantitative, analogue experimental approach: *Basin Research*, **v. 13**, p. 269-292.

Van Wagoner, J.C., Mitchum, R.M., K.M., C., and Rhamanian, V.D., 1990, Siliciclastic sequence stratigraphy in Well logs, Cores and Outcrop: Concepts for high resolution correlation of time and facies., American Association of petroleum Geologists Methods in Exploration Series, Volume **7**, p. 55.

Vandenberghe, J., 2001, A typology of Pleistocene cold-based rivers: *Quaternary International*, **v. 79**, p. 111-121.

Veldkamp, A., and van Dijke, J.J., 2000, Simulating internal and external controls on fluvial terrace stratigraphy: a qualitative comparison with the Maas record: *Geomorphology*, **v. 33**, p. 225-236.

Wood, L.J., Ethridge, F.G., and Schumm, S.A., 1993, The effects of rate of base-level fluctuation on coastal-plain, shelf, and slope depositional systems: an experimental approach, *in* Posamentier, H.W., Summerhayes, C.P., Haq, B.U., and Allen, G.P., eds., Sequence Stratigraphy and Facies Associations, Volume **18**: *International Association of Sedimentologists Special Publication*, Blackwell Scientific Publications, p. 43-54.

Yalin, M.S., 1971, Theory of Hydraulic Models: London, Macmillan, 266 p.

Zhang, P.Z., Molnar, P., and Downs, W.R., 2001, Increased sedimentation rates and grain sizes 2-4 Myr ago due to the influence of climate change on erosion rates: *Nature*, **v. 410**, p. 891-897.

Samenvatting

(Summary in Dutch)

Het fluviatiele systeem

Riviersystemen zorgen voor ongeveer 95% van het transport van klastische sedimenten naar de oceaanbekkens (Hay, 1998). Sediment wordt via delta's en de shelf (continentale marges) naar de randen van de oceanische bekkens getransporteerd. Tijdens periodes waarin de zeespiegel relatief hoog is worden grote hoeveelheden sediment voor langere tijd op de shelf opgeslagen. Wanneer de zeespiegel zakt tot een niveau lager dan de randen van de shelf, wordt een deel van deze sedimenten door riviersystemen verder in de richting van de oceaanbekkens getransporteerd. De stratigrafie van riviersystemen en gerelateerde afzettingen bevat informatie over de geschiedenis van de processen die het riviersysteem beïnvloeden. Klimaat, tektoniek en zeespiegelfluctuaties zijn daarbij de belangrijkste. De stratigrafie van riviersystemen biedt een min of meer continu archief van klimaatsveranderingen in het Quartair.

Riviersystemen zijn van economisch belang. Zo vormen zij bijvoorbeeld belangrijke reservoirs voor olie, gas en water, en kunnen steenkool en zogenaamde 'placer deposits' (met bijv. diamanten en edelmetalen) bevatten. Inzicht in de vorming van de stratigrafie van riviersystemen en hun controle over het transport van sedimenten naar sedimentaire bekkens is dus ook in dit opzicht zeer relevant.

Riviersystemen bestaan uit drie hoofdonderdelen: het brongebied, waar water en sediment worden verzameld, de vallei van de hoofdrivier, waar sediment doorheen wordt getransporteerd, en het sedimentaire bekken, waarin de sedimenten uiteindelijk afgezet worden (Fig. 2.1).

De vallei van de hoofdrivier is niet enkel een transportband die het ontvangen sediment automatisch vervoert naar het sedimentaire bekken. Het longitudinale profiel van een rivier wordt, onder andere, bepaald door de hoeveelheid water en sediment die er doorheen worden getransporteerd. De gradiënt is evenredig met de hoeveelheid getransporteerd sediment en omgekeerd evenredig met het debiet van de rivier. Met andere woorden: een grote hoeveelheid sediment en/of een laag debiet in de rivier resulteren in een steil rivierprofiel en *vice versa*. Veranderingen in de helling van het rivierprofiel zorgen voor veranderingen in het volume van de sedimenten die (tijdelijk) opgeslagen zijn in de riviervallei. Hierdoor heeft de rivier een bufferwerking: als reactie op veranderingen in hoeveelheid sediment en/of water in de rivier wordt sediment toegevoegd aan of vrijgemaakt uit de tijdelijke opslag.

Het klimaat heeft een grote invloed op de productie en het beschikbaar maken van sedimenten in het brongebied, op het transport van sediment door het riviersysteem, en daardoor ook op de hoeveelheid sediment die uiteindelijk aan het sedimentaire bekken wordt geleverd. Twee andere belangrijke externe processen die het riviersysteem beïnvloeden zijn tektoniek en zeespiegelfluctuaties. Tektoniek is van invloed op de hoeveelheid verweringsproducten die beschikbaar worden gemaakt in het brongebied en de accomodatieruimte en gradiënt in de riviervallei en het sedimentaire bekken. Zeespiegelfluctuaties beïnvloeden de accomodatieruimte in het riviersysteem en op de shelf en de positie van de kustlijn, waaraan het (evenwichts)profiel van de rivier zich aanpast.

Het samenspel tussen deze drie externe processen zorgt ervoor dat het gedrag van riviersystemen zeer complex is. Zowel de invloed van de individuele processen als hun relatieve sterkte en onderlinge interactie worden nog slechts deels begrepen. Deze processen spelen zich af over periodes van duizenden tot miljoenen jaren; daarom is het alleen mogelijk om hun effecten te bestuderen aan de hand van het eindproduct, de stratigrafie van riviersystemen. Hierdoor is het maken van een correcte interpretatie en het begrijpen van het ontstaan ervan moeilijk. Daarnaast zijn de klimaatsomstandigeheden waaronder de meest recente en dus best bewaarde riviersystemen gevormd zijn niet representatief voor het verdere verleden. Zo zijn de zeespiegelfluctuaties in het Quartair bijvoorbeeld veel groter en sneller dan in periodes zonder ijstijden. Tenslotte zorgt 'equifinality' (Schumm, 1998), het idee dat (combinaties van) verschillende processen tot vergelijkbare eindproducten kunnen leiden, voor extra onzekerheid in de interpretatie van stratigrafie.

Conceptuele modellen verklaren de ontwikkeling van sedimentaire systemen aan de hand van een beperkt aantal externe processen, die een eenduidige invloed op het systeem uitoefenen. Een goed voorbeeld hiervan, dat veel wordt gebruikt, is het 'sequence stratigraphy' concept van Vail et al. (1977), dat de (snelheid van) eustatische zeespiegelverandering als belangrijkste bepalende factor bij het vormen van de stratigrafische architectuur van sedimentaire systemen op passieve continentale marges beschouwt. De eenvoud van dit concept maakt het zeer aantrekkelijk en in veel systemen biedt het zonder twijfel een plausibele verklaring voor de grootschalige stratigrafische architectuur. Een beperking van het concept is dat het nog niet gelukt is om het concept uit te breiden naar continentale (delen van) sedimentaire systemen. Daarnaast is het niet zeker dat andere externe processen niet een vergelijkbare invloed op sedimentaire systemen kunnen hebben. Het bredere concept van 'genetic stratigraphy' (Galloway, 1989) heeft tot doel stratigrafie onder te verdelen in systematische opeenvolgingen, die gevormd worden in periodes van depositie en begrensd worden door hiaten, zonder deze eenheden te koppelen aan de processen die verantwoordelijk zijn voor hun vorming. Hierdoor kan dit concept worden toegepast op elk sedimentair systeem. Het accent ligt echter op het beschrijven van stratigrafische opeenvolgingen, en niet op het verklaren van hun ontstaan. Om tot een verklaring van de stratigrafische opeenvolging te komen zijn aanvullende concepten nodig, die de invloed van individuele processen, hun relatieve belang en hun interactie beschrijven. Daarvoor is meer inzicht nodig in de invloed van de externe processen die sedimentaire systemen beïnvloeden (zeespiegelfluctuaties, klimaat en tektoniek).

Het doel van dit proefschrift is om de invloed van klimaat, dat wil zeggen de aanvoer van water en sediment, op de ontwikkeling van de stratigrafische architectuur van riviersystemen op passieve marges te analyseren. Dit impliceert:

- het bepalen van de relatieve invloed van klimaat ten opzichte van zeespiegelfluctuaties op de ontwikkeling van de stratigrafische architectuur van riviersystemen en de daarmee geassocieerde afzettingen op de shelf in een passieve setting,
- het bepalen van de invloed van veranderingen in de aanvoer van enerzijds water en anderzijds de aanvoer van sediment op het riviersysteem en op de hoeveelheid sediment die de rivier naar het bekken transporteert,
- het reconstrueren van de ontwikkeling van model riviersystemen aan de hand van hun stratigrafische architectuur, en
- het vergelijken van de uitkomsten met natuurlijke voorbeelden.

Benadering

We hebben gekozen voor het gebruik van een analoog model om deze vraagstelling te onderzoeken. De complexiteit van riviersystemen maakt het onmogelijk om de processen die het ontstaan van hun afzettingen bepalen op een eenvoudige en betrouwbare manier te reconstrueren en te kwantificeren. Numerieke en analoge modellen maken het mogelijk om dit probleem (deels) op te lossen. Analoge modellen kunnen het best worden beschouwd als miniatuurlandschappen die belangrijke aanwijzingen geven voor de gevoeligheid van het systeem voor verschillende parameters, iets wat moeilijk is te bereiken met numerieke modellen. Analoge modellen kunnen de processen die in een echt riviersysteem plaatsvinden niet reproduceren - analoge modellen zijn dus geen schaalmodellen -, wel reproduceren ze de gemiddelde effecten van deze processen over lange tijd. Deze benadering, waarbij alleen het grootschalige gedrag van het systeem wordt bestudeerd, zorgt ervoor dat complexiteit van het resultaat sterk wordt gereduceerd. Dit resulteert in een grootschalig kader waarbinnen meer gedetailleerde antwoorden kunnen worden gezocht. Voorbeelden van succesvol onderzoek middels analoge modellen zijn onder andere te vinden in Wood et al. (1993), Koss et al. (1994), Heller et al. (2001) en Van Heijst en Postma (2001).

Resultaten

In **hoofstuk 2** wordt de interactie tussen zeespiegelfluctuaties en klimaat behandeld. De resultaten van Van Heijst and Postma (2001) met betrekking tot de invloed van zeespiegelfluctuaties onder constante aanvoer van sediment en water worden vergeleken met de resultaten van experimenten met constante, maar per experiment verschillende waardes voor de sediment- en wateraanvoer in combinatie met een telkens identieke zeespiegelfluctuatie. De resultaten geven aan dat zeespiegelfluctuatie de belangrijkste factor is in het bepalen van de grootschalige stratigrafische architectuur van het systeem, dat wil zeggen: de positie van het depocentrum en periode waarin erosie plaatsvindt. De aanvoer van sediment en water, die bepaald worden door het klimaat en, bij sedimentaanvoer, door tektoniek in het brongebied, spelen een ondergeschikte maar niet onbelangrijke rol. Ze hebben geen grote invloed op de grootschalige architectuur van het systeem, maar zijn wel bepalend voor de stratigrafische architectuur op kleinere schaal: ze beïnvloeden de snelheid, mate en locatie van erosie en de relatieve afmetingen van de verschillende eenheden binnen de stratigrafie.

Hoofdstuk 3 beschrijft de gevolgen van veranderingen in de aanvoer van sediment en water uit het brongebied voor de hoeveelheid sediment die de rivier aan de monding verlaat. Uit de experimenten blijkt dat er fundamentele verschillen zijn in de manier waarop het systeem reageert op veranderingen in sedimentaanvoer ten opzichte van de reactie op veranderingen in de aanvoer van water. Bij veranderingen in wateraanvoer reageert het riviersysteem snel en met sterke veranderingen in de afvoer van sediment, terwijl de reactie op veranderingen in de sedimentaanvoer minder sterk en trager is. Hierdoor werkt het riviersysteem als een buffer voor snelle veranderingen in sedimentaanvoer. Het gevolg ervan is dat de kleinschalige stratigrafische architectuur aan de monding van het riviersysteem vooral beïnvloed wordt door veranderingen in de wateraanvoer, terwijl de stratigrafische architectuur op grotere schaal vooral wordt bepaald door (veranderingen in) de aanvoer van sediment vanuit het brongebied en eventuele zeespiegelfluctuaties. Kleinschalige stratigrafie zegt dus vooral veel over veranderingen in waterafvoer en grootschalige architectuur zegt meer over sedimentafvoer over langere tijd, die met name bepaald wordt door tektoniek in het

brongebied. De accumulatie van sedimenten aan de riviermonding kan zo worden gebruikt, in combinatie met de grootschalige architectuur van het riviersysteem, om veranderingen in de aanvoer van sediment en water uit het brongebied te reconstrueren.

In **hoofdstuk 4** wordt de complexe reactie van een model van een riviersysteem op een eenvoudige verandering van de wateraanvoer bestudeerd. Het gevonden gedrag is een eenvoudige verklaring voor het ontstaan van een stratigrafische architectuur, waarbij verschillende rivierterrassen elkaar ver van de monding van de rivier kruisen. De Rijn laat een voorbeeld van een dergelijke geometrie zien. Gezien de afstand tot de monding van de rivier ten tijde van de vorming van deze afzettingen, kan dit fenomeen niet worden verklaard in termen van zeespiegelfluctuatie in combinatie met klimaatsverandering. Het gedrag van het model biedt een goede verklaring voor het ontstaan van de kruisende rivierterrassen in de Rijn als gevolg van enkel en alleen klimaatsverandering. Wanneer de wateraanvoer wordt verhoogd op een moment dat de rivier niet in evenwicht is, kan snelle erosie in het bovenstroomse deel van de rivier optreden in combinatie met gelijktijdige benedenstroomse depositie, waarbij twee kruisende terrassen gevormd worden, zoals in de Rijn.

In **hoofdstuk 5** wordt een nieuwe manier van het analyseren en presenteren van de resultaten van analoge modellen uitgelegd. De belangrijkste meetresultaten bestaan uit series nauwkeurige hoogtemodellen, zogenaamde 'digital elevation models', DEMs, die de ontwikkeling van het oppervlak van het model gedurende een experiment weergeven. Door opeenvolgende DEMs met elkaar te vergelijken kunnen erosie en depositie tussen de momenten waarop de scans zijn gemaakt, worden bepaald. In de meeste studies is dit de voornaamste manier waarop deze gegevens gebruikt worden. Echter, een serie opeenvolgende DEMs van het oppervlak is het equivalent van een serie isochrone oppervlakken, en daarom is alle informatie voorhanden om voor elke tijdstap een driedimensionaal model van de stratigrafie van het model te maken. Deze informatie kan vervolgens als geologische kaarten, geologische doorsneden, fence diagrammen en Wheeler diagrammen worden gepresenteerd. In dit hoofdstuk wordt de logica beschreven die gebruikt wordt in de software die ontwikkeld is om de meetgegevens te analyseren en om te zetten tot 'synthetische stratigrafie'. Het genereren van synthetische stratigrafie uit de meetgegevens van de experimenten is een grote vooruitgang met betrekking tot de hoeveelheid en kwaliteit van de informatie die kan worden verkregen uit het model en draagt bij aan de interpretatie door een betere visualisatie van de resultaten.

Dankwoord

(Acknowledgements)

In de eerste plaats gaat mijn dank uit naar mijn promotor, Poppe de Boer, en mijn copromotor, George Postma, voor hun ondersteuning, begeleiding en de prettige samenwerking tijdens mijn promotieonderzoek. In de vele discussies bood het grote enthousiasme van George een goed tegenwicht tegen mijn soms wat te grote voorzichtigheid ten aanzien van het modelleerwerk. Poppe ben ik in het bijzonder dankbaar voor de snelle en goede feedback op mijn manuscripten.

Experimenteel werk is onmogelijk zonder goed werkende apparatuur. Ik ben dan ook Tony van der Gon Netscher zeer dankbaar voor de uitstekende technische ondersteuning en de slimme oplossingen voor de vele praktische problemen.

Rory Dalman heeft me wegwijs gemaakt in het werken met de stroomgoot. Romée Kars heeft geholpen met het uitvoeren van een aantal belangrijke experimenten. Joris Eggenhuisen heeft met een eigen experiment, zijn numeriek modelleerwerk en bijzonder scherpe discussies een flinke bijdrage geleverd aan mijn onderzoek.

Ik bedankt Marjolein Boonstra voor de secretariële ondersteuning, Marjan Reith en Paul Anten voor de logistieke ondersteuning en Jan Jansen voor zijn hulp in de bibliotheek, de leden van de leescommissie voor hun commentaar op dit proefschrift, Paul Meijer en Quintijn Clevis voor hun commentaar op hoofdstuk 5 van dit proefschrift, Peter van den Berg en Maurits van Dijk voor hun commentaar op de opmaak van dit proefschrift, Robbert van Vossen, Geert Strik en Quintijn Clevis voor alle tips omtrent het afronden van een proefschrift en Max van Heijst voor het overdragen van zijn collectie vakliteratuur.

Quintijn Clevis, Xander Meijer, Alexander Okx, Maurits van Dijk, Peter van den Berg, Joris Eggenhuisen en Arjan de Leeuw, met wie ik in de afgelopen jaren voor korte of langere tijd kamer N308 heb gedeeld, de overige medewerkers van de projectgroep Sedimentologie, Bernard de Jong, mijn onafscheidelijke partner in crime Geert Strik, de leden van het promovendiplatform, en de overige mede-promovendi en collegae bedank ik voor de prettige werksfeer, de koffie, de lunches, de borrels, en alle zinnige en minder zinnige discussies.

Onder alle veldwerken, excursies en practica die ik heb begeleid neemt het veldwerk in Aliaga in 2003 een bijzondere plaats in. Bernard, Hugo, Kim, Geert, Joris en Saskia: nihil nec optimum!

Buiten het werk hebben mijn jaargenoten en vrienden Frodo, Geert, Hubert, Jerfaas, Kees-Jan, Martijn, Michiel en Steven, evenals Sacha, De Buurvrouw en Buurman, mijn broer Bart, mijn overige vrienden en vriendinnen en de (oud)leden van Geologisch College Miölnir voor een hoop noodzakelijke ontspanning gezorgd. Tamar bedank ik daarnaast voor het becommentariëren van de samenvatting in het Nederlands. Ook bedank ik alle squashpartners, vooral Steven, die een jarenlange staat van dienst heeft. Ik bedank Hennie Thijssen en de leden van Thijssen Taekwon-do Academie voor de vele aangename trainingen.

En niet in de laatste plaats bedank ik mijn ouders, die mij altijd hebben gestimuleerd om te leren en me altijd hebben gesteund in mijn beslissingen.

Curriculum Vitae

De auteur werd geboren op 29 augustus 1974 te Wageningen. Tussen 1986 en 1992 doorliep hij het VWO/Gymnasium aan Het Wagenings Lyceum te Wageningen, waarna hij Geologie studeerde aan de faculteit Aardwetenschappen van de Universiteit Utrecht vanaf 1992 tot 1997. Na het behalen van het doctoraal diploma werkte hij als programmeur en softwareontwerper bij twee verschilende bedrijven. In 2001 begon hij met het promotieonderzoek aan de faculteit Aardwetenschappen / Geowetenschappen van de Universiteit Utrecht waarvan de resultaten in dit proefschrift worden beschreven.

The author was born on the 29th of August, 1974 in Wageningen, The Netherlands. Between 1986 and 1992 he attended secondary school at 'Het Wagenings Lyceum'. Between 1992 and 1997 he studied Geology at Utrecht University. After his graduation he worked for two different companies as a software engineer and software designer, and in 2001 he started his PhD study, the results of which are described in this thesis.